Entanglement entropy and Page curve from the M-theory dual of thermal QCD above T_c at intermediate coupling

Gopal Yadav[*] and Aalok Misra[†]

Department of Physics, Indian Institute of Technology Roorkee, Roorkee 247667, India

Exploration of entanglement entropy (EE) and obtaining the Page curve in the context of eternal black holes associated with top-down nonconformal holographic thermal duals at intermediate coupling has been entirely unexplored in the literature. We fill this gap by obtaining the Page curve of an eternal neutral black hole from a doubly holographic setup relevant to the M-theory dual of thermal QCD-like theories at high temperatures (i.e., above T_c) and intermediate coupling (effected by inclusion of terms quartic in curvature in M theory). Remarkably, excluding the higher derivative terms, the EE of the Hawking radiation from the on-shell Wald entanglement entropy integral (for appropriate choices of constants of integration appearing in the embeddings) increases *almost* linearly due to dominance of entanglement entropy contribution from the Hartman-Maldacena (HM)-like surface $S_{\mathrm{EE}}^{\mathrm{HM},\beta^0}, \beta \sim l_p^6$. This imparts a "Swiss-cheese" structure to $S_{\mathrm{EE}}^{\mathrm{HM},\beta^0}$ effecting a "Large N scenario" (LNS). Then after the Page time, the EE contribution from the island surface (IS) $S_{\mathrm{EE}}^{\mathrm{IS},\beta^0}$ dominates and saturates the linear time growth of the entanglement entropy of Hawking radiation and leads to the Page curve. The same is also obtained via the areas of the Hartman-Maldacena-like/island surfaces. Requiring the (IS) EE ($S_{\mathrm{EE}}^{\mathrm{IS},\beta^0}$) per unit Hawking-Beckenstein entropy (S_{BH}) post the Page time to be around 2, and positivity of the Page time, set respectively a lower and upper bound on the horizon radius r_h (the nonextremality parameter). Further, with the inclusion of the $\mathcal{O}(R^4)$ terms in M theory, the fact the turning point associated with the HM-like surface is in the deep IR, requires a relationship between l_p and r_h along with a conjectural $\gamma \equiv e^{-\mathcal{O}(1)N^{1/3}}$-suppression (motivated by the aforementioned requirement $\frac{S_{\mathrm{EE}}^{\mathrm{IS},\beta^0}}{S_{\mathrm{BH}}} \sim 2$ up to leading order). We obtain a hierarchy with respect to γ in $S_{\mathrm{EE}}^{\mathrm{HM},\beta^0}, S_{\mathrm{EE}}^{\mathrm{IS},\beta^0}$ and $S_{\mathrm{EE}}^{\mathrm{HM},\beta}, S_{\mathrm{EE}}^{\mathrm{HM},\beta}$ [at $\mathcal{O}(\beta)$]. This is due to the existence of massless graviton corresponding to a null mass eigenvalue of the Laplace-Beltrami equation in the internal space.

I. INTRODUCTION AND MOTIVATION

According to Hawking, black holes evolve from the pure state to a mixed state, i.e., Hawking radiation is thermal radiation. Evaporation of the black holes has no information about the initial state of the black hole which means information is lost in the black hole evaporation process [1]. But it has to respect the fundamental principle of quantum mechanics which is unitarity. Entanglement entropy of the Hawking radiation starts decreasing after the Page time [2] of the evaporating black hole and for eternal

[*]gyadav@ph.iitr.ac.in
[†]aalok.misra@ph.iitr.ac.in

black holes it reaches a constant value. Unitary evolution of black holes thus for has been understood via AdS/CFT correspondence [3]. In gauge-gravity duality, on gravity dual side, we have black hole and on the gauge theory side we have conformal field theory which respects unitarity. Therefore, we can study the unitary evolution of the black holes on the CFT side via gauge-gravity duality. A similar construction for QCD-like theories (equivalence class of theories which are IR confining, UV conformality and quarks transforms in the fundamental representation) at intermediate coupling was done in [4] where M-theory dual $\mathcal{O}(R^4)$ corrections were considered. We are studying the black hole information paradox via gauge-gravity duality in M-theory dual of [4]. For a review on the black hole information paradox, see [5,6].

There is a prescription to calculate entanglement entropy in field theories which have a gravity dual. For conformal field theories it was given in [7] that entanglement entropy will be given by the area of the codimension two minimal

surface in the bulk gravity dual. Generalization of the Ryu-Takayanagi formula for nonconformal theories was given in [8] and used made in [9] to discuss deconfinement phase transition in thermal QCD-like theories from entanglement entropy point of view. Further, if we consider higher derivative gravity theories then we can calculate entanglement entropy using [10]. Authors in [11] included quantum corrections to the Ryu-Takayanagi formula at all order in $\hbar$ and entanglement entropy which is known as generalized entropy. At leading order in $\hbar$ in generalized entropy formula, we recover the Ryu-Takayanagi formula [7]. In Englehardt-Wall prescription one is required to extremize the generalized entropy, and surfaces which extremize the generalized entropy are known as quantum extremal surfaces (QES). The island proposal was first introduced in [12], where the authors discussed that at late times islands come into the picture which contribute to the entanglement entropy. In this case, one is required to extremize the generalized entropylike functional over all islands which include contribution from the island surfaces, and then minimize over all possible extrema. Islands which extremize the aforementioned generalized entropy-like functional are known as quantum extremal islands (QEI).

In doubly holographic models we consider a black hole in the gravitational dual is coupled to an external conformal field theory (CFT) bath [13]. For example, gravity (which contains the black hole) in d-dimensions is coupled to external bath in d-dimensions, where d-dimensional external bath has its own holographic dual in $(d+1)$-dimensions. In these kinds of models we consider two copies of the setup described earlier. We consider two kinds of surfaces. First is the Hartman-Maldacena-like surface [14], which starts from the point where gravity is coupled to external bath, i.e., defect and crosses the black hole horizon and reaches up to the defect of thermofield double of doubly holographic models, and entanglement entropy contribution from this surface has linear time dependence which leads to information paradox at late times. Second, is the island surface, which start from the external bath and hit the Karch-Randall brane [15,16]. Entanglement entropy contribution from the island surface is independent of time and dominates after the Page time. After combining the entanglement entropy contributions from both surfaces we obtain the Page curve. Doubly holographic model with gravitating bath was discussed in [17] and with non-gravitating baths models were discussed in [18–21]. Page curve calculation for the neutral Gauss-Bonnet black hole was done in [22].[1]

There is one more way via which information paradox was resolved. In this approach, initially we calculate the entanglement entropy contribution without the island

surface using Cardy's formula [23] which depends on time and is responsible for the appearance of information paradox. Later, island surfaces emerge which contribute to the entanglement entropy and this contribution is independent of time which dominates after the Page time. Combining these two contributions we obtain the Page curve. Based on this approach some examples were discussed in [24–28]. Since there is no known Cardy-like formula for nonconformal theories therefore we are following the doubly holographic models approach discussed earlier in our calculations. Islands and Page curves were studied in type IIB string theory in [29–31] and for flat space black holes, see [32]. Page curves of the Reissner-Nordström black hole in the presence of higher derivative terms was studied in [33].

To study thermal QCD-like theories via gauge-gravity duality in the UV complete type IIB holographic dual, the authors started in [34] where they constructed type IIB string dual of large-N thermal QCD-like theories in the strong coupling limit. To study the finite coupling regime of thermal QCD-like theories authors constructed type IIA mirror of the aforementioned type IIB setup then uplifted it to the M-theory in [35,36]. Applications of the same were studied in [37–40]. Further, to have analytical control on the intermediate coupling regime of thermal QCD-like theories, the authors in [4] incorporated HD terms on the gravity dual side. We are working with [4] too in this paper to obtain the Page curve of a neutral black hole in the presence of higher derivative terms. The model [4] has been reviewed in [9,41] and the latter references are applications of the same. One of us (GY) studied the effect of rotation on the deconfinement temperature of thermal QCD-like theories at intermediate coupling from M-theory in [42].

In this paper we are calculating the Page curve of a neutral black hole where we have a nonconformal bath. In our case, on the gravity dual side we have M-theory dual inclusive of higher derivative terms and on the gauge theory side we have thermal QCD-like theories at intermediate coupling which is a nonconformal theory. In this paper we are considering a doubly holographic setup similar to [18,19] where on the gauge theory side authors have a conformal theory but the story is different in our setup because we have a nonconformal theory. Similar to [18,19], we consider two kinds of candidate surfaces: Hartman-Maldacena-like surface and island surface. Hartman-Maldacena-like surface is responsible for the linear time growth of the entanglement entropy of Hawking radiation [14]. After the Page time, the entanglement entropy contribution from the island surface dominates which is independent of time and we obtain the Page curve from M-theory dual inclusive of $\mathcal{O}(R^4)$ corrections.

We have organized the paper in the following way. In Sec. II via two subsections II A and II B, we have described

---

[1]One of us (GY), thanks R. X. Miao to bring their work to our attention.

the holographic dual of thermal QCD-like theories from top-down approach in subsection II A and construction of doubly holographic setup in M-theory dual in subsection II B. Section III is devoted to discussion of end-of-the-world (ETW) "brane" embedding in the M-theory dual. First, we have discussed that ETW-"brane" has constant embedding at the level of Einstein gravity in III A and then we have shown in III B that when restricted to the aforementioned constant ETW-"brane" embedding, there are no boundary terms generated from the most dominant J_0 terms at $\mathcal{O}(R^4)$ in the "MQGP limit" in the eleven dimensional supergravity action that would have covariant derivatives of the metric variation, and hence would have required suitable boundary terms to be constructed to cancel the same (much like the GHY boundary terms to cancel off similar terms in the EH action in Einstein gravity). Section IV is divided into three subsections. Subsections IV A and IV B involve calculations of the entanglement entropy of the Hawking radiation from the areas of Hartman-Maldacena-like and island surfaces, and in subsection IV C we have obtained the Page curve of eternal neutral black hole in the absence of higher derivative terms in eleven dimensional supergravity action. We do the Page curve calculation of the neutral black hole in the presence of higher derivative terms in Sec. V via four subsections V A, V B, V C and V D. In Secs. V A and V C we obtain the entanglement entropies of the Hawking radiation for the Hartman-Maldacena-like and island surfaces in the presence of higher derivative terms, and then we obtain the Page curve in Sec. V D. In Sec. V B we discuss the "Swiss-cheese" structure of entanglement entropy contribution from the Hartman-Maldacena-like surface. Section VI has a discussion on showing the existence of massless graviton by showing the existence of a null eigenvalue of the Laplace-Beltrami differential equation for the graviton wave function along the internal coordinates and hence provide a physical reason for the exponential-in-N suppression of entanglement entropies in particular for the Island Surface. We discuss our results and conclusion in Sec. VII.

Additionally there are four appendices. By dividing the appendix A into two parts, we have computed angular integrals used in this paper in A 1 and turning point of the island surface in A 2. In appendix B we have listed various r dependent functions in entanglement entropy expression of the HM-like surface at $\mathcal{O}(\beta^0)$ and $\mathcal{O}(\beta)$, apart from that we have also computed EOM of the HM-like surface embedding in the same appendix. In appendix C we have listed r dependent functions appearing in the $\mathcal{O}(\beta)$ term of the entanglement entropy of island surface and then computed the derivatives of the Lagrangian with respect to embedding function and derivatives of the embedding function. In appendix D, we have listed all the possible terms that we obtain in the holographic entanglement entropy for Hartman-Maldacena-like and island surfaces in D 1 and D 2.

II. SETUP

In this section we will first summarize (in II A) the type IIB/IIA mirror dual of thermal QCD-like theories (i.e., IR-confining, UV-conformal with quarks in the fundamental representation of flavor and color) and its no-braner M-theory uplift worked out in [4,34,36]. We will then discuss (in II B) the doubly holographic setup in the M-theory uplift.

A. Top-down UV-complete holographic dual of thermal QCD-like theories

From the point of view of construction of a string/M-theory holographic dual truly close to realistic thermal QCD-like theories, one needs to consider finite gauge coupling (g_s) and finite number of colors (N). From the point of view of gauge-gravity duality, this entails looking at the strong-coupling limit of string theory—M theory—the same was dubbed as the "MQGP limit" in [36] wherein $g_s \lesssim 1, N_f \equiv \mathcal{O}(1), (N, M) \gg 1$ such that $\frac{g_s M^2}{N} \ll 1$.

(1) *Brane configuration of [34]*: Brane setup of [34] has N D3-branes, M D5-branes and M $\overline{D5}$-branes, N_f D7-branes N_f $\overline{D7}$-branes. World volume coordinates are the aforementioned D-branes are summarized in Table I. M D5-branes and M $\overline{D5}$-branes are wrapping the same vanishing two cycle $S^2(\theta_1, \phi_1)$ but located at antipodal points (average separation is $\mathcal{R}_{D5/\overline{D5}}$) of resolving $S_a^2(\theta_2, \phi_2)$. $\mathcal{R}_{D5/\overline{D5}}$ is the boundary between UV ($r > \mathcal{R}_{D5/\overline{D5}}$) and IR ($r < \mathcal{R}_{D5/\overline{D5}}$) on the gravity dual side in terms of radial coordinate. Flavor D7-branes were embedded holomorphically [43] in the resolved conifold geometry (1):

$$(r^6 + 9a^2 r^4)^{\frac{1}{4}} e^{\frac{i}{2}(\psi - \phi_1 - \phi_2)} \sin\left(\frac{\theta_1}{2}\right) \sin\left(\frac{\theta_2}{2}\right) = \mu_{\text{Ouyang}},$$

(1)

where μ_{Ouyang} is the Ouyang embedding parameter. N_f $\overline{D7}$-branes are present only in the UV and UV-IR interpolating region whereas N_f D7-branes are present in the UV, UV-IR interpolating region and in the IR too. This provides a realization of chiral symmetry breaking in the setup and UV conformality in the theory which we will explain in the next point.

(2) Based on earlier discussion, we can see that product color and flavor gauge groups are $SU(N + M) \times SU(N + M)$ and $SU(N_f) \times SU(N_f)$ when we are in the UV, i.e., $r > \mathcal{R}_{D5/\overline{D5}}$. When one is going from UV ($r > \mathcal{R}_{D5/\overline{D5}}$) to IR ($r < \mathcal{R}_{D5/\overline{D5}}$) via RG group flow then $SU(N_f) \times SU(N_f)$ changes into $SU(N_f)$ (because there are no N_f $\overline{D7}$-branes in the IR). This

process can be interpreted as chiral symmetry breaking in the setup. Effect of transition from UV to IR at $r = \mathcal{R}_{D5/\overline{D5}}$ on the product color gauge group is that it changes $SU(N + M) \times SU(N + M)$ to $SU(N + M) \times SU(N)$ (because no $M \overline{D5}$-branes in the IR). This triggers Sieberg-like duality in the setup and if we perform repeated Sieberg-like dualities then in the IR we will be left with $SU(M)$ gauge theory where M can be identified with number of colors in the theory and M can be set to 3 [44] in the "MQGP" limit discussed later in this subsection.

(3) Now let us see how we can say that the theory is nonconformal. This can be seen from the following RG-flow equations of the gauge couplings of the product gauge group:

$$4\pi^2 \left(\frac{1}{g_{SU(N+M)}^2} + \frac{1}{g_{SU(N)}^2} \right) e^\phi \sim \pi;$$

$$4\pi^2 \left(\frac{1}{g_{SU(N+M)}^2} - \frac{1}{g_{SU(N)}^2} \right) e^\phi \sim \frac{1}{2\pi\alpha'} \int_{S^2} B_2. \quad (2)$$

If $\int_{S^2} B_2 = 0$, then we will have a conformal theory and this is true in the UV in this setup because of presence of $M \overline{D5}$-branes in the UV. In the IR, $\int_{S^2} B_2 \neq 0$, which implies nonconformality in the theory from (2). $N_f \overline{D7}$-branes cancels the net N_f flavor $D7$-branes charges in the UV which corresponds to constancy of dilaton in the UV.

(4) *String dual of thermal QCD-like theories [34]*: On the gauge theory side we want to have finite temperature QCD. As we know that there are two phases of QCD: confining phase ($T < T_c$) and the deconfined phase ($T > T_c$). In the deconfined phase, finite temperature can be introduced by a black hole in the holographic dual side and in the confining phase, finite temperature can be introduced by a thermal background in the holographic dual side. In addition to finite temperature there is finite separation between the $M D5$-branes and $M \overline{D5}$, this corresponds to nontrivial resolution of the conifold geometry. Further, we need IR confinement in thermal QCD and it will be obtained on the gauge theory side by deforming the three cycle in the gravity dual side. From the aforementioned discussion it is clear that gravity dual of type IIB setup is a resolved warped deformed conifold. Further, we have fluxes [which contains the backreaction (also in the warp factor)] in the IR which are coming from $D3$-branes and the $D5$-branes.

(5) *Number of colors, i.e., $N_c = 3$*: Number of colors N_c can be identified with M when Sieberg-like duality cascade ends in the IR [44], and M can be set to 3 in the MQGP limit. The idea is as follows: we can write N_c as the sum of effective number of $D3$-branes and $D5$-branes, i.e., $N_c = N_{\text{eff}}(r) + M_{\text{eff}}(r)$, where $N_{\text{eff}}(r)$ and $M_{\text{eff}}(r)$ are defined from $\tilde{F}_5$ and $\tilde{F}_3$:

$$\tilde{F}_5 \equiv dC_4 + B_2 \wedge F_3 = \mathcal{F}_5 + *\mathcal{F}_5; \qquad \mathcal{F}_5 \equiv N_{\text{eff}} \times \text{Vol(Base of Resolved Warped Deformed Conifold)},$$

$$M_{\text{eff}}(r) = \int_{S^3} \tilde{F}_3, \qquad\qquad\qquad\qquad\qquad\qquad\qquad\qquad\qquad (3)$$

where $\tilde{F}_3 (\equiv F_3 - \tau H_3) \propto M_{\text{eff}}(r) \equiv M \frac{1}{1 + e^{\alpha(r - \mathcal{R}_{D5/\overline{D5}})}}$, $\alpha \gg 1$ with $\mathcal{R}_{D5/\overline{D5}}$ being the $D5 - \overline{D5}$ separation along the blown-up S^2 which in turn is estimated to be $\sqrt{3}a$ in the type IIB dual with the same therefore acting as the outer boundary of the UV-IR interpolating region in same as well as its type IIA mirror gravity dual and its M-theory uplift, and S^3 is dual to $e_\psi \wedge (\sin\theta_1 d\theta_1 \wedge d\phi_1 - B_1 \sin\theta_2 \wedge d\phi_2)$, where $e_\psi \equiv d\psi + \cos\theta_1 d\phi_1 + \cos\theta_2 d\phi_2)$ and B_1 is an "asymmetry factor" defined in [34]. Since $N_{\text{eff}} \in [N_{\text{UV}}, 0_{\text{IR}}]$ and $M_{\text{eff}} \in [0_{\text{UV}}, M_{\text{IR}}]$, therefore $N_c = M_{\text{IR}}$, where M_{IR} implies that in the IR, number of colors is equal to M and this can be set to 3 in the MQGP limit. Further we can also take $N_f = 2(u/d) + 1(s)$. Therefore we can see that $\frac{N_f}{N_c}$ is fixed in the IR (Veneziano-like limit [45]; but N_f and N_c remain finite themselves).

(6) *The MQGP limit, type IIA Strominger-Yau-Zaslow (SYZ) mirror of [34] and its M-theory uplift at intermediate gauge coupling*:
(a) The MQGP limit is defined as below [35,36]:

$$g_s \sim \frac{1}{\mathcal{O}(1)}, \qquad M, N_f \equiv \mathcal{O}(1),$$

$$N \gg 1, \qquad \frac{g_s M^2}{N} \ll 1, \qquad \frac{(g_s M^2) g_s N_f}{N} \ll 1. \quad (4)$$

MQGP limit (4) involves finite string coupling (intermediate gauge coupling on gauge theory side) and finite M which is number of colors in the IR, i.e., $N_c = M$. Therefore M theory dual is holographic dual of thermal QCD-like theories at intermediate gauge coupling [4].

TABLE I. Brane configuration of [34].

Serial number	Branes	World Volume
1.	N $D3$	$\mathbb{R}^{1,3}(t,x^{1,2,3}) \times \{r=0\}$
2.	M $D5$	$\mathbb{R}^{1,3}(t,x^{1,2,3}) \times \{r=0\} \times S^2(\theta_1,\phi_1) \times \mathrm{NP}_{S_a^2(\theta_2,\phi_2)}$
3.	M $\overline{D5}$	$\mathbb{R}^{1,3}(t,x^{1,2,3}) \times \{r=0\} \times S^2(\theta_1,\phi_1) \times \mathrm{SP}_{S_a^2(\theta_2,\phi_2)}$
4.	N_f $D7$	$\mathbb{R}^{1,3}(t,x^{1,2,3}) \times \mathbb{R}_+(r \in [|\mu_{\mathrm{Ouyang}}|^{\frac{2}{3}}, r_{\mathrm{UV}}]) \times S^3(\theta_1,\phi_1,\psi) \times \mathrm{NP}_{S_a^2(\theta_2,\phi_2)}$
5.	N_f $\overline{D7}$	$\mathbb{R}^{1,3}(t,x^{1,2,3}) \times \mathbb{R}_+(r \in [\mathcal{R}_{D5/\overline{D5}} - \epsilon, r_{\mathrm{UV}}]) \times S^3(\theta_1,\phi_1,\psi) \times \mathrm{SP}_{S_a^2(\theta_2,\phi_2)}$

(b) One can obtain the M-theory uplift of type IIB setup by constructing the type IIA Strominger-Yau-Zaslow (SYZ) mirror (which is obtained by implementing triple T-duality along the three isometry directions) setup of type IIB setup and then uplift the type IIA mirror to M-theory. Three isometry directions produces a local special Lagrangian (sLag) T^3–which could be identified with the T^2-invariant sLag of [46] with a large base $\mathcal{B}(r,\theta_1,\theta_2)$ [for a $T^3(\phi_1,\phi_2,\psi)$-fibration over $\mathcal{B}(r,\theta_1,\theta_2)$] [35,47][2] Three isometry directions are x, y, z which are toroidal analogue of ϕ_1, ϕ_2, ψ.[3] From Table I we see that T duality along the ψ direction converts the N $D3$-branes, M fractional $D3$-branes and N_f flavor $D7$-branes into N $D4$-branes wrapping the ψ circle, M $D4$-branes straddling a pair of orthogonal N $S5$-branes and N_f flavor $D6$-branes. Now, from second and third T duality along the ϕ_1 and ϕ_2 directions, we obtain N $D6$-branes, M $D6$-branes and N_f $D6$-branes "wrapping" a noncompact three-cycle $\Sigma^{(3)}(r,\theta_1,\phi_2)$. Now if we uplift the type IIA mirror to M-theory

then it was found that $D6$-branes are converted into KK monopoles (variants of Taub-NUT spaces). Therefore we have no branes in the M-theory and we will be left with M-theory with a G_2-structure manifold—a no-braner uplift.

(7) *M-theory uplift including $\mathcal{O}(R^4)$ and G-structure torsion classes*:

One of us (AM) along with V. Yadav, worked out $O(l_p^6)$ corrections to the M-theory M-theory metric in the "MQGP" limit in [4] and using the afore-mentioned M-theory metric, G-structure torsion classes were worked out for the six-, seven- and eight-folds of the M-theory uplift and summarized in Table II. The eleven-fold M_{11} in the M theory uplift obtained in [36] turns out to be a warped product of $S^1(x^0) \times \mathbb{R}_{\mathrm{conformal}}$ and $M_7(r,\theta_{1,2},\phi_{1,2},\psi,x^{10})$, the latter being a cone over $M_6(\theta_{1,2},\phi_{1,2},\psi,x^{10})$ with $M_6(\theta_1,\phi_{1,2},$
$\psi,x^{10})$ possessing the following nested fibration structure:

$$\mathcal{M}_6(\theta_{1,2},\phi_{1,2},\psi,x_{10}) \leftarrow S^1(x^{10})$$
$$\downarrow$$
$$\mathcal{M}_5(\theta_{1,2},\phi_{1,2},\psi) \leftarrow \mathcal{M}_3(\phi_1,\phi_2,\psi). \quad (5)$$
$$\downarrow$$
$$\mathcal{B}_2(\theta_1,\theta_2)$$

As shown in [36], $p_1^2(M_{11}) = p_2(M_{11}) = 0$ up to $\mathcal{O}(\beta^0)$ where p_a is the a-th Pontryagin class of M_{11}. This hence implied that $X_8 = 0$ in (14) up to $\mathcal{O}(\beta^0)$.

From the above discussions we find that the type IIB setup has the following properties: IR confinement, UV conformality, quarks transform in the fundamental representation of flavor and color groups and well defined in the confining and deconfined phases. Therefore it is an ideal holographic dual of thermal QCD-like theories.

The type IIB setup of [34], its Strominger-Yau-Zaslow type IIA mirror and its M-theory uplift as constructed in [35,36] as well as [4] (M-theory uplift at intermediate 't Hooft coupling effected by inclusion of $\mathcal{O}(R^4)$ terms) are summarized in Fig. 1.

---

[2]In [44] it was discussed in a footnote that to implement SYZ mirror symmetry idea is similar to [48], we need to replace the pair of S^2s by pair of T^2s from which we can get the correct T-duality coordinates. After getting the type IIA mirror, similar to the [48] pertaining to $D5$-branes wrapping a vanishing S^2, uplift it to M-theory with a bonafide G_2-structure that is free of the angular delocalization. One can descend back to type IIA which will therefore be free of delocalization now.

[3]As explained in [49], the T^3-valued (x,y,z) (used for effecting SYZ mirror in [35,36]) are defined via:

$$\phi_1 = \phi_{10} + \frac{x}{\sqrt{h_2}[h(r_0,\theta_{10,20})]^{\frac{1}{4}}\sin\theta_{10} \, r_0},$$

$$\phi_2 = \phi_{20} + \frac{y}{\sqrt{h_4}[h(r_0,\theta_{10,20})]^{\frac{1}{4}}\sin\theta_{20} \, r_0},$$

$$\psi = \psi_0 + \frac{z}{\sqrt{h_1}[h(r_0,\theta_{10,20})]^{\frac{1}{4}} r_0},$$

$h_{1,2,4}$ defined in [34], and one works up to linear order in (x,y,z). In the IR, it can be shown [50] that $\theta_{10,20}$ can be promoted to global coordinates $\theta_{1,2}$ in all the results in the paper.

TABLE II. IR G-structure classification of six-/seven-/eight-folds in the type IIA/M-theory duals of thermal QCD-like theories (at high temperatures) and for $r \in$ IR; $\times_w$ denotes a warped product.

Serial number	Manifold	G-Structure	Nontrivial Torsion Classes
1.	$M_6 =$ non-Kähler conifold	$SU(3)$	$T^{\text{IIA}}_{SU(3)} = W_1 \oplus W_2 \oplus W_3 \oplus W_4 \oplus W_5 : W_4 \sim W_5$
2.	$M_7 = S^1_{\mathcal{M}} \times_w M_6$	G_2	$T^{\mathcal{M}}_{G_2} = W_1 \oplus W_7 \oplus W_{14} \oplus W_{27}$
			$\downarrow r \sim (1 + \alpha_a)a, \ \alpha_a \sim 0.1\text{–}0.3$
			$W_1 = \mathcal{O}\left(\frac{1}{N^{\alpha_{W_1}}}\right), \ \alpha_{W_1} > 1,$
			therefore disregarded up to $\mathcal{O}\left(\frac{1}{N}\right)$;
			$W_7 \approx 0$
			$\Rightarrow T^{\mathcal{M}}_{G_2} = W_{14} \oplus W_{27}$
3.	$M_8 = S^1_t \times_w M_7$	$SU(4)$	$T^{\mathcal{M}}_{SU(4)} = W_2 \oplus W_3 \oplus W_5$
4.	M_8	Spin(7)	$T^{\mathcal{M}}_{\text{Spin}(7)} = W_1 \oplus W_2$

B. Doubly holographic setup

Let us first review the doubly holographic setup [13]. There are three equivalent descriptions of doubly holographic models which are summarized below:

(1) A bath which is a boundary CFT(BCFT) living at the boundary of AdS$_{d+1}$ whose boundary is (d-1) dimensional defect [51,52], to collect the Hawking radiation.
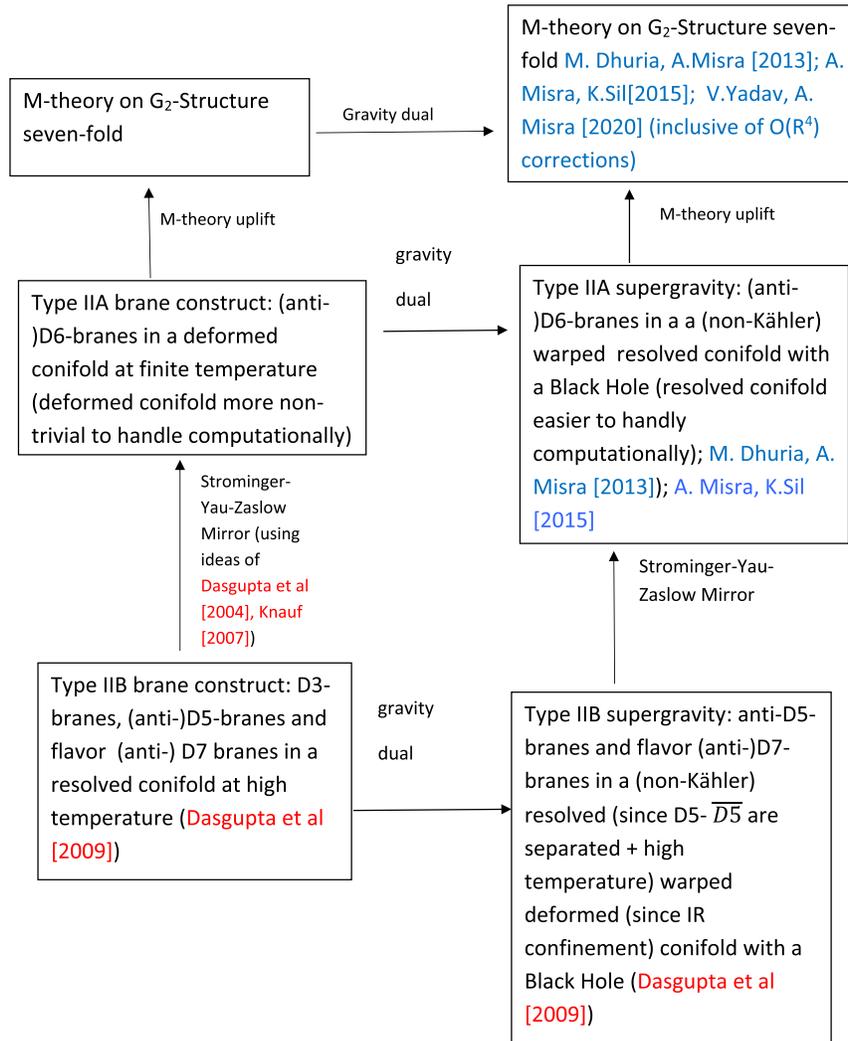

FIG. 1. Type IIB dual of large-N thermal QCD like theories, its SYZ type IIA mirror and M-theory uplift.

(2) Conformal field theory in d dimensions is coupled to gravity on an "end-of-the-world" (ETW) brane in an asymptotically AdS_d space $\mathcal{M}_d$ with a half-space bath CFT coupled to $\mathcal{M}_d$ via "transparent boundary conditions" at the defect (the intersection of the ETW-brane and the bath).

(3) Einstein gravity in $\mathcal{M}_{d+1}$ asymptotic to AdS_{d+1}, the holographic dual of d-dimensional BCFT, containing $\mathcal{M}_d$ as an ETW brane [15,16,53].

Let $S(\mathcal{R})$ be the von Neumann entropy of subregion $\mathcal{R}$ defined on constant time slice in description 1. In the second description it will be given by the island-rule ($\mathcal{I}$) [12] as,

$$S(\mathcal{R}) = \min_{\mathcal{I}} \mathrm{ext}_{\mathcal{I}} S_{\mathrm{gen}}(\mathcal{R} \cup \mathcal{I}), \qquad (6)$$

where generalized entropy functional is defined as [11]:

$$S_{\mathrm{gen}}(\mathcal{R} \cup \mathcal{I}) = \frac{A(\partial \mathcal{I})}{4G_N} + S_{\mathrm{matter}}(\mathcal{R} \cup \mathcal{I}), \qquad (7)$$

where the first term in the above equation is the area of the boundary of the island surface and second term is the matter contribution from bath as well as island regions. In the third description, generalized entropy functional defined in semi-classical geometry can be computed classically using the Ryu-Takayanagi formula in $(d+1)$ dimensions [7] from the area of the codimension two minimal surface:

$$S_{\mathrm{gen}}(\mathcal{R} \cup \mathcal{I}) = \frac{A(\gamma)}{4G_N^{(d+1)}}, \qquad (8)$$

where γ is the codimension two surface in the $\mathcal{M}_{(d+1)}$ dimensional bulk space-time. Therefore one can calculate very easily entanglement entropy of the Hawking radiation in doubly holographic models using the classical Ryu-Takayanagi formula in third description.

There is also a similar setup available in the literature as constructed in [19]. In [19], authors constructed a similar setup as discussed earlier but in this setup bath is a warped conformal field theory(WCFT) [54] instead of CFT. This setup has also three equivalent descriptions which are summarized below:

(1) Boundary warped conformal field theory(BWCFT) in two dimensions with one dimensional boundary.

(2) Two dimensional JT gravity coupled to WCFT in two dimensions at the interface point via transparent boundary conditions.

(3) Einstein gravity on $\mathcal{M}_3$ asymptote to AdS_3 space containing $\mathcal{M}_2$ as a Planck brane [12].

Similar to earlier discussion one can calculate the entanglement entropy of the Hawking radiation classically in the third description when one has warped conformal field theory in two dimensions as a bath using Ryu-Takayanagi formula [7]. Doubly holographic models have been studied in the literature mentioned in Sec. I and also in [55–66].

Motivated by these constructions we are generalizing these kinds of setups to our case. After a double Wick-rotation, we have QCD_{2+1} at r = 0, along $x^{1,2}$ and Wick-rotated x^3. One can think of a fluxed ETW-hypersurface or "brane" $M_{10} = \mathbb{R}^2(x^{2,3}) \times_w M_8$ where M_8 is the (non-compact) $SU(4)/\mathrm{Spin}(7)$-structure ([4], Table II) eight-fold $M_8^{SU(4)/\mathrm{Spin}(7)}(r,t,\theta_{1,2},\phi_{1,2},\psi,x^{10})$ at $x^1 = 0$ which has a black hole. The ETW-hypersurface can be interpreted as $\mathbb{R}^2(x^{2,3}) \times_w M_8^{SU(4)/\mathrm{Spin}(7)}(t,r,\theta_{1,2},\phi_{1,2},\psi,x^{10})$ containing black $M5$-brane at $x^1 = 0$ with world volume $\Sigma^{(6)} = S^1(t) \times_w \mathbb{R}_{\geq 0}(r) \times \Sigma^{(4)}$ where $\Sigma^{(4)} = n_1 S^3(\theta_1,\phi_1,\psi) \times [0,1]_{\theta_2} + n_2 S^2(\theta_1,\phi_1) \times S^2(\theta_2,x^{10})$ with n_1 determined by $\int_{S^3 \times [0,1]} G_4$ and n_2 by $\int_{S^2 \times S^2} G_4$; the QCD_{2+1} can be thought of as living on $M2$-branes with world volume $\Sigma^{(3)}(x^{1,2,3})$. QCD_{2+1} at $r = 0$ would interact gravitationally via the pull-back of the ambient $M_{11} = \mathbb{R}^{1,2,3} \times_w M_8 = \mathbb{R}(x^1) \times_w M_{10}$ metric used to contract the non-Abelian field strength in the gauge kinetic term obtained as part of the $M2$-brane($x^{1,2,3}$) world-volume action. This has some similarity with points 2. and 3. of the first paragraph of this section as regards the doubly holographic setup as described in [13]. Let us be more specific and briefly describe the three equivalent descriptions alluded to toward the beginning of this subsection. The doubly holographic setup constructed from the bottom-up approach (usually followed in the literature) as described at the beginning of this subsection, has the following M-theory description (the one we follow) of top-down double holography with QCD_{2+1} bath with the numbering matches the one used in the aforementioned three equivalent description:

(1) *Boundarylike description:* QCD_{2+1} (could be thought of as supported on an $M2$-brane with world volume $\Sigma^{(3)}(x^{1,2,3})$, and) is living at the tip ($r = 0$) of a noncompact seven-fold of G_2 structure which is a cone over a warped non-Kähler resolved conifold. The two-dimensional "defect" $\Sigma^{(2)} \cong \Sigma^{(3)}(x^{2,3}; x^1 = 0) \cong \mathbb{R}^2(x^{2,3})$.

(2) *Nonconformal bath-ETW interv c maction description:* Fluxed end-of-the-world (ETW) hypersurface $M_{10} \cong \mathbb{R}^2(x^{2,3}) \times_w M_8^{SU(4)/\mathrm{Spin}(7)}(t,r,\theta_{1,2},\phi_{1,2},\psi,x^{10})$ containing black $M5$-brane at $x^1 = 0$ coupled to QCD_{2+1} bath living on $M2$ brane with world volume $\Sigma^{(3)}(x^{1,2,3})$ along the defect $\Sigma^{(2)} \cong M_{10} \cap \Sigma^{(3)}(x^{1,2,3})|_{x^1=0}$ via exchange of massless graviton.

(3) *Bulk description:* $QCD_{2+1}(x^{1,2,3})$ has holographic dual which is eleven dimensional $[M_{11} \cong \mathbb{R}(x^1) \times_w M_{10} \cong S^1(t) \times_w \mathbb{R}^3(x^{1,2,3}) \times_w M_7^{G_2}(r,\theta_{1,2},\phi_{1,2},\psi,x^{10})]$ M-theory background (compactified on a seven-fold with G_2 structure) containing the fluxed ETW-hypersurface $M_{10}(x^1 = 0)$.
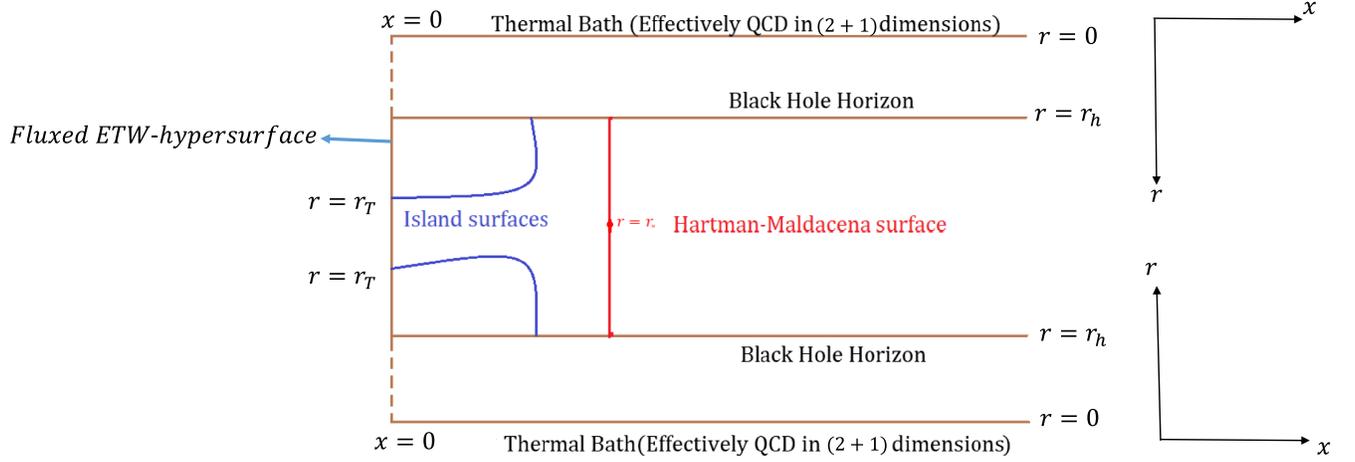
FIG. 2.   Doubly holographic setup in M-theory dual. ETW-black "brane" is coupled the thermal bath (at the tip of seven-fold of G_2-structure which is a cone over a warped non-Kähler resolved conifold), where the Hawking radiation is collected, which effectively is thermal QCD_{2+1} along $x^{1,2,3}$ after Wick-rotation along x^3 at $r = 0$. Blue curves correspond to the island surfaces and red curve corresponds to the Hartman-Maldacena-like surface.

The pictorial representation of the aforementioned ETW-brane(containing a black $M5$-brane)/$M2$-brane(supporting the nonconformal "bath"—QCD_{2+1})-setup focusing only on the $x^1 - r$-plane, along with the Hartmann-Maldacena-like surface and island surface, is given in Fig. 2. Unlike [12,13,17], the (nonconformal) bath is at $r = 0$ instead of the UV cutoff $r = r_{\rm UV}$.[4] In the high temperature $(T > T_c)$ M-theory dual (15), evidently $r \geq r_h$ [the metric component $g_{tt}^{\mathcal{M}}$ being proportional to a warp factor e^B where $B \sim \log\left(1 - \frac{r_h^4}{r^4} + \mathcal{O}\left(\frac{g_s M^2}{N}\right)\right)$ from the solutions to the supergravity EOM implies that for $B \in \mathbb{R}$, $r \geq r_h$ in the MQGP limit (4)].[5]

If $S(\mathcal{R})$ be the von Neumann entropy of subregion $\mathcal{R}$ defined on constant time slice in description 1 then

in the second description it will be given by the island-rule [12] as:

$$S(\mathcal{R}) = \min_{\mathcal{I}} \text{ext}_{\mathcal{I}} S_{\rm gen}(\mathcal{R} \cup \mathcal{I}), \tag{9}$$

where $\mathcal{I}$ is the island surface and generalized entropy functional is defined as [11]:

$$S_{\rm gen}(\mathcal{R} \cup \mathcal{I}) = \frac{A(\partial \mathcal{I})}{4G_N} + S_{\rm matter}(\mathcal{R} \cup \mathcal{I}). \tag{10}$$

As discussed earlier that in doubly holographic models we can calculate the generalized entropy functional defined in semiclassical geometry using classical Ryu-Takayanagi formula [7] in eleven dimensions in the third description as below:

$$S_{\rm gen}(\mathcal{R} \cup \mathcal{I}) = \frac{A(\gamma)}{4G_N^{(11)}}, \tag{11}$$

where $A(\gamma)$ is the area of the minimal surface, γ, which is a codimension two surface in the eleven dimensional bulk space-time. By following [18] we obtain the Page curve of a neutral black hole using (11) without higher derivative terms in Sec. IV from M-theory dual.

For higher derivative gravity theories we can calculate the entanglement entropy in the holographic dual theories from the results of [10]. Since we are working with M-theory dual therefore we can write the analogue of the generalized entropy functional defined in Eq. (11) using [10] as below:

$$S_{\rm gen}(\mathcal{R} \cup \mathcal{I}) = S_{\rm gravity}, \tag{12}$$

where

---

[4]The cutoff, unlike most references in the literature is not at infinity but is such that $r_{\rm UV} \lesssim L \equiv (4\pi g_s N)^{1/4}$ thereby justifying dropping the "1" in the 10-dimensional warp factor h in [4,34,36] [that appears in (15)], which otherwise would have been $1 + \frac{L^4}{r^4}\left[1 + \mathcal{O}\left(\frac{g_s M^2}{N}\right)\right]$.

[5]Further, as will be shown later, the area/entanglement entropy (inclusive of $\mathcal{O}(R^4)$ contributions) of the HM surface [see (48), (52), (86), (89) and (129)] as well as the IS [see (64), (65), (118), and (132)] are proportional to a positive power of M—the number of fractional $D3$-branes in the parent type IIB dual [34]. Now, the contribution to r integral from $r \in$ UV, i.e., $r > \sqrt{3}a \sim \left[1 + \mathcal{O}\left(\frac{\sqrt{\beta}}{N}\right) + \mathcal{O}\left(\frac{g_s M^2}{N}\right)\right]r_h \sim (1 + \epsilon)r_h, |\epsilon| \ll 1$ [41] will involve replacing M by $M^{\rm UV} \equiv M_{\rm eff}(r \in$ UV $\Leftrightarrow r > \sqrt{3}a)$—the UV-valued effective number of fractional $D3$-branes in the aforementioned parent type IIB dual—which is vanishing small [see the discussion beneath (3)] ensuring UV conformality. Therefore all integrals $\int_{r_* \text{ or } r_T}^{r_{\rm UV}}$ of integrands relevant to the HM/IS areas or entanglement entropies, will vanish as $r_{*,T} > r_h$ though being nearer to r_h than $\sqrt{3}a$.

$$S_{\text{gravity}} = \frac{S_{\text{EE}}}{4G_N^{(11)}}, \qquad (13)$$

where S_{EE} can be calculated using [10]. We will use Eq. (12) to obtain the Page curve from M-theory dual in the presence of higher derivative terms in Sec. V. The idea is that we need to calculate Eq. (12) for the Hartman-Maldacena-like surface which may produce a linear time growth of entanglement entropy of the Hawking radiation and for the island surface which dominates after the Page time. Combining these two contributions will generate the analog of the Page curve.

III. ETW-"BRANE" EMBEDDING

In the doubly-holographic approach, end of the world (ETW)-"brane" embedding is an important issue

related to the existence of islands. The issue is well understood at the level of Einstein gravity at LO (i.e., Einstein-Hilbert(EH) action and the boundary Gibbons-Hawking-York surface terms), but not much is known for higher derivative gravity, e.g., $D = 11$ supergravity at $\mathcal{O}(R^4)$; in top-down models such as the one considered by us, the ETW-"brane" would be a fluxed hypersurface $\mathcal{W}$.[6] We will now address this issue in this section as two subsections—in the first we will obtain the ETW embedding at the level of EH + GHY action, and in the second we will show that in the MQGP limit (4), the aforementioned LO embedding receives no corrections.

The $\mathcal{N} = 1$, $D = 11$ supergravity action without higher derivative terms is given by:

$$S = \frac{1}{2\kappa_{11}^2} \int_{M_{11}} \sqrt{-G^{\mathcal{M}}} \left[\mathcal{R} *_{11} \wedge 1 - \frac{1}{2} G_4 \wedge *_{11} G_4 - \frac{1}{6} C \wedge G \wedge G \right] + \frac{1}{\kappa_{11}^2} \int_{r=r_{\text{UV}}} d^{10}x \sqrt{h} K + \frac{1}{\kappa_{11}^2} \int_{\mathcal{W}} d^{10}x \sqrt{\gamma}(\mathcal{K} - 9T). \qquad (14)$$

γ, $\mathcal{K}$ and T in (14) are the induced metric, trace of extrinsic curvature ($\mathcal{K}_{mn}$) and tension of the ETW brane ($\mathcal{W}$: $\partial M_{11} = \{r = r_{\text{UV}}\} \cup \mathcal{W}$). Metric for the M-theory dual when $T > T_c$ on gauge theory side is given by:

$$ds_{11}^2 = e^{-\frac{2\phi^{\text{IIA}}}{3}} \left[\frac{1}{\sqrt{h(r, \theta_{1,2})}} \left(-g(r)dt^2 + (dx^1)^2 + (dx^2)^2 + (dx^3)^2 \right) \right.$$
$$\left. + \sqrt{h(r, \theta_{1,2})} \left(\frac{dr^2}{g(r)} + ds_{\text{IIA}}^2(r, \theta_{1,2}, \phi_{1,2}, \psi) \right) \right] + e^{\frac{4\phi^{\text{IIA}}}{3}} \left(dx^{11} + A_{\text{IIA}}^{F_1^{\text{IIB}} + F_3^{\text{IIB}} + F_5^{\text{IIB}}} \right)^2, \qquad (15)$$

where $A_{\text{IIA}}^{F_{i=1,3,5}^{\text{IIB}}}$ are the type IIA RR 1-forms obtained from the triple T/SYZ-dual of the type IIB $F_{1,3,5}^{\text{IIB}}$ fluxes in the type IIB holographic dual of [34], and $g(r) = 1 - \frac{r_h^4}{r^4}$. Near the $\psi = 2n\pi$, $n = 0, 1, 2$-coordinate patch, we can write the metric (15) in the following form (explicit form of the metric in terms of the parameters of the model can be read off from the appendix A of [9]):

$$ds^2 = \alpha(r)[-g(r)dt^2 + \sigma(r)dr^2 + dx_\mu dx^\mu] + g_{mn}dx^m dx^n, \qquad (16)$$

where x_μ ($\mu = 1, 2, 3$) represent spatial coordinates, r is the radial coordinate and x^m ($m = 5, 6, 7, 8, 9, 10$) represent six angular coordinates $(\theta_{1,2}, \phi_{1,2}, \psi, x^{10})$ in the conifold geometry. The volume of the compact six-fold can be obtained by the following equation:

$$\mathcal{V}_{\text{int}} = \int \prod_m dx^m \sqrt{-g}. \qquad (17)$$

On comparing Eqs. (15) and (16), we obtain:

$$\alpha(r, \theta_{1,2}) = \frac{e^{-\frac{2\phi^{\text{IIA}}}{3}}}{\sqrt{h(r, \theta_{1,2})}},$$
$$\sigma(r, \theta_{1,2}) = \frac{h(r, \theta_{1,2})}{g(r)}, \qquad (18)$$

where ϕ^{IIA} is the type IIA dilaton profile and can be defined as $G_{x_{10}x_{10}}^{\mathcal{M}} = e^{\frac{4\phi^{\text{IIA}}}{3}}$. For M-theory dual, the expressions for $\alpha(r, \theta_{1,2}), \sigma(r, \theta_{1,2}), H(r, \theta_{1,2}) \equiv \mathcal{V}_{\text{int}}^2(r, \theta_{1,2})\alpha(r, \theta_{1,2})^3$ can be easily read off from (15) and (18).

The ETW-"brane" $\mathcal{W}$: $AdS_4^\infty \times_w M_6$ with G_4 fluxes threading a homological sum of four-cycles $S^3 \times [0, 1]$ and $S^2 \times S^2$ in $M_6 = M_5(\theta_{1,2}, \phi_{1,2}, \psi) \times S^1(x^{10}) \hookrightarrow M_8^{SU(4)/\text{Spin}(7)}(t, r, \theta_{1,2}, \phi_{1,2}, \psi, x^{10})$ (in the large-N MQGP limit) implies: $\partial M_{11} = \{r = r_{\text{UV}}\} \cup \mathcal{W}$. Assuming the ETW-"brane" embedding,

---

[6]One of us (GY) would like to thank C. F. Uhlemann for a brief clarification on this point.

$$x^1 = x^1(r), \qquad (19)$$

and substituting the same into (16) yields:

$$ds^2 = \alpha(r)\left[-g(r)dt^2 + \left(\sigma(r) + \left(\frac{dx^1}{dr}\right)^2\right)dr^2 \right.$$
$$\left. + \sum_{\mu=2}^{3} dx_\mu dx^\mu\right] + g_{mn}dx^m dx^n. \qquad (20)$$

A. At $\mathcal{O}(\beta^0)$

Assuming T to be the tension of the ETW-"brane," and if $\mathcal{K}$ and $\mathcal{K}_{\tilde{m}\tilde{n}}$, $\tilde{m}, \tilde{n} = r, t, \mu, m$ are respectively the extrinsic curvature scalar and tensor on the ETW-brane, then [67],

$$\mathcal{K}_{mn} - \mathcal{K}h_{mn} = -9Th_{mn}, \qquad (21)$$

where h_{mn} is the induced metric on the ETW-brane. Let us look at the rr-component of (21) in the IR. One can argue that in the IR, the embedding function $x^1(r) = x(r)$ always appears as $x'(r)$, $x''(r)$ in (21), and writing $a = (b + \mathcal{O}(\frac{g_s M^2}{N}))r_h$ [47], the terms LO and NLO in N and

$$\mathcal{K}(N, g_s; r_h) \sim -\kappa_K \frac{(3b^2 - 1)\sqrt{r_h}(\log N - 9\log(r_h))}{\sqrt[4]{g_s}\sqrt[4]{N}\sqrt{r - r_h}((3b^2 - 1)\log N + 9\log(r_h))\sqrt[3]{N_f}(\log N - 3\log(r_h))}$$

$$\mathcal{K}_{rr}(N, M, N_f, g_s; r_h; x'(r); x''(r)) \sim -\kappa_{K_{rr}}^{(1)} \frac{\sqrt{g_s N}\Sigma(r_h; N, N_f)}{r_h(r - r_h)^2} + \kappa_{K_{rr}}^{(2)} \frac{g_s{}^3 M^2 N_f \log(r_h)(\log N - 12\log(r_h))\Sigma(r_h; N, N_f)}{r_h{}^2\sqrt{g_s N}(r - r_h)^2}$$

$$+ \kappa_{K_{rr}}^{(3)} \frac{r_h x'(r)\Sigma(r_h; N, N_f)}{\sqrt{g_s N}} + \kappa_{K_{rr}}^{(4)} \frac{r_h{}^2 x''(r)\Sigma(r_h; N, N_f)}{\sqrt{g_s N}},$$

$$h_{rr}(N, M, N_f, g_s; r_h; x'(r)) \sim -2\kappa_{K_{rr}}^{(1)} \frac{\sqrt{g_s N}\Sigma(r_h; N, N_f)}{r_h(r - r_h)} - \kappa_{K_{rr}}^{(3)} \frac{r_h{}^2 x'(r)\Sigma(r_h; N, N_f)}{\sqrt{g_s N}}$$

$$- 2\kappa_{K_{rr}}^{(2)} \frac{3g_s{}^3 M^2 N_f \log(r_h)(\log N - 12\log(r_h))\Sigma(r_h; N, N_f)}{r_h\sqrt{g_s N}(r - r_h)}, \qquad (22)$$

wherein $\Sigma(r_h; N, N_f) \equiv (6\log NN_f - 3N_f\log(9a^2 r_h{}^4 + r_h{}^6))^{2/3}$ the numerical pre-factors are respectively collected in $\kappa_K, \kappa_{K_{rr}}^{(i=1,2,3,4)}$. As $b = \frac{1}{\sqrt{3}} + \epsilon$, (e.g., in the $\psi = 2n\pi, n = 0, 1, 2$-coordinate patches, $|\epsilon| \sim r_h^2$ $(|\log r_h|)^{9/2}N^{-9/10-\alpha_b}$, $\alpha_b > 0$ [4]), one can approximate (21) by $K_{mn} \sim -9Th_{mn}$. Looking then at $m = n = r$ component of the same, one notes that unlike $\mathcal{K}_{rr}(N, M, N_f, g_s; r_h; x'(r); x''(r))$, $h_{rr}(N, M, N_f, g_s; r_h; x'(r))$ does not have an $x''(r)$ term. Therefore,

$$x''(r) = 0. \qquad (23)$$

Further, we note that the LO-in-N terms in the IR $(r = \mathcal{O}(1)r_h$ of$)$ $\mathcal{K}_{rr}(N, M, N_f, g_s; r_h; x'(r); x''(r))$ are proportional to $h_{rr}(N, M, N_f, g_s; r_h; x'(r))$ with a proportionality constant -2 resulting in the ETW-brane tension

$$T \sim \frac{1}{r_h}. \qquad (24)$$

But, at NLO in N, the coefficients of the same are proportional to each other but with a proportionality constant that is -1. These two can be reconciled by $x'(r) = 0$, i.e.,

$$x^1(r) = \text{constant}, \qquad (25)$$

and we take the constant to be zero.

B. No boundary terms generated at $\mathcal{O}(R^4)$

Eleven dimensional supergravity action including $\mathcal{O}(R^4)$ terms is given by:

$$S = \frac{1}{2\kappa_{11}^2}\int_{M_{11}} \sqrt{-G^{\mathcal{M}}}\left[\mathcal{R} *_{11} 1 - \frac{1}{2}G_4 \wedge *_{11}G_4 - \frac{1}{6}C \wedge G \wedge G\right] + \frac{1}{\kappa_{11}^2}\int_{r=r_{\text{UV}}} d^{10}x\sqrt{h}K$$

$$+ \frac{1}{(2\pi)^4 3^2 2^{13}}\left(\frac{2\pi^2}{\kappa_{11}^2}\right)^{\frac{1}{3}}\int_{M_{11}} d^{11}x\sqrt{-G^{\mathcal{M}}}\left(J_0 - \frac{1}{2}E_8\right) + \left(\frac{2\pi^2}{\kappa_{11}^2}\right)\int C_3 \wedge X_8 + \frac{1}{\kappa_{11}^2}\int_{\mathcal{W}} d^{10}x\sqrt{\gamma}(\mathcal{K} - 9T), \qquad (26)$$

where:

$$J_0 = 3 \times 2^8 \left(R^{HMNK} R_{PMNQ} R_H{}^{RSP} R^Q{}_{RSK} + \frac{1}{2} R^{HKMN} R_{PQMN} R_H{}^{RSP} R^Q{}_{RSK} \right)$$

$$E_8 = \frac{1}{3!} \epsilon^{ABCM_1 N_1 \dots M_4 N_4} \epsilon_{ABCM'_1 N'_1 \dots M'_4 N'_4} R^{M'_1 N'_1}{}_{M_1 N_1} \dots R^{M'_4 N'_4}{}_{M_4 N_4},$$

$$\kappa_{11}^2 = \frac{(2\pi)^8 l_p^9}{2}; \tag{27}$$

κ_{11}^2 being related to the eleven-dimensional Newtonian coupling constant, and $G = dC$ with C being the $\mathcal{M}$-theory three-form potential with the four-form G being the associated four-form field strength. Givent the hierarchy $|t_8^2 G^2 R^3| < |E_8| < |J_0|$ [4] in the MQGP limit (4), we will only work with J_0; γ, $\mathcal{K}$ and T in (26) are defined earlier.

From [4],

$$\delta J_0 \sim -\delta g_{\tilde{M}\tilde{N}} \left[g^{M\tilde{M}} R^{H\tilde{N}NK} + g^{N\tilde{N}} R^{HM\tilde{M}K} + g^{K\tilde{M}} R^{HMN\tilde{N}} \right] \tilde{\chi}_{HMNK}$$

$$- \frac{1}{2} \left[g^{H\tilde{H}} \left(D_{[N_1} \left(D_{K_1]} \delta g_{M_1 \tilde{H}} + D_{M_1} \delta g_{|K_1|\tilde{H}} - D_{\tilde{H}} \delta g_{|K_1|M_1} \right) \right) \chi_H{}^{M_1 N_1 K_1} \right], \tag{28}$$

where,

$$\tilde{\chi}_{HMNK} \equiv R_{PMNQ} R_H{}^{RSP} R^Q{}_{RSK} - \frac{1}{2} R_{PQKN} R_H{}^{RSP} R^Q{}_{RSM};$$

$$\chi_H{}^{M_1 N_1 K_1} \equiv R_P{}^{M_1 N_1}{}_Q R_H{}^{RSP} R^Q{}_{RS}{}^{K_1}$$

$$- \frac{1}{2} R_{PQ}{}^{M_1 N_1} R_H{}^{RSP} R^Q{}_{RS}{}^{K_1}. \tag{29}$$

We thus see that a typical boundary term involving covariant derivatives of the metric variations that one would need to cancel out by an appropriate boundary term (using Stokes theorem) is

$$\int_{\mathcal{W}} D_{[K_1|} \delta g_{M_1 \tilde{H}} \chi^{\tilde{H}M_1[N_1 K_1]} d\Sigma_{|N_1]}$$

$$= \int_{\mathcal{W}} D_{[K_1|} \delta g_{M_1 \tilde{H}} \chi^{\tilde{H}M_1[N_1 K_1]} \eta_{|N_1]} \sqrt{-h} d^{10} y. \tag{30}$$

The (dual to the) unit normal vector to $\mathcal{W}$ given by:

$$\eta_M = (\eta_r, \eta_x, \eta_{M \neq r,x}) = \frac{\left(-\frac{dx^1(r)}{dr} \sqrt{G_{\mathcal{M}}^{rr}}, \sqrt{G_{\mathcal{M}}^{x^1 x^1}}, \mathbf{0} \right)}{\sqrt{(G_{\mathcal{M}}^{xx})^2 + (G_{\mathcal{M}}^{rr})^2 \left(\frac{dx^1(r)}{dr} \right)^2}}. \tag{31}$$

Therefore,

$$\eta_M |_{x^1(r) = \text{constant}} = \left(0, \sqrt{G_{\mathcal{M}}^{xx}}, \mathbf{0} \right). \tag{32}$$

What we will now show that the ETW embedding (25) continues to hold even with the inclusion of $\mathcal{O}(l_p^6)$ corrections. From (32), one sees that one will be required to consider $\chi^{HM[x^1 N]}$. Using that the only linearly independent nonvanishing Riemann curvature tensor for the metric (16) with one index along x^1 is $R_{x^1 t x^1 t}$, and (29), one obtains:

$$\chi^{tx^1 tx^1} = \frac{1}{2} (g_{x^1 x^1}^{\mathcal{M}})^2 (R_t{}^{x^1 x^1 t})^2 R^{tx^1 x^1 t}. \tag{33}$$

[7]We therefore see from (30) $(\chi^{ttx^1 t} = \chi^{x^1 x^1 x^1 t} = 0)$:

[7]Using

$$R_t^{x^1 x^1 t} \sim -\frac{(9a^2 + r_h^2)}{N_f r_h^2 (6a^2 + r_h^2)(\log N - 3 \log(r_h)) \sqrt[3]{\frac{12\pi}{g_s} + 3 \log N N_f - 9 N_f \log(r_h)}};$$

$$R^{tx^1 tx^1} \sim \frac{(9a^2 (g_s \log N N_f + 4\pi) - 3 g_s N_f (9a^2 + r_h^2) \log(r_h) + g_s \log N N_f r_h^2)}{\sqrt{g_s} N_f^3 r_h^3 (6a^2 + r_h^2)(r - r_h)(\log N - 3 \log(r_h))^3}.$$

We therefore see that up to LO in N and $\log N$, $|\log r_h|$, and in the IR (near $r = r_h$)

$$\beta \chi^{tx^1 tx^1} |_{x^1 = \text{constant}} \sim \frac{\beta}{N} \frac{1}{\sqrt{g_s} N_f^{25/3} r_h^3 (r - r_h)(\log N - 3|\log r_h|)^{10/3}}.$$

$$\int_{\mathcal{W}} D_{[K_1|}\delta g^{\mathcal{M}}_{M_1\tilde{H}}\chi^{\tilde{H}M_1[N_1K_1]}d\Sigma_{|N_1]}\Big|_{x^1=\text{constant}}$$
$$\sim \int_{\mathcal{W}} D_t \delta g^{\mathcal{M}}_{x^1 t}\chi^{tx^1[x^1 t]}\eta_{x^1}\sqrt{-h}d^{10}y. \quad (34)$$

Now, $g^{\mathcal{M}}_{x^1 t} = 0$. We therefore see that restricted to $x^1 = $ constant, there is no surface term generated if one chooses $\delta g^{\mathcal{M}}_{x^1 t} = 0$—we will assume to do so in the rest of the paper.

IV. PAGE CURVE WITHOUT HIGHER DERIVATIVE TERMS

To obtain the page curve we are required to calculate the entanglement entropy contribution from Hartman-Maldacena-like surface and island surface and then we have to see behavior of these entropies as function of time.

In this section we are going to perform this analysis in a M-theory uplift of type IIB setup [34] without inclusion of higher derivative terms in eleven dimensional supergravity action, i.e., up to $\mathcal{O}(\beta^0)$ term (14), which is holographic dual of thermal QCD-like theories in four dimensions at finite coupling. We are following [18] to obtain the Page curve of an eternal black hole by computing areas of the Hartman-Maldacena-like and Island surfaces. We are considering the doubly holographic setup as discussed in Sec. II. We are collecting the radiation of a black hole in a bath (which is effectively a thermal QCD-like theories in $2 + 1$D). In this setup we have two kinds of extremal surfaces- Hartman-Maldacena-like surface and island surface. In Sec. IV A we will calculate entanglement entropy contribution from Hartman-Maldacena-like surface and in Sec. IV B we will calculate entanglement entropy contribution from island surface. We will obtain the Page curve of an eternal neutral black hole in the absence of higher derivative terms in Sec. IV C by combining the entanglement entropies of Hartman-Maldacena-like and island surfaces.

A. Entanglement entropy contribution from Hartman-Maldacena-like surface

In this subsection we are going to compute the entanglement entropy of the Hartman-Maldacena-like surface by computing area of the codimension two surface in the bulk similar to [18].

To compute the time dependent entanglement entropy of Hartman-Maldacena-like surface, we consider induced metric on constant x^1 slice and can be obtained from Eq. (16) as below:

$$ds^2|_{x^1=x_R} = \alpha(r)[(-g(r)\dot{t}(r)^2 + \sigma(r))dr^2 + (dx^2)^2 + (dx^3)^2] + g_{mn}dx^m dx^n. \quad (35)$$

Area density functional of Hartman-Maldacena-like Surface can be obtained from Eq. (35) as:

$$\mathcal{A}_{\text{HM}}(t_b) = \frac{A}{\mathcal{V}_2} = \int dt \sqrt{(-g(r)H(r) + \sigma(r)H(r)\dot{r}(t)^2)}$$
$$\equiv \int dt \mathcal{L}, \quad (36)$$

where $H(r) = \mathcal{V}^2_{\text{int}}\alpha(r)^3$ and $\mathcal{V}_2 = \int\int dx^2 dx^3$. Due to absence of explicit t dependence in the Lagrangian, we have constant of motion E (which is the energy of the minimal surface):

$$E = \frac{\partial \mathcal{L}}{\partial \dot{r}(t)}\dot{r}(t) - \mathcal{L}, \quad (37)$$

where $\dot{r}(t) = \frac{dr(t)}{dt}$. Therefore using Eq. (36) we can simplify the above equation as,

$$E = \frac{g(r)H(r)}{\sqrt{(-g(r)H(r) + \sigma(r)H(r)\dot{r}(t)^2)}}. \quad (38)$$

On solving the above equation for $\dot{r}(t)$, we get:

$$\dot{r}(t) = \pm\sqrt{\left(\frac{g(r)}{\sigma(r)}\left(1 + \frac{g(r)H(r)}{E^2}\right)\right)} \quad (39)$$

If there is a surface at $r = r^*$ at which,

$$\dot{r}(t)|_{r=r^*} = 0 \quad (40)$$

Then Eq. (39) will be simplified as,

$$\frac{g(r^*)}{\sigma(r^*)}\left(1 + \frac{g(r^*)H(r^*)}{E^2}\right) = 0. \quad (41)$$

From the above equation we get:

$$E^2 = -g(r^*)H(r^*), \quad (42)$$

r^* is the maximum value of r for a surface with energy E. In the full geometry Hartman-Maldacena-like surface can be viewed as a surface which starts at $x^1 = x_\mathcal{R}$ reaches up to r^* and then goes to its thermofield double partner. Equation (36) can be rewritten as:

$$\mathcal{A}_{\text{HM}}(t_b) = \int dr \sqrt{-\frac{g(r)H(r)}{\dot{r}(t)^2} + \sigma(r)H(r)}. \quad (43)$$

From Eqs. (39) and (43), we get:

$$\mathcal{A}_{\text{HM}}(t_b) = 2\int_{r_h}^{r^*} dr \frac{\sqrt{\sigma(r)g(r)}H(r)}{E\sqrt{\left(1 + \frac{g(r)H(r)}{E^2}\right)}}. \quad (44)$$

Let us define time using the following integral:

$$\int_{r_h}^{r^*} \frac{dr}{\dot{r}(t)} = t_* - t_b, \tag{45}$$

where $t_* = t(r^*)$ and t_b is the boundary time at $r = r_h$. From Eqs. (39) and (45) we obtain the boundary time in terms of energy as:

$$t_b = -P \int_{r_h}^{r^*} \frac{dr}{\sqrt{\frac{g(r)}{\sigma(r)} \left(1 + \frac{g(r)H(r)}{E^2}\right)}}. \tag{46}$$

Therefore entanglement entropy of the Hartman-Maldacena-like surface is

$$\mathcal{S}_{\mathrm{HM}}(t_b) = \frac{\mathcal{A}_{\mathrm{HM}}(t_b)}{4G_N^{(11)}}. \tag{47}$$

1. Hartman-Maldacena-like surface analytics/numerics

The area of the Hartman-Maldacena-like surface after integrating out the angular coordinates and therefore incorporating a $(2\pi)^4$ arising from integration with respect to $\phi_{1,2}, \psi, x^{10}$, and is thus given as:

$$A_{\mathrm{HM}} \sim (2\pi)^4 \int_{r_h}^{r^*} dr (\pi^9 E M^2 \sqrt[10]{N} \log^2(2)(\log(64) - 1)^2 N_f^4 g_s^{9/4} \log^2(r)(\log(N) - 3\log(r))^4$$
$$\times (N_f g_s (r^2(2\log(N) - 18\log(r) + 3) - 2r_h^2(\log(N) - 54r\log(r))) + 8\pi r_h^2)^2). \tag{48}$$

Assuming $|\log r_h| \gg \log N$ [68] in (A4), one obtains:

$$A_{\mathrm{HM}} \sim \mathcal{O}(1) \times 10^5 M^2 \sqrt[10]{N} N_f^6 g_s^{17/4} r_h^4 (r_* - r_h) \log^4(r_h)(\log(N) - 3\log(r_h))^4. \tag{49}$$

Now, t_b is given by the principal value of the following integral:

$$t_b \sim \mathcal{P} \int_{r_h}^{r^*} dr \left(\frac{E^2 \sqrt{N} r^2 \sqrt{g_s} (N_f g_s (r^2(2\log(N) - 18\log(r) + 3) - 2r_h^2(\log(N) - 54r\log(r))) + 8\pi r_h^2)^2}{(r^4 - r_h^4)(N_f g_s((2r^2 - 6a^2)\log(N) + 3r(108a^2\log(r) + r - 6r\log(r))) + 24\pi a^2)^2} \right)$$

$$\sim \lim_{\epsilon_1 \to 0} \left[4\pi^{33/2} E^2 \sqrt{g_s} \sqrt{N} \left(\frac{\log(r_h - r)}{4r_h} - \frac{\log(r + r_h)}{4r_h} + \frac{\tan^{-1}\left(\frac{r}{r_h}\right)}{2r_h} \right) \right]_{r=r_h+\epsilon_1}^{r=r_*}$$

$$- \frac{E^2 \sqrt{g_s} \sqrt{N}(\log(-\epsilon) - \log(r_h - r_*))}{r_h} + \frac{\pi^{33/2} E^2 \sqrt{g_s} \sqrt{N}(r_* - r_h)}{2r_h^2} + \mathcal{O}((r_* - r_h)^2). \tag{50}$$

The principal value requires: $r_* = r_h + \epsilon_1$. Writing $a = \left(\frac{1}{\sqrt{3}} + \epsilon\right)r_h$, up to leading order in ϵ, one obtains:

$$t_b = \frac{E^2 \pi^{33/2} \sqrt{N} \sqrt{g_s}(r_* - r_h)}{2r_h^2}. \tag{51}$$

Writing $\epsilon_1 = \tilde{\epsilon}_1 r_h$, one sees that for (i) $\tilde{\epsilon}_1 \sim 0.5$, one will have to include terms up to $\mathcal{O}(\tilde{\epsilon}_1^2)$ in t_b, (ii) $\tilde{\epsilon}_1 \sim \frac{1}{\sqrt{2}}$,

one will have to include terms up to $\mathcal{O}(\tilde{\epsilon}_1^3)$ in t_b, (iii) $\tilde{\epsilon}_1 \sim 1$, one will have to include terms up to $\mathcal{O}(\tilde{\epsilon}_1^4)$ in t_b, and (iv) $\tilde{\epsilon}_1 \sim \sqrt{5}$, one will have to include terms up to $\mathcal{O}(\tilde{\epsilon}_1^5)$ in t_b. We see that up to the Page time, $\tilde{\epsilon}_1 \ll 1$ and therefore one is justified in retaining terms only linear in $\tilde{\epsilon}_1$ as in (51).

From Eqs. (49) and (51), one obtains the entanglement entropy corresponding to Hartman-Maldacena-like surface as:

$$S_{\mathrm{HM}}^{\beta^0} = \frac{A_{\mathrm{HM}}}{4G_N^{(11)}} \sim \frac{\mathcal{O}(1) \times 10^{-4} M^2 N_f^6 g_s^{15/4} r_h^6 \log^4(r_h)(\log(N) - 3\log(r_h))^4}{E^2 G_N^{(11)} N^{2/5}} t_b. \tag{52}$$

We therefore obtain a linear growth of the entanglement entropy corresponding to Hartman-Maldacena-like surface

B. Entanglement entropy contribution from island surface

In this subsection we compute the entanglement entropy corresponding to the island surface by computing area of the codimension two surface in the bulk by following [18]. Embedding for the island surface is $x(r)$.

To compute the entanglement entropy of island surface we consider constant t slice. Therefore using Eq. (16), we can write induced metric of the island surface in the following form:

$$ds^2|_{\text{constt-time}} = \alpha(r)[(\sigma(r) + \dot{x}(r)^2)dr^2 + (dx^2)^2 + (dx^3)^2] + g_{mn}dx^m dx^n, \tag{53}$$

here we have represented $x^1(r)$ by $x(r)$ and $\dot{x}(r) \equiv \frac{dx(r)}{dr}$. Now we can calculate area density functional of the island surface as given below:

$$\mathcal{A}_{\text{IS}} = \frac{A}{\mathcal{V}_2} = \int dr\sqrt{(H(r)\sigma(r) + H(r)\dot{x}(r)^2)} \equiv \int dr\mathcal{L}, \tag{54}$$

where,

$$H(r) = \mathcal{V}_{\text{int}}^2\alpha(r)^3. \tag{55}$$

Since $x(r)$ is cyclic coordinate therefore conjugate momentum corresponding to $x(r)$, i.e., $p_{x(r)} = \frac{\partial \mathcal{L}}{\partial \dot{x}(r)}$ is constant of motion:

$$p_{x(r)} = \mathcal{C}, \tag{56}$$

where $\mathcal{C}$ is a constant. Using Eq. (54) we simplify the Eq. (56) as

$$\frac{H(r)\dot{x}(r)}{\mathcal{L}} = \mathcal{C}. \tag{57}$$

On solving the above equation for $\dot{x}(r)$, we obtained:

$$\dot{x}(r) = \pm\mathcal{C}\sqrt{\frac{\sigma(r)}{H(r) - \mathcal{C}^2\sigma(r)}} \tag{58}$$

Let us assume that there is a turn around point at $r = r_T$ at which island surface satisfies following condition:

$$\left(\frac{dr}{dx}\right)_{r=r_T} = 0. \tag{59}$$

From Eqs. (58) and (59), constant $\mathcal{C}$ can be obtained which is given below:

$$\mathcal{C} = \pm\sqrt{\frac{H(r_T)}{\sigma(r_T)}}. \tag{60}$$

Using the aforementioned value of $\mathcal{C}$, Eq. (57) simplifies to the following form:

$$\frac{dx(r)}{dr} = \pm\sqrt{\frac{H(r_T)\sigma(r_T)}{H(r)\sigma(r_T) - H(r_T)\sigma(r)}}. \tag{61}$$

Now from Eqs. (54) and (61) area density functional of the island surface simplifies as,

$$\mathcal{A}_{\text{IS}} = 2\int_{r_h}^{r_T}\sqrt{H(r)\sigma(r) + \frac{H(r)H(r_T)\sigma(r)}{H(r)\sigma(r_T) - H(r_T)\sigma(r)}}. \tag{62}$$

Therfore entanglement entropy contribution from the island surface is:

$$S_{\text{IS}} = \frac{\mathcal{A}_{\text{IS}}}{4G_N^{(11)}} \tag{63}$$

From the above equation it is clear that entanglement entropy contribution from island surface is independent of time. Therefore entropy contribution to the Hawking-radiation from island surface will be constant all the time.

1. Island surface analytics

The entanglement entropy upon evaluation of (62) yields:

$$\mathcal{A}_{\mathcal{IS}} = \int_{r_h}^{r_T}\left(\frac{2\sqrt{2}\pi MN^{3/10}rN_f^2g_s^{11/8}\log(r)(\log(N) - 3\log(r))^2}{\sqrt{r^4 - r_h^4}}\right.$$
$$\left. \times (N_fg_s(r^2(2\log(N) - 18\log(r) + 3) - 2r_h^2(\log(N) - 54r\log(r))) + 8\pi r_h^2)\right), \tag{64}$$

which hence obtains:

$$\mathcal{S}_{\text{IS}} \sim \frac{1}{4G_N^{(11)}} \left[MN^{3/10} N_f^3 g_s^{19/8} \log(r_h)(\log(N) - 3\log(r_h))^2 \left(216 r_h \tilde{r}_T \log(r_h)_2 F_1 \left(-\frac{1}{4}, \frac{1}{2}; \frac{3}{4}; \frac{1}{\tilde{r}_T^4} \right) \right. \right.$$
$$\left. \left. - r_h \left(\log(N) \left(2\log \left(\sqrt{1 - \frac{1}{\tilde{r}_T^4}} + 1 \right) - \log \left(\frac{1}{\tilde{r}_T^4} \right) \right) + \sqrt{\tilde{r}_T^4 - 1} (18\log(r_h) - 2\log(N) - 3) + 73\sqrt{\pi} r_h \log(r_h) \right) \right) \right],$$

(65)

where $\tilde{r}_T \equiv \frac{r_T}{r_h} > 1$; r_T is estimated in (A5)–(A7) (and the text containing the same).

C. Page curve at $\mathcal{O}(\beta^0)$ from areas of Hartman-Maldacena-like and island surfaces

In this subsection we will obtain the Page curve of an eternal neutral black hole in the absence of higher derivative terms in the eleven dimensional supergravity action, explicitly by using the results of previous two subsections.

From (52), for the aforementioned values of g_s, M, N_f, N, r_h, $S_{\text{EE}}^{\text{HM}} = \frac{5 \times 10^{-4} t_b}{E^2}$, and from Eq. (65) we see that entanglement entropy contribution of the island surface is independent of time, and for the aforementioned values, is given by 421. This contribution dominates after the Page time. As we saw in Sec. IV A that entanglement entropy of the Hartman-Maldacena-like surface has linear time dependence therefore when we combine both the contributions then we will find that initially entanglement entropy of the Hawking radiation will increase with
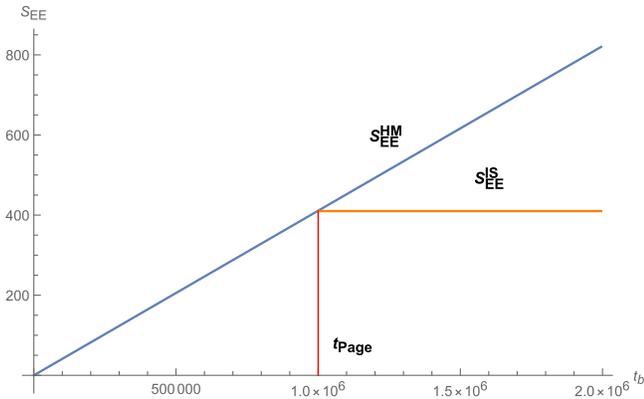
FIG. 3. Page curve up to $\mathcal{O}(\beta^0)$ of an eternal black hole from doubly holographic setup in M-theory dual. Blue line in the graph corresponds to the entanglement entropy contribution from the Hartman-Maldacena-like surface's area, and orange line corresponds to the entanglement entropy contribution from the island surface's area; E in (52) is set to be 1.1 to get the same order of magnitude of t_{Page} as in Fig. 8.

boundary time then after the Page time it is the island surface contribution that dominates therefore entanglement entropy will stop increasing and reach a constant value. Therefore we will obtain the Page curve of an eternal black hole in the absence of higher derivative terms from a doubly holographic setup where gravity dual is M-theory. The same is plotted in Fig. 3. The Page time is given by: $t_{\text{Page}} = 8.5 \times 10^5 E^2$. To obtain the same t_{Page} after inclusion of $\mathcal{O}(\beta)$ "anomaly terms" as will be obtained in V D, $E = 1.1$. With this t_{Page}, one sees that $\tilde{\epsilon}_1 \sim 10^{-5} \ll 1$, as stated beneath (51). We have also plotted the Page curve in Sec. V in Fig. 7 where we have done our calculations in the presence of higher derivative terms.

V. PAGE CURVE WITH HIGHER DERIVATIVE TERMS

In this section we are going to obtain the Page curve of a neutral black hole in the presence of higher derivative terms which are quartic in Riemann curvature tensor. We have divided this section into four subsections. In Sec. V A, we will compute the entanglement entropy of the HM-like surface, in Sec. V B, we will discuss the "Swiss-cheese" structure of the same, in Sec. V C, we will compute the entanglement entropy of the island surface and then finally in Sec. V D, we will obtain the Page curve of an eternal black hole using the results obtained in previous subsections.

We will perform the same analysis as we did in previous section. In the presence of higher derivative terms we will compute entanglement entropy of Hartman-Maldacena-like surface and island surface using [10].

Holographic entanglement entropy in general higher derivative gravity theories can be calculated using the following formula in $\text{AdS}_{d+2}/\text{CFT}_{d+1}$ correspondence [10]:

$$S_{EE} = \int d^d y \sqrt{-g} \left[\frac{\partial \mathcal{L}}{\partial R_{z\bar{z}z\bar{z}}} + \sum_\alpha \left(\frac{\partial^2 \mathcal{L}}{\partial R_{zizj} \partial R_{\bar{z}m\bar{z}l}} \right)_\alpha \frac{8 K_{zij} K_{\bar{z}ml}}{(q_\alpha + 1)} \right], \quad (66)$$

where g is the determinant of the induced metric on codimension two surface, (a, b) are along the normal directions, (i, j, k, l) are along tangential directions, $K_{zij} = \frac{1}{2} \partial_z G_{ij}$ and its trace is defined as $K_z = K_{zij} G^{ij}$. First term in the above equation is Wald entanglement entropy and to calculate the second term one is required to go through the following steps:

(i) Label each term as α after differentiating twice the Lagrangian with respect to Riemann tensor.

(ii) Do the following transformations of the specific components of Riemann tensors in each term.

$$
\begin{aligned}
R_{abij} &= r_{abij} + g^{ml}(K_{ajm}K_{bil} - K_{aim}K_{bjl}) \\
R_{aibj} &= r_{aibj} + g^{ml}K_{ajm}K_{bil} - Q_{abij} \\
R_{ijml} &= r_{ijml} + g^{ab}(K_{ail}K_{bjm} - K_{aij}K_{bml}),
\end{aligned} \tag{67}
$$

where $Q_{abij} = \partial_a K_{bij}$.

(iii) In the αth term, let number of Q_{aaij} and Q_{bbij} be γ and number of K_{aij}, R_{abci}, and R_{aijk} be δ. Then q_α for the αth term is defined as:

$$
q_\alpha = \gamma + \frac{\delta}{2}. \tag{68}
$$

(iv) By using Eq. (67) one can then obtain values of r_{abij}, r_{aibj}, r_{ijml} and then substitute back in Eq. (66). By doing so we will obtain the entanglement entropy expression in terms of original Riemann tensors, i.e., in terms of R_{abij}, R_{aibj} etc.

Let us outline that how we can calculate the holographic entanglement entropy (66) in general higher derivative gravity theories:

(i) If holographic dual is $(d + 1)$ dimensional gravitational background then obtain the induced metric for the codimension two surface, i.e., in $(d - 1)$ dimensions in terms of the embedding function.

(ii) Calculate (66) for the aforementioned induced metric. By doing so we will obtain the holographic entanglement entropy in terms of embedding function and its derivatives.

(iii) Work out the equation of motion of the embedding function and find its solution.

(iv) Substituting the solution obtained in previous step into the action will give the holographic entanglement entropy in higher derivative gravity theories.

Contribution from J_0 term:

We obtain the four terms from Wald entanglement entropy formula, i.e., $\frac{\partial J_0}{\partial R_{z\bar{z}z\bar{z}}}$ for both the extremal surfaces. which are listed in appendix D 1 for Hartman-Maldacena-like surface and in D 2 for the island surface.

$$
\frac{\partial J_0}{\partial R_{z\bar{z}z\bar{z}}} = -4x^2 \left(\frac{\partial J_0}{\partial R_{txtx}} \right). \tag{69}
$$

To calculate the second term in Eq. (66), we are required to calculate the four kinds of differentiations for Hartman-Maldacena-like and island surfaces as given below:

$$
\left(\frac{\partial^2 J_0}{\partial R_{zizj} \partial R_{\bar{z}m\bar{z}l}} \right) K_{zij} K_{\bar{z}ml} = \left(\frac{\partial^2 J_0}{\partial R_{xixj} \partial R_{xmxl}} + x^4 \frac{\partial^2 J_0}{\partial R_{titj} \partial R_{tmtl}} - 2x^2 \frac{\partial^2 J_0}{\partial R_{titj} \partial R_{xmxl}} + 4x^2 \frac{\partial^2 J_0}{\partial R_{tixj} \partial R_{xmtl}} \right)
$$
$$
\times \left(\frac{1}{x^2} K_{tij} K_{tml} + K_{xij} K_{xml} - \frac{i}{x} K_{tij} K_{xml} + \frac{i}{x} K_{xij} K_{tml} \right), \tag{70}
$$

Coefficient appearing in the numerator and denominators of the above equation is $x = x_R$ for Hartman-Maldacena-like surface and $x = x(r)$ for the island surface. We have calculated and listed all four kinds of differentiations appearing in Eq. (70) for Hartman-Maldacena-like surface in appendix D 1 and for the island surface in appendix D 2.

A. Entanglement entropy contribution from Hartman-Maldacena-like surface

In this subsection we will be calculating the entanglement entropy corresponding to the Hartman-Maldacena-like surface using Dong's formula (66).

In M-theory dual, Hartman-Maldacena-like surface is a codimension two surface which is located at $x^1 = x_R$.

Therefore using Eq. (66) we can write expression for the entanglement entropy for Hartman-Maldacena-like surface in the following form:

$$
S_{EE} = \int dr dx^2 dx^3 d\theta_1 d\theta_2 dx dy dz dx^{10}
$$
$$
\times \sqrt{-g} \left[\frac{\partial \mathcal{L}}{\partial R_{z\bar{z}z\bar{z}}} + \sum_\alpha \left(\frac{\partial^2 \mathcal{L}}{\partial R_{zizj} \partial R_{\bar{z}m\bar{z}l}} \right)_\alpha \frac{8 K_{zij} K_{\bar{z}ml}}{(q_\alpha + 1)} \right], \tag{71}
$$

where g is the determinant of the induced metric (35) on the codimension two surface.

Contribution from $\mathcal{O}(\beta^0)$ action: For the metric (35) first term in Eq. (71) simplifies to the following form for the

$\mathcal{O}(\beta^0)$ term in action (26):

$$\int d\mathcal{V}_9 \sqrt{-g}\left(\frac{\partial R}{\partial R_{z\bar{z}z\bar{z}}}\right) = \int d\mathcal{V}_9 \mathcal{L}_0^{\rm HM} \sim \int dr \left(x_R^2 \lambda(r) \sqrt{\alpha(r)\left(\sigma(r) - \left(1 - \frac{r_h^4}{r^4}\right)t'(r)^2\right)} \right), \tag{72}$$

where x_R is constant and $\alpha(r)$, $\sigma(r)$, $\lambda(r)$ are given in (B1).

Contribution from $\mathcal{O}(\beta)$ term: At $\mathcal{O}(\beta)$, one is required to calculate two type of terms, first one is Wald entanglement entropy term and the second one is the anomaly term.

Wald entanglement entropy term, i.e., $\left(\frac{\partial J_0}{\partial R_{z\bar{z}z\bar{z}}}\right)$:

For a Hartman-Maldacena-like surface, we obtain:

$$\frac{\partial J_0}{\partial R_{z\bar{z}z\bar{z}}} = -4x_R^2 \frac{\partial J_0}{\partial R_{txtx}}. \tag{73}$$

Out of four terms that we have listed for $\frac{\partial J_0}{\partial R_{txtx}}$ in appendix D 1, most dominant terms that contribute to the Lagrangian in the large N limit are given below [which have been calculated for the metric (35)].

$$\int d\mathcal{V}_9 \sqrt{-g}\frac{\partial J_0}{\partial R_{z\bar{z}z\bar{z}}} = \int d\mathcal{V}_9 \mathcal{L}_{\mathcal{W}}^{\rm HM} = \int dr \left(-4x_R^2 (\lambda_1(r) + \lambda_2(r)) \sqrt{\alpha(r)\left(\sigma(r) - \left(1 - \frac{r_h^4}{r^4}\right)t'(r)^2\right)} \right), \tag{74}$$

where $\lambda_{1,2}(r)$ are given in (B2).

Anomaly term: Using Eq. (70) and appendix D 1, we find that following are the possible most dominant terms in the large-N limit that contribute the Lagrangian from second term in Eq. (71):

$$\int d\mathcal{V}_9 \mathcal{L}_{\mathcal{A}}^{\rm HM} = \int d\mathcal{V}_9 \sqrt{-g}\left(\frac{\partial^2 J_0}{\partial R_{zizj}\partial R_{\bar{z}m\bar{z}l}}K_{zij}K_{\bar{z}ml}\right) = \int d\mathcal{V}_9 \sqrt{-g}\left(\frac{\partial^2 J_0}{\partial R_{zizj}\partial R_{\bar{z}m\bar{z}l}}\frac{K_{tij}K_{tml}}{x_R^2}\right),$$

$$\int d\mathcal{V}_9 \mathcal{L}_{\mathcal{A}}^{\rm HM} = \int dr \frac{1}{x_R^2}\left(Z(r)\mathcal{L}_1 + x_R^4 W(r)\mathcal{L}_2 - 2x_R^2 U(r)\mathcal{L}_3 + 4x_R^2(U(r) + 2V(r))\mathcal{L}_4\right), \tag{75}$$

where $\mathcal{L}_{1,3}$ are given in (B3), $Z(r)$, $W(r)$, $U(r)$, $V(r)$ are given in (B7), and use has been made of (B4).

From Eqs. (72), (74), (75), and (B3), total holographic entanglement entropy corresponding to Hartman-Maldacena-like surface can be written as:

$$S_{\rm EE}^{\rm total,HM} = \int dr \mathcal{L}_{\rm Total}^{\rm HM} = \int dr (\mathcal{L}_0^{\rm HM} + \mathcal{L}_{\mathcal{W}}^{\rm HM} + \mathcal{L}_{\mathcal{A}}^{\rm HM}) \tag{76}$$

Using (B8)–(B11), and writing $t(r) = t_0(r) + \beta t_1(r)$, the EOM up to $\mathcal{O}(\beta^0)$ is:

$$N^{3/10}(r - r_h)^{5/2}p_1(r_h)t_0''(r)$$
$$+ \frac{5}{2}N^{3/10}(r - r_h)^{3/2}p_1(r_h)t_0'(r) = 0. \tag{77}$$

The solution to (77) will be given by:

$$t_0(r) = c_2 - \frac{2c_1}{3(r - r_h)^{3/2}}. \tag{78}$$

Substituting (78) into (B11), one obtains:

$$t_1(r) = c_3 + \frac{2r_h^{3/2}\sqrt{\kappa_\sigma}(11r_h^7(p_8^\beta(r_h) + p_9^\beta(r_h)) - 3(r - r_h)^7(p_8^\beta(r_h) + p_9^\beta(r_h)) - 11c_1^3 c_2 p_1(r_h))}{33c_1^3 M N_f^{5/3} g_s^{7/3}(r - r_h)^{3/2}\sqrt{\kappa_\alpha}\kappa_\lambda \log(r_h)(\log(N) - 9\log(r_h))(\log(N) - 3\log(r_h))^{5/6}}. \tag{79}$$

Retaining the term up to leading order in N we can write embedding function $t(r)$ as:

$$t(r) = c_2 - \frac{2c_1}{3(r - r_h)^{3/2}} + \beta\left(c_3 - \frac{2c_2}{3(r - r_h)^{3/2}}\right), \quad (80)$$

where it is understood that $t(r = r_h) \equiv t_b$ is evaluated as $t(r_h[1 + \frac{1}{N^{n_{t_b}}}]), n_{t_b} \equiv \mathcal{O}(1)$, in the large-$N$ limit. Since (in $\mathcal{R}_{D5/\overline{D5}} = 1$-units) $\frac{c_1}{r_h^{3/2}} \sim c_2$, i.e., $c_1 \sim r_h^\alpha c_2$ implying $\alpha = 3/2$, i.e., $l_p^6 \sim r_h^{3/2}$ or $l_p \sim r_h^{1/4}$ i.e.,

$$l_p \sim \left(g_s^{\frac{4}{3}}\alpha'^2\left(\frac{r_h}{\mathcal{R}_{D5/\overline{D5}}}\right)\right)^{\frac{1}{4}}. \quad (81)$$

To determine the turning point i.e., r_* of the Hartman-Maldacena-like surface we need to impose the following condition:

$$\left(\frac{1}{t'(r)}\right)_{r=r_*} = \frac{(r_* - r_h)^{5/2}}{c_1} - \frac{\beta c_2(r_* - r_h)^{5/2}}{c_1^2} = 0, \quad (82)$$

Since $\frac{c_1}{r_h^{3/2}} \sim c_2$, therefore (82) can be approximated by the following equation for the purpose of estimating r_*:

$$(r_* - r_h)^{3/2} - \beta\kappa_{r_*}^\beta = 0, \quad (83)$$

whose solution is

$$r_* = r_h + \beta^{2/3}(\kappa_{r_*}^\beta)^{2/3} \quad (84)$$

Now we can calculate the entanglement entropy of the Hawking radiation for the Hartman-Maldacena-like surface as follow:

$$S_{EE}^{\beta^0,\text{HM}} = \int_{r_h}^{r_*} dr\left(\lambda(r)\sqrt{\alpha(r)\left(\sigma(r) - \left(1 - \frac{r_h^4}{r^4}\right)t_0'(r)^2\right)}\right), \quad (85)$$

using Eqs. (B1) and (78) above equation can be rewritten as

$$S_{EE}^{\beta^0,\text{HM}} \sim \int_{r_h}^{r_*}\left(\frac{\sqrt{(r - r_h)r_h}\log(r_h)(\log(N) - 9\log(r_h))(\log(N) - 3\log(r_h))^{5/6}}{r_h^3\sqrt{r_h^2}}\right)$$

$$\times\left(-\frac{2^{5/6}MN^{13/10}\log(2)(\log(64) - 1)N_f^{5/3}g_s^{10/3}\sqrt{\kappa_\alpha}\kappa_\lambda\sqrt{\kappa_\sigma}}{81\,3^{2/3}\pi^{11/12}}\right)$$

$$\sim \frac{2(r_* - r_h)^{3/2}\log(r_h)(\log(N) - 9\log(r_h))(\log(N) - 3\log(r_h))^{5/6}}{3r_h^{7/2}}$$

$$\times\left(-\frac{2^{5/6}MN^{13/10}\log(2)(\log(64) - 1)N_f^{5/3}g_s^{10/3}\sqrt{\kappa_\alpha}\kappa_\lambda\sqrt{\kappa_\sigma}}{81\,3^{2/3}\pi^{11/12}}\right)$$

$$\sim \frac{2(\beta^{2/3}(\kappa_{r_*}^\beta)^{2/3})^{3/2}\log(r_h)(\log(N) - 9\log(r_h))(\log(N) - 3\log(r_h))^{5/6}}{3r_h^{7/2}}$$

$$\times\left(-\frac{2^{5/6}MN^{13/10}\log(2)(\log(64) - 1)N_f^{5/3}g_s^{10/3}\sqrt{\kappa_\alpha}\kappa_\lambda\sqrt{\kappa_\sigma}}{81\,3^{2/3}\pi^{11/12}}\right)$$

$$\sim -\frac{2\,2^{5/6}\beta g_s^{10/3}\sqrt{\kappa_\alpha}\kappa_{r_*}^\beta\kappa_\lambda\sqrt{\kappa_\sigma}MN^{13/10}\log(2)(\log(64) - 1)N_f^{5/3}\log(r_h)(\log(N) - 9\log(r_h))(\log(N) - 3\log(r_h))^{5/6}}{243\,3^{2/3}\pi^{11/12}r_h^{7/2}} \quad (86)$$

If $t_b = t(r = r_h + \epsilon)$ where $\epsilon = \frac{r_h}{N^{n_{t_b}}}$, $n_{t_b} \equiv \mathcal{O}(1)$ then

$$t_{b_0} = c_2 - \frac{2c_1N^{3n_{t_b}/2}}{3r_h^{3/2}}, \quad (87)$$

we obtain the r_h from the above equation as below:

$$r_h = \frac{\left(\frac{2}{3}\right)^{2/3}}{\left(\frac{(c_2 - t_{b_0})N^{-\frac{3n_{t_b}}{2}}}{c_1}\right)^{2/3}} \tag{88}$$

It will be argued when discussing the computation of the entanglement entropy corresponding to the island surface, that β turns out to be related to black hole horizon radius [see the discussion around (123)]. If $|\log(r_h)| \gg \log(N)$ then Eq. (86), using (123), can be approximated by

$$S_{EE}^{\beta^0,HM} \sim e^{-\frac{3\kappa_{l_p}N^{\frac{1}{3}}}{2}} \frac{MN^{13/10}N_f^{5/3}(|\log(r_h)|)^{17/6}}{r_h^2}. \tag{89}$$

Since $\frac{1}{r_h^2} \sim \left(\frac{c_2}{c_1} - \frac{t_{b_0}}{c_1}\right)^{4/3} N^{-2n_{t_b}} = \left(\frac{c_2}{c_1}\right)^{2/3}\left(1 - \frac{t_{b_0}}{c_2}\right)^{4/3} N^{-2n_{t_b}}$. For $t_{b_0} \ll c_2$, $\frac{1}{r_h^2} \sim \left(\frac{c_2}{c_1}\right)^{4/3}\left(1 - \frac{4t_{b_0}}{3c_2}\right)N^{-2n_{t_b}}$. Therefore,

$$S_{EE}^{\beta^0,HM} \sim e^{-\frac{3\kappa_{l_p}N^{\frac{1}{3}}}{2}} MN^{13/10}N_f^{5/3}\left(1 - \frac{4t_{b_0}}{3c_2}\right)\left(\frac{2}{3}\log\left(\frac{c_2 - t_{b_0}}{c_1}\right) - n_{t_b}\log(N)\right)^{\frac{17}{6}}$$

$$\approx e^{-\frac{3\kappa_{l_p}N^{\frac{1}{3}}}{2}} MN^{13/10}N_f^{5/3}\left(1 - \frac{4t_{b_0}}{3c_2}\right)\left(\frac{2}{3}\log\left(\frac{c_2}{c_1}\right) - n_{t_b}\log(N)\right)^{\frac{17}{6}}, \tag{90}$$

when $c_1, c_2 < 0$. The Fig. 4 for $N = 10^{3.3}$, $M = N_f = 3$, $g_s = 0.1$, $c_1 = -10^3$, $c_2 = -10^8$, $n_{t_b} = 1$ obtained from (91), shows the linearization assumed in obtaining the last line of (90), can be approximately justified. In it,

$$S_{EEHM1} \sim 51.024\left(\frac{t_{b_0}}{7.5 \times 10^7} + 1\right)\left(\frac{2}{3}\log\left(\frac{t_{b_0} + 10^8}{10^3}\right) - 7.6\right)^{\frac{17}{6}},$$

$$S_{EEHM2} \sim 51.024\left(\frac{t_{b_0}}{10^8} + 1\right)^{4/3}\left(\frac{2}{3}\log\left(\frac{t_{b_0} + 10^8}{10^3}\right) - 7.6\right)^{\frac{17}{6}},$$

$$S_{EEHM3} \sim 0.0354\left(\frac{t_{b_0}}{7.5 \times 10^7} + 1\right). \tag{91}$$

From Eq. (90) we see that entanglement entropy of the Hawking radiation coming from the Hartman-Maldacena-like surface has linear time dependence. Therefore it is increasing with time and diverges at late times, i.e., when $t_{b_0} \to \infty$.
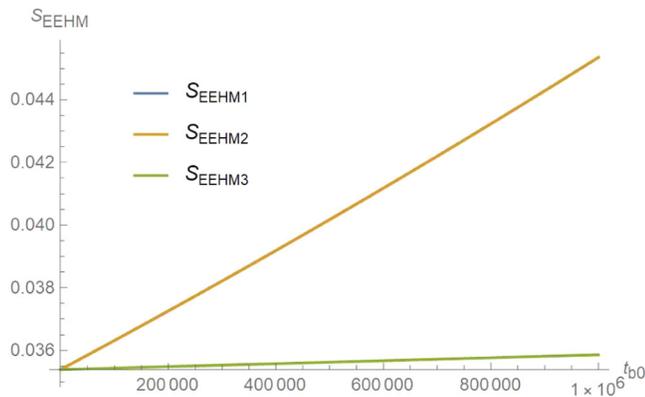
FIG. 4. Hartman-Maldacena-like surface entanglement entropy as a function of t_{b_0}.

B. "Swiss-cheese" structure of $S_{EE}^{\beta^0,HM}$ in a large-N-scenario

In this subsection we discuss the "Swiss-cheese" structure of entanglement entropy of the Hawking radiation corresponding to the Hartman-Maldacena-like surface at $O(\beta^0)$.

The expression for $S_{EE}^{\beta^0,HM}$ in (90) for the values of constants of integration $c_{1,2}$ used beneath the same, suggests the following hierarchy:

$$|c_2| \sim e^{\kappa_{c_2}|c_1|^{1/3}}, \qquad |c_1| \sim N. \tag{92}$$

Further, assuming $c_{1,2} < 0$, (90) can be rewritten as:

$$S_{EE}^{\beta^0,HM} \sim e^{-\frac{3\kappa_{l_p}N^{\frac{1}{3}}}{2}} MN^{13/10}N_f^{5/3}\left(1 + \frac{4t_{b_0}}{3|c_2|}\right)$$

$$\times \left(\frac{2}{3}\log\left(\frac{|c_2| + t_{b_0}}{|c_1|}\right) - n_{t_b}\log(N)\right)^{\frac{17}{6}}. \tag{93}$$

We thus see,

$$\frac{\partial S_{\text{EE}}^{\beta^0,\text{HM}}}{\partial |c_2|} \sim e^{-\frac{3\kappa l_p N^{\frac{1}{3}}}{2}} MN^{13/10}N_f^{5/3}\left[-\frac{4t_{b_0}}{3|c_2|^2}\left(\frac{2}{3}\log\left(\frac{|c_2|+t_{b_0}}{|c_1|}\right) - n_{t_b}\log(N)\right)^{\frac{17}{6}}\right.$$
$$\left. +\frac{17}{6}\frac{2}{3|c_2|}\left(1 + \frac{4t_{b_0}}{3|c_2|}\right)\left(\frac{2}{3}\log\left(\frac{|c_2|+t_{b_0}}{|c_1|}\right) - n_{t_b}\log(N)\right)^{\frac{11}{6}}\right]. \tag{94}$$

For $N = 10^{3.3}$, $M = N_f = 3$, $g_s = 0.1$, $c_1 = -10^3$, $c_2 = -10^8$, $n_{t_b} = 1$ as in the previous subsection, as $t_b \leq t_{\text{Page}} \sim 10^6$,

$$\frac{\partial S_{\text{EE}}^{\beta^0,\text{HM}}}{\partial |c_2|} \sim e^{-\frac{3\kappa l_p N^{\frac{1}{3}}}{2}}MN^{13/10}N_f^{5/3}[- \leq 10^{6-16}\times\mathcal{O}(1) + \mathcal{O}(1)\times\mathcal{O}(1)\times 10^{-8}] \approx \mathcal{O}(1)\times 10^{-8}$$

$$\sim e^{-\frac{3\kappa l_p N^{\frac{1}{3}}}{2}}MN^{13/10}N_f^{5/3}\mathcal{O}(1)\times 10^{-8} > 0. \tag{95}$$

Similarly,

$$\frac{\partial S_{\text{EE}}^{\beta^0,\text{HM}}}{\partial |c_1|} \sim -e^{-\frac{3\kappa l_p N^{\frac{1}{3}}}{2}}MN^{13/10}N_f^{5/3}\left[\left(1 + \frac{4t_{b_0}}{3|c_2|}\right)\frac{1}{|c_1|}\right] < 0. \tag{96}$$

We also note that in the $|c_2| \gg |c_1|$-limit and assuming $|c_1| \sim N$,

$$S_{\text{EE}}^{\beta^0,\text{HM}} \sim e^{-\frac{3\kappa l_p N^{\frac{1}{3}}}{2}}MN^{13/10}N_f^{5/3}(\log|c_2|)^{11/6}$$
$$\times (12\log|c_2| - (34 + 51n_{t_b})\log|c_1|), \tag{97}$$

which mimics a Swiss-cheese volume written out in terms of a single "large divisor" volume $\log|c_2|$ and a single "small divisor" volume $\log|c_1|$ (with 12 and $34 + 51n_{t_b}$ encoding information about some version of "classical intersection numbers" of these "divisors"). Alternatively,
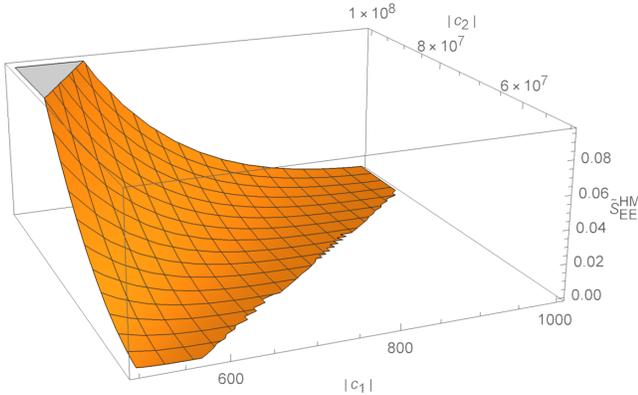
FIG. 5. Plot of $\tilde{S}_{\text{EE}}^{\text{HM}}$ as a bifunction of $(|c_1|, |c_2|)$ at $t = t_{\text{Page}} = 10^6$.

defining $S_{\text{EE}}^{\beta^0,\text{HM}} \equiv e^{-\frac{3\kappa l_p N^{\frac{1}{3}}}{2}}MN^{13/10}N_f^{5/3}\tilde{S}_{\text{EE}}^{\text{HM}}$, one can think of (97) as an open Swiss-cheese surface (in the same sense as (96) and (97), i.e., $\tilde{S}_{\text{EE}}^{\text{HM}}$ decreases as $|c_1|$ increases and $\tilde{S}_{\text{EE}}^{\text{HM}}$ increases as $|c_2|$ increases) in $\mathbb{R}_{\geq 0}(\tilde{S}_{\text{EE}}^{\text{HM}})\times \mathbb{R}_+^2(|c_1|,|c_2|)$—see Fig. 5.

Therefore, (92) along with (95), (96) and (97), suggests very curiously a "Swiss-cheese" structure of $S_{\text{EE}}^{\beta^0,\text{HM}}$ in a large N scenario (reminiscent of the "large volume scenario" in moduli stabilizations in string theory [69,70]).

C. Entanglement entropy contribution from island surface

In this subsection we are calculating the entanglement entropy corresponding to the island surface using Dong's formula (66).

Similar to Hartman-Maldacena-like surface, island surface is also a codimension two surface and located at constant time slice. Therefore we can write the expression for the holographic entanglement entropy similar to Hartman-Maldacena-like surface in the following form:

$$S_{\text{EE}} = \int drdx^2dx^3d\theta_1d\theta_2dxdydzdx^{10}$$
$$\times \sqrt{-g}\left[\frac{\partial\mathcal{L}}{\partial R_{z\bar{z}z\bar{z}}} + \sum_\alpha\left(\frac{\partial^2\mathcal{L}}{\partial R_{zizj}\partial R_{\bar{z}m\bar{z}l}}\right)_\alpha\frac{8K_{zij}K_{\bar{z}ml}}{(q_\alpha + 1)}\right], \tag{98}$$

where all the quantities in the above equation are same as Eq. (71).

Contribution from $\mathcal{O}(\beta^0)$ term: Holographic entanglement entropy contribution to the Lagrangian (26) from the induced metric (53) for the island surface at $\mathcal{O}(\beta^0)$ turns out to be

$$\int d\mathcal{V}_9 \sqrt{-g} \left(\frac{\partial R}{\partial R_{z\bar{z}z\bar{z}}} \right) = \int d\mathcal{V}_9 \mathcal{L}_0^{\mathrm{IS}} = \int dr \left(4\lambda_5(r) x(r)^2 \sqrt{\alpha(r)(\sigma(r) + x'(r)^2)} \right), \tag{99}$$

where,

$$\lambda_5(r) = \kappa_{\lambda_5} \frac{M N^{17/10} N_f^{4/3} g_s^{5/2} r_h^2 \log(N) \log(r) \sqrt[3]{\log(N) - 3\log(r)}}{r^4 \alpha_{\theta_1}^3 \alpha_{\theta_2}^2}$$

$$\sim \frac{M N^{21/20} \log(2)(\log(64) - 1) N_f^{4/3} g_s^{13/4} r_h^2 \kappa_{\lambda_5} \log(N) \log(r) \sqrt[3]{\log(N) - 3\log(r)}}{r^4}, \tag{100}$$

where κ_{λ_5} is the numerical factor. Angular integrations in Eqs. (100), (C1), and (C2) have been performed using (A2) and (A3).

Contribution from $\mathcal{O}(\beta)$ *term:* At $\mathcal{O}(\beta)$ we are required to calculate the two terms to obtain the holographic entanglement entropy (98). First term is coming from $\left(\frac{\partial J_0}{\partial R_{z\bar{z}z\bar{z}}} \right)$ and is given below:

$$\frac{\partial J_0}{\partial R_{z\bar{z}z\bar{z}}} = -4x(r)^2 \frac{\partial J_0}{\partial R_{txtx}}, \tag{101}$$

from appendix D 2 we find that following terms are the most dominant terms in the large-N limit:

$$\int d\mathcal{V}_9 \sqrt{-g} \frac{\partial J_0}{\partial R_{z\bar{z}z\bar{z}}} = \int d\mathcal{V}_9 \mathcal{L}_{\mathcal{W}}^{\mathrm{IS}}$$

$$= \int dr \left(4x(r)^2 (\lambda_3(r) + \lambda_4(r)) \right)$$

$$\times \sqrt{\alpha(r)(\sigma(r) + x'(r)^2)} \right), \tag{102}$$

where $\lambda_{3,4}$ are given in (C1). We obtain the second term in Eq. (98) using (70) and appendix D 2. For the island surface, most dominant terms in the large-N limit that contribute to the Lagrangian are given below:

$$\int d\mathcal{V}_9 \mathcal{L}_{\mathcal{A}}^{\mathrm{IS}} = \int d\mathcal{V}_9 \sqrt{-g} \left(\frac{\partial^2 J_0}{\partial R_{ziz j} \partial R_{\bar{z}m\bar{z}l}} K_{zij} K_{\bar{z}ml} \right) = \int d\mathcal{V}_9 \sqrt{-g} \left(\frac{\partial^2 J_0}{\partial R_{ziz j} \partial R_{\bar{z}m\bar{z}l}} K_{xij} K_{xml} \right),$$

$$= \int dr (Z_1(r)\mathcal{L}_1 + x(r)^4 W_1(r)\mathcal{L}_2 - 2x(r)^2 U_1(r)\mathcal{L}_3 + 4x(r)^2 (U_1(r) + 2V_1(r))\mathcal{L}_4), \tag{103}$$

where,

$$\mathcal{L}_1 = \mathcal{L}_2 = \frac{\sqrt{\alpha(r)(\sigma(r) + x'(r)^2)}(\alpha'(r)(\sigma(r) + x'(r)^2) + \alpha(r)(\sigma'(r) + 2x'(r)x''(r)))^2}{x'(r)^2(\sigma(r) + x'(r)^2)^4};$$

$$\mathcal{L}_3 = \mathcal{L}_4 = \frac{\sqrt{\alpha(r)(\sigma(r) + x'(r)^2)}}{x'(r)^2}, \tag{104}$$

and various r dependent functions appearing in Eq. (103) are given in (C2). From Eqs. (99), (102), and (103), we find that total holographic entanglement entropy from $\mathcal{O}(\beta^0)$ and $\mathcal{O}(\beta)$ terms for the action (26) corresponding to island surface is given by:

$$S_{\mathrm{EE}}^{\mathrm{total}} = \int dr \mathcal{L}_{\mathrm{Total}}^{\mathrm{IS}} = \int dr (\mathcal{L}_0^{\mathrm{IS}} + \mathcal{L}_{\mathcal{W}}^{\mathrm{IS}} + \mathcal{L}_{\mathcal{A}}^{\mathrm{IS}}). \tag{105}$$

Using appendix C, $x(r)$ EOM $\frac{\delta \mathcal{L}_{\mathrm{Total}}^{\mathrm{IS}}}{\delta x(r)} - \frac{d}{dr} \left(\frac{\delta \mathcal{L}_{\mathrm{Total}}^{\mathrm{IS}}}{dx'(r)} \right) + \frac{d^2}{dr^2} \left(\frac{\delta \mathcal{L}_{\mathrm{Total}}^{\mathrm{IS}}}{\delta x''(r)} \right) = 0$, turns out to be,

$$- \frac{N^{3/10} x(r)(F_1(r_h)(4(r - r_h)x'(r)^2 + x(r)(2(r - r_h)x''(r) + x'(r))) - 2N f_1(r_h))}{2\sqrt{r - r_h}}$$

$$+ \frac{\beta}{4N^{7/10}(r - r_h)^{3/2} x'(r)^4} \left[2N^{7/10} F_4^{\beta}(r_h) x(r)(4(r_h - r)x'(r)^2 + x(r)(6(r - r_h)x''(r) + x'(r))) \right.$$

$$\left. + (r - r_h)x'(r)^4 (3\mathcal{F}_1^{\beta}(r_h) + 3\mathcal{F}_2^{\beta}(r_h) + 4N^2 x(r)Y_1(r_h)) \right] = 0. \tag{106}$$

Writing $x(r) = x_0(r) + \beta x_1(r)$, and making an ansatz:

$$x_0(r) = \sqrt{\frac{a_3}{a_2} + r} \sqrt{\frac{F_1(r_h)}{N f_1(r_h)}}. \tag{107}$$

Defining $X(r) \equiv \dfrac{x_0(r)\sqrt{\frac{F_1(r)}{N f_1(r_h)}}}{\sqrt{2}}$, one notes that $X(r)$ must satisfy:

$$X(r)(2(r - r_h)X''(r) + X'(r)) + 4(r - r_h)X'(r)^2 - 1 = \frac{a_3(a_1^2 a_2 - 2) + a_2(2r(a_1^2 a_2 - 1) - a_1^2 a_2 r_h)}{2(a_2 r + a_3)} = 0. \tag{108}$$

If $a_1^2 a_2 = 2$, then the left-hand side (lhs) of (108) becomes proportional to $\frac{r - r_h}{\frac{a_3}{a_2} + r}$, which in the deep IR, i.e., $r \sim r_h$ becomes negligible if $\frac{a_3}{a_2 r} \gg 1$. Therefore,

$$x_0(r) = \sqrt{\frac{a_3}{a_2} + r} \sqrt{\frac{F_1(r_h)}{N f_1(r_h)}}. \tag{109}$$

One therefore sees,

$$x_1(r) = \frac{N^{3/10}}{2\sqrt{r - r_h}} \Big[2N f_1(r_h)x_1(r) - F_1(r_h)\Big(x_0(r)(2(r - r_h)(2x_1(r)x_0''(r) + x_0(r)x_1''(r)) + x_0(r)x_1'(r))$$

$$+ 2x_0(r)x_0'(r)(4(r - r_h)x_1'(r) + x_1(r)) + 4(r - r_h)x_1(r)x_0'(r)^2 \Big) \Big]$$

$$= \frac{2a_2 N^2 f_1(r_h)^2 x_1(r) - F_1(r_h)^2(x_1'(r)(5a_2 r - 4a_2 r_h + a_3) + 2(r - r_h)(a_2 r + a_3)x_1''(r) + a_2 x_1(r))}{2a_2 N^{7/10} f_1(r_h)\sqrt{r - r_h}}, \tag{110}$$

and,

$$\frac{\beta}{4N^{7/10}(r - r_h)^{3/2} x_0'(r)^4}(2N^{7/10}F_4^\beta(r_h)x_0(r)(4(r_h - r)x_0'(r)^2 + x_0(r)(6(r - r_h)x_0''(r) + x_0'(r))))$$

$$+ (r - r_h)x_0'(r)^4(3\mathcal{F}_1^\beta(r_h) + 3\mathcal{F}_2^\beta(r_h) + 4N^2 x_0(r)Y_1(r_h)))$$

$$= \frac{4(a_2 r + a_3)\sqrt{\frac{a_3}{a_2} + r}(a_2(5r_h - 4r) + a_3)F_4^\beta(r_h)}{a_2^2(r - r_h)^{3/2}\sqrt{\frac{F_1(r_h)}{N f_1(r_h)}}} + \frac{4N^2 \sqrt{\frac{a_3}{a_2} + r}Y_1(r_h)\sqrt{\frac{F_1(r_h)}{N f_1(r_h)}} + 3\mathcal{F}_1^\beta(r_h) + 3\mathcal{F}_2^\beta(r_h)}{4N^{7/10}\sqrt{r - r_h}}. \tag{111}$$

Therefore equation of motion corresponding to embedding $x_1(r)$ for the island surface is given by:

$$\frac{2a_2 N^2 f_1(r_h)^2 x_1(r) - F_1(r_h)^2(x_1'(r)(5a_2 r - 4a_2 r_h + a_3) + 2(r - r_h)(a_2 r + a_3)x_1''(r) + a_2 x_1(r))}{2a_2 N^{7/10} f_1(r_h)\sqrt{r - r_h}}$$

$$+ \frac{4(a_2 r + a_3)\sqrt{\frac{a_3}{a_2} + r}(a_2(5r_h - 4r) + a_3)F_4^\beta(r_h)}{a_2^2(r - r_h)^{3/2}\sqrt{\frac{F_1(r_h)}{N f_1(r_h)}}} + \frac{4N^2 \sqrt{\frac{a_3}{a_2} + r}Y_1(r_h)\sqrt{\frac{F_1(r_h)}{N f_1(r_h)}} + 3\mathcal{F}_1^\beta(r_h) + 3\mathcal{F}_2^\beta(r_h)}{4N^{7/10}\sqrt{r - r_h}} = 0, \tag{112}$$

which near $r = r_h$ simplifies to:

$$\frac{4\sqrt{\frac{a_3}{a_2} + r_h}(a_2 r_h + a_3)^2 F_4^\beta(r_h)}{a_2^2(r - r_h)^{3/2}\sqrt{\frac{F_1(r_h)}{N f_1(r_h)}}} + \frac{N^{13/10}x_1(r)f_1(r_h) - \frac{F_1(r_h)^2((a_2 r_h + a_3)x_1'(r) + a_2 x_1(r))}{2a_2 N^{7/10} f_1(r_h)}}{\sqrt{r - r_h}} = 0. \tag{113}$$

The solution to (113) is given by,

$$x_1(r) = \frac{8\sqrt{\frac{a_3}{a_2} + r_h}(a_2 r_h + a_3)F_4^\beta(r_h)\log(r - r_h)}{a_2 N^{3/10}F_1(r_h)\left(\frac{F_1(r_h)}{Nf_1(r_h)}\right)^{3/2}}, \quad (114)$$

implying,

$$x(r) \approx \sqrt{\frac{a_3}{a_2} + r}\sqrt{\frac{F_1(r_h)}{Nf_1(r_h)}}$$

$$+ \beta N^{\frac{11}{5}}\left(\frac{8\left(r_h + \frac{a_3}{a_2}\right)^{\frac{3}{2}}F_4^\beta(r_h)\log(r - r_h)}{F_1(r_h)\left(\frac{F_1(r_h)}{f_1(r_h)}\right)^{3/2}}\right). \quad (115)$$

To determine the turning point via r_T: $1/x'(r_T) = 0$, one therefore obtains:

$$\frac{32\beta N^{11/5}(a_2 r_T + a_3)\sqrt{\frac{a_3}{a_2} + r_h}(a_2 r_h + a_3)F_4^\beta(r_h)}{a_2^2(r_T - r_h)F_1(r_h)\left(\frac{F_1(r_h)}{f_1(r_h)}\right)^{5/2}}$$

$$- \frac{2\sqrt{\frac{a_3}{a_2} + r_T}}{\sqrt{\frac{F_1(r_h)}{Nf_1(r_h)}}} = 0, \quad (116)$$

whose solution is given by

$$r_T = r_h + \frac{128\beta^2}{a_2^4 F_1(r_h)^6}\left(a_2 N^{17/5}(a_2 r_h + a_3)^3 f_1(r_h)^4 F_4^\beta(r_h)^2 + a_2 a_3^3 N^{17/5}f_1(r_h)^4 F_4^\beta(r_h)^2\right.$$

$$+ a_2^4 N^{17/5}r_h^3 f_1(r_h)^4 F_4^\beta(r_h)^2 + 3a_2^3 a_3 N^{17/5}r_h^2 f_1(r_h)^4 F_4^\beta(r_h)^2 + 3a_2^2 a_3^2 N^{17/5}r_h f_1(r_h)^4 F_4^\beta(r_h)^2\right)$$

$$\sim r_h + \frac{289(\frac{3}{2})^{2/3}\pi^{17/3}\beta^2 M^2 N^{17/5}(107 - 540\log(2))^2 g_s^7 \kappa_\sigma^6 \kappa_{U_1}^2 \log^2(N)(3a_2 a_3^2 r_h + 3a_2^2 a_3 r_h^2 + 2a_2^3 r_h^3 + a_3^3)}{50a_2^3 \log^2(2)(\log(64) - 1)^2 N_f^{2/3}r_h^{20}\kappa_{\lambda_5}^2(-\log(r_h))^{2/3}}$$

$$\equiv r_h + \delta \in \text{IR}, \quad (117)$$

in $\mathcal{R}_{D5/\overline{D5}} = 1$-units. One therefore obtains the $\mathcal{O}(\beta^0)$ on-shell entanglement entropy:

$$S_{\text{EE}}^{\beta^0,\text{IS}}$$

$$= \int_{r_h}^{r_h + \delta\mathcal{R}_{D5/\overline{D5}}} dr\left(\frac{\kappa_{\lambda_5}\log NMN^{17/10}N_f^{4/3}r_h^2 x(r)^2\log(r)\sqrt[3]{\log N - 3\log(r)}\sqrt{\alpha(r)(\sigma(r) + x'(r)^2)}}{r^4\alpha_{\theta_1}^3\alpha_{\theta_2}^2}\right)$$

$$\sim \int_{r_h}^{r_h + \delta} dr\left(\frac{2^{2/3}MN^{3/10}\log(2)(\log(64) - 1)N_f^{5/3}g_s^{10/3}\kappa_{\lambda_5}\log(N)(a_2 r_h + a_3)F_1(r_h)\log(r_h)\sqrt{\kappa_\alpha\kappa_\sigma}(\log(N) - 3\log(r_h))^{2/3}}{81\,3^{5/6}\pi^{11/12}a_2\sqrt{r - r_h}r_h^{5/2}f_1(r_h)}\right)$$

$$\sim \left(\frac{\sqrt{\delta}MN^{3/10}N_f^{5/3}g_s^{7/3}\sqrt{r_h}\kappa_\alpha\kappa_{\lambda_5}\log(N)(a_2 r_h + a_3)\log(r_h)|\log(r_h)|^{2/3}}{a_2\sqrt{\kappa_\alpha\kappa_\sigma}}\right)$$

$$\sim \frac{\beta M^2 N^2 N_f^{4/3}g_s^{35/6}\log^2(N)(a_2 r_h + a_3)|\log(r_h)|^{4/3}}{a_2^{5/2}r_h^{19/2}}\sqrt{3a_2 a_3^2 r_h + 3a_2^2 a_3 r_h^2 + 2a_2^3 r_h^3 + a_3^3}. \quad (118)$$

Now, this appears to present a contradiction—$S_{\text{EE}}^{\beta^0,\text{IS}} \sim \beta$. The resolution, using (81), is that $\beta \propto r_h^{\frac{3}{2}}$.

The Hawking BH entropy is given by:

$$S_{\text{BH}} \sim \frac{g_s^{7/4}MN_f^3 r_h^3\log(N)\log^4(r_h)(2 - \beta(\mathcal{C}_{zz}^{\text{BH}} - 2\mathcal{C}_{\theta_1 z}^{\text{BH}}))}{N^{3/4}}, \quad (119)$$

From the above equation we see that $\mathcal{O}(\beta^0)$ contribution to the black hole thermal entropy scale as $S_{\text{BH}}^{\beta^0} \sim r_h^3\log^4(r_h)$.

The $\mathcal{O}(\beta)$-corrections to the MQGP background of [36] as worked out in [4] and as quoted in appendix A, were worked out in the $\psi = 2n\pi, n = 0, 1, 2$-patches, by setting the $\mathcal{O}(\beta)$-corrections to the M-theory three-form potential, to zero. This required $\mathcal{C}_{zz}^{\text{BH}} = 2\mathcal{C}_{\theta_1 z}^{\text{BH}}$. One therefore sees that the BH entropy receives no higher-derivative corrections at $\mathcal{O}(R^4)$.

From (118) and (119), as well as $\beta = \kappa_\beta(g_s, N)$ $\left(\frac{r_h}{\mathcal{R}_{D5/\overline{D5}}}\right)^{\frac{3}{2}}\alpha'^3$ from the discussion beneath (118), one sees,

$$\frac{S_{\mathrm{EE}}^{\beta^0,IS}}{S_{\mathrm{BH}}} \sim \frac{\kappa_\beta(g_s,N)g_s^{49/12}\log NM N^{11/4}(a_2 r_h + a_3)\sqrt{3a_2^2 a_3 r_h^2 + 2a_2^3 r_h^3 + 3a_2 a_3^2 r_h + a_3^3}}{a_2^{5/2}N_f^{5/3}r_h^{11}|\log(r_h)|^{8/3}}. \tag{120}$$

If $a_2 r_h \gg a_3$ then,

$$\frac{S_{\mathrm{EE}}^{\beta^0,IS}}{S_{\mathrm{BH}}} \sim \frac{\kappa_\beta(g_s,N)g_s^{49/12}\log NM N^{11/4}}{N_f^{5/3}r_h^{17/2}|\log(r_h)|^{8/3}}$$
$$\times \left[1 + \sum_{n=1}^{\infty}\mathcal{A}_n\left(\frac{a_3}{a_2 r_h}\right)^n\right], \tag{121}$$

where, e.g., $\mathcal{A}_1 = \frac{7}{4}, \mathcal{A}_2 = \frac{39}{32}$, etc. Now, one expects:

$$\frac{S_{\mathrm{EE}}^{\beta^0,IS}}{S_{\mathrm{BH}}} = 2 + \sum_{n=1}^{\infty}a_n\left(\frac{G_N^D}{r_h^{D-2}}\right)^n, \tag{122}$$

for a D-dimensional black-hole (the central charge for conformal backgrounds is absorbed into the a_n's) [71]; a_3 in (121) is the nonconformal analog of the conformal charge "c" figuring in [71]. It is rather nontrivial to obtain a somewhat similar expression for the nonconformal backgrounds considered in this paper in (121). To ensure that (121)–(122), one needs to cure the large-N and IR (via small r_h) enhancements in the (121). Utilizing the estimate in [68] of the $r = r_0 \sim r_h$: $N_{\mathrm{eff}}(r_0 = 0)$ (N_{eff} being the effective number of color $D3$-branes in [34]—the type IIB dual of thermal QCD-like theories), and in particular the exponential N-suppression therein,[8] we therefore propose $\kappa_\beta(g_s,N) \sim e^{-\kappa_{l_p}N^{1/3}}$, i.e.,

$$\beta \sim \left(g_s^{\frac{4}{3}}\alpha'^2 e^{-\kappa_{l_p}N^{1/3}}\frac{r_h}{\mathcal{R}_{D5/\overline{D5}}}\right)^{3/2}. \tag{123}$$

In particular then,

$$S_{\mathrm{EE}}^{\beta^0,IS} \sim \frac{M^2 e^{-\frac{3\kappa_{l_p}N^{\frac{1}{3}}}{2}}N_f^{4/3}g_s^{35/6}\log^2(N)|\log(r_h)|^{4/3}}{r_h^{11/2}}. \tag{124}$$

Setting $N = 10^{3.3}, M = N_f = 3, g_s = 0.1$, one sees [without worrying about numerical multiplicative constants in (124) and (119)] from (119), $11.4 r_h^3|\log r_h|^4 = S_{\mathrm{BH}}$. This is solved to yield,

$$r_h = e^{\frac{4}{3}W\left(0.4 S_{\mathrm{BH}}^{\frac{1}{4}}\right)}. \tag{125}$$

From Fig. 6 and using (125), it is evident that (121) $\sim$ (122) implies there will be a lower bound on r_h, the nonextremality parameter in the M-theory dual of large-N thermal QCD.

From Eq. (124) we find that entanglement entropy contribution from the island surface reaches a constant value. Now considering both the contribution together, i.e., Hartman-Maldacena-like surface and island surface, we obtain the Page curve as follows. Initially entanglement entropy of the Hawking radiation is increasing linearly with time and will diverge at late times. But due to presence of the island surface entanglement entropy contribution from this surface dominates after the Page time and stops the linear time growth of the entanglement entropy of the Hawking radiation and reaches a constant value. In this way we obtain the Page curve of an eternal black hole from M-theory dual where bath is a nonconformal theory.
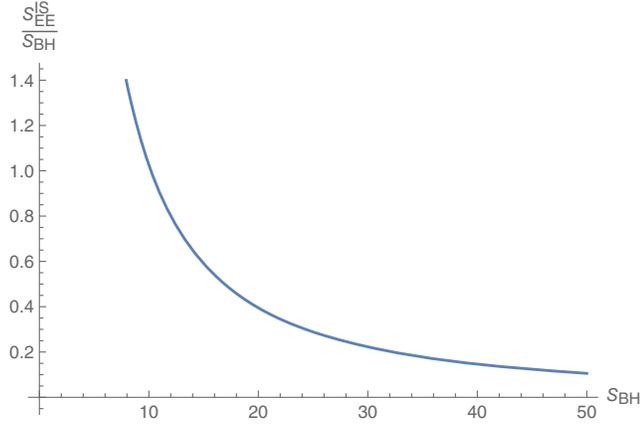
---

[8]To find an appropriate r_0/r_h it would be easier to work with the type IIB side instead of its type IIA mirror as the mirror *a la* SYZ keeps the radial coordinate unchanged. To proceed then, let us define an *effective* number of three-brane charge as:

$$N_{\mathrm{eff}}(r) = \int_{\mathbb{M}_5} F_5^{\mathrm{IIB}} + \int_{\mathbb{M}_5} B_2^{\mathrm{IIB}} \wedge F_3^{\mathrm{IIB}},$$

where $B_2^{\mathrm{IIB}}, F_3^{\mathrm{IIB}}$ and F_5^{IIB} are given in [34]. The five-dimensional internal space $\mathbb{M}_5$, with coordinates (θ_i, ϕ_i, ψ), is basically the base of the resolved warped-deformed conifold. As shown in [68],

$$N_{\mathrm{eff}}(r_0) = N + \frac{3g_s M^2 \log r}{10 r^4}\left\{18\pi r(g_s N_f)^2 \log N \sum_{k=0}^{1}(18a^2(-1)^k \log r + r^2)\left(\frac{108a^2 \log r}{2k+1} + r\right)\right.$$
$$\left. + 5(3a^2(g_s - 1) + r^2)(3g_s N_f \log r + 2\pi)(9g_s N_f \log r + 4\pi)\left[9a^2 g_s N_f \log\left(\frac{e^2}{r^3}\right) + 4\pi r^2\right]\right\},$$
$$= N\left[1 + 6\pi \log r(3g_s N_f \log r + 2\pi)(9g_s N_f \log r + 4\pi)\frac{g_s M^2}{N}\right] + \mathcal{O}\left[\frac{g_s M^2}{N}(g_s N_f)^2 \log N\right].$$

Note that the assumption of small r_0 is crucial here as the same implies the dominance of $g_s N_f|\log r_0|$ over other constant pieces. Solving for r_0: $N_{\mathrm{eff}}(r_0) = 0$ yields $r_0 \sim r_h \sim e^{-\kappa_{r_h}(M,N_f,g_s)N^{\frac{1}{3}}}$.

FIG. 6. $\frac{S_{EE}^{\beta^0,IS}}{S_{BH}}$-versus-$S_{BH}$ for $N = 10^{3.3}, M = N_f = 3, g_s = 0.1, \kappa_{l_p} = 0.47$.
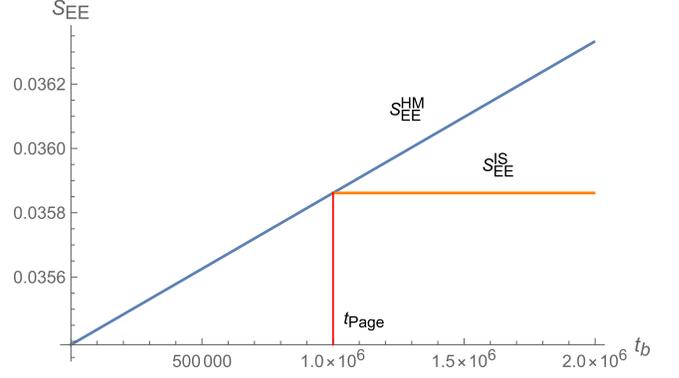

FIG. 7. Page curve of an eternal black hole from doubly holographic setup in M-theory dual. Blue line in the graph corresponds to the entanglement entropy contribution from the Hartman-Maldacena-like surface and orange line corresponds to the entanglement entropy contribution from the island surface.

D. Page curve and an exponential(-in-N) hierarchy of entanglement entropies up to $\mathcal{O}(R^4)$ before/after the Page time

In this subsection we will obtain the Page curve of an eternal neutral black hole appearing on the gravity dual of thermal QCD-like theories at intermediate coupling, and show that a hierarchy in powers of $e^{-\kappa_{l_p} N^{1/3}}$ in the entanglement entropies arising from the EH + GHY terms and the $\mathcal{O}(R^4)$ corrections to the same, before and after the Page time, naturally arises. For this purpose we will use the results of Secs. V A and V C.

Since we are equipped with all the results therefore we are going to obtain the Page curve in this subsection. For this purpose we are plotting the entanglement entropy contribution from the Hartman-Maldacena-like surface obtained in Sec. V A and entanglement entropy of the Hawking radiation coming from the island surface obtained in Sec. V C.

Entanglement entropy of the Hawking radiation corresponding to the Hartman-Maldacena-like surface is given in Eq. (90) and for the island surface it is given in Eq. (124). For the numerical values of the parameters of the model we obtain the following plot.

We have plotted $S_{EE}^{\beta^0,HM}$ and S_{EE}^{IS} in Fig. 7 for $N = 10^{3.3}$, $M = N_f = 3, g_s = 0.1, \kappa_{l_p} = 0.47, c_2 = -10^8, c_1 = -10^3$.

From Fig. 7 it is clear that initially entanglement entropy of the Hawking radiation is increasing linearly with time. After the Page time entanglement entropy of the Hawking radiation coming from the island surface dominates therefore entanglement entropy stops increasing and we obtain the Page curve. The values of S_{EE} in Fig. 3 and Fig. 7 differ because, e.g., the latter did not include the factor of $(2\pi)^4$ arising from integrations with respect to $\phi_{1,2}, \psi, x^{10}$, etc.
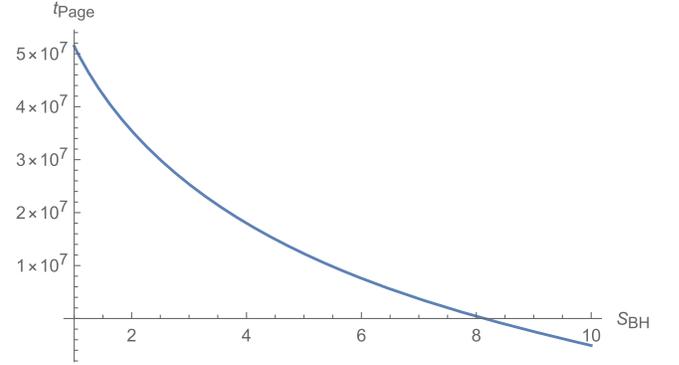
FIG. 8. Page time for $N = 10^{3.3}, M = N_f = 3, g_s = 0.1$, $c_2 = -10^8, c_1 = -10^3$.

The Page time is obtained by equality of the entanglement entropies for the Hartman-Maldacena-like surface and island surface (at the Page time). This yields:

$$t_{Page} = \frac{3}{4} c_2 \left(1 - \frac{93^{5/6} g_s^{35/6} M N^{7/10} \log^2(N) |\log(r_h)|^{4/3}}{\sqrt[3]{N_f} r_h^{11/2} (-3 n_{t_b} \log(N) + 2 \log(\frac{c_2}{c_1}))^{17/6}} \right).$$

(126)

The Page time, implicitly assumes choosing the time evolution of S_{EE}^{HM} which is (approximately) linear in time up to the Page time beyond which, the constant contribution to the entanglement entropy from the island, takes over. The behavior of the Page time as a function of the Black-hole entropy [using (125)] is given in Fig. 8. This also shows that positivity of the Page time requires an upper bound on the black-hole entropy and therefore the IR cutoff r_h. Given that r_h, the nonextremality parameter, is essentially a constant of integration [72] and requiring the same

(in units of $\mathcal{R}_{D5/\overline{D5}}$) to be less than unity, can be effected, e.g., by noting from (125) that r_h is an increasing function of S_{BH}, and therefore: $r_h(S_{\mathrm{BH}}) \to \frac{r_h(S_{\mathrm{BH}})}{r_h(S^0_{\mathrm{BH}}:t_{\mathrm{Page}}(S^0_{\mathrm{BH}})>0)}$. Therefore, for the values of $N, M, g_s, c_1, c_2, n_{t_b}, \kappa_{l_p}$ chosen, this would imply $r_h \to \frac{r_h(S_{\mathrm{BH}})}{r_h(S_{\mathrm{BH}}\approx 8)}$.

It appears we have disregarded $S^\beta_{\mathrm{EE,HM}}$ altogether. Let us now discuss why the same is justified and how a exponential-large-N-suppression hierarchy is generated in the process.

One can show that:

$$S^\beta_{\mathrm{EE,HM}} \sim \frac{\beta^{4/3} x_R^2 g_s^{\frac{23}{6}} M^3 N_f^{\frac{2}{3}} \log^2(r_h)(\log(N) - 12\log(r_h))(\log(N) - 9\log(r_h))}{r_h^{\frac{5}{2}}(\log N - 3\log r_h)^{\frac{7}{6}}}$$
$$\times \left(-216\left(16+\sqrt{2}\right)g_s^4\kappa_{\lambda_1}M^4 N_f^2 \log(N)\log^3(r_h) + 9\left(16+\sqrt{2}\right)g_s^4\kappa_{\lambda_1}M^4 N_f^2 \log^2(N)\log^2(r_h)\right.$$
$$\left. +1296\left(16+\sqrt{2}\right)g_s^4\kappa_{\lambda_1}M^4 N_f^2\log^4(r_h) + 4096\left(4+\sqrt{2}\right)\pi^4\kappa_{\lambda_2}\right), \tag{127}$$

which in the $|\log r_h| \gg \log N$-limit, approximates to:

$$\frac{\beta^{4/3} g_s^{47/6} M^7 N^{3/10} N_f^{8/3} x_R^2 \log(2)(-\log(r_h))^{41/6}}{r_h^{5/2}}. \tag{128}$$

Using (123), (128) yields,

$$\frac{g_s^{47/6} M^7 N^{3/10} N_f^{8/3} x_R^2 e^{-2\kappa_{l_p}N^{\frac{1}{3}}}(-\log(r_h))^{41/6}}{\sqrt{r_h}}. \tag{129}$$

Similarly,

$$S^\beta_{\mathrm{EE,IS}} \sim \frac{\beta^2 g_s^{15/2}\sqrt{\kappa_\alpha}\kappa_\sigma^{5/2}\kappa_{U_1}M^2 N \log^2(N)(a_2 r_h + a_3)\sqrt{3a_2^2 a_3 r_h^2 + 2a_2^3 r_h^3 + 3a_2 a_3^2 r_h + a_3^3}}{a_2^{5/2}\kappa_{\lambda_5}r_h^{35/2}(-\log(r_h))^{2/3}}$$
$$\times \left(6561\sqrt[6]{2}\left(1+8\sqrt{2}\right)g_s^{17/6}\kappa_{\lambda_3}M^6 N_f^{7/3} r_h^8\log^6(r_h) + 1048576\sqrt[3]{6}\pi^{47/6}\kappa_\alpha^2\kappa_{Z_1}N^2(-\log(r_h))^{2/3}\right)$$
$$\approx \frac{17\beta^2 g_s^{15/2}\log N^2 M^2 N^3(a_2 r_h + a_3)\sqrt{3a_2^2 a_3 r_h^2 + 2a_2^3 r_h^3 + 3a_2 a_3^2 r_h + a_3^3}}{a_2^{5/2}r_h^{35/2}}, \tag{130}$$

which in the $a_2 r_h \gg a_3$-limit yields,

$$\frac{\beta^2 g_s^{15/2}\log N^2 M^2 N^3}{r_h^{15}}. \tag{131}$$

Using (123), (131) yields:

$$\frac{g_s^{15/2}\log N^2 M^2 N^3 e^{-3\kappa_{l_p}N^{\frac{1}{3}}}}{r_h^{12}}. \tag{132}$$

From (90), (124), (129), and (132), one sees the following hierarchy:

$$S^{\mathrm{HM},\beta^0}_{\mathrm{EE}} : S^{\mathrm{IS},\beta^0}_{\mathrm{EE}} : S^{\mathrm{HM},\beta}_{\mathrm{EE}} : S^{\mathrm{IS},\beta}_{\mathrm{EE}} \sim \gamma^{\frac{3}{2}} : \gamma^{\frac{3}{2}} : \gamma^2 : \gamma^3, \tag{133}$$

where $\gamma \equiv e^{-\kappa_{l_p}N^{\frac{1}{3}}}$. From the above equation we can see that $O(\beta)$ corrections to entanglement entropies for the Hartman-Maldacena-like and island surfaces are more exponentially large-N suppressed. Therefore we have disregarded those contributions for the computation of Page curve.

VI. MASSLESS GRAVITON—THE PHYSICAL REASON FOR EXPONENTIALLY SUPPRESSED ENTANGLEMENT ENTROPIES

We now aim at presenting a physical reason behind the exponential suppression of the entanglement entropies of the HM-like and island surfaces in Sec. V D. The essence of the discussion is the following. We will show that despite the coupling of a nongravitational bath to the ETW-brane,

(imposition of Dirichlet boundary condition at the horizon on the radial profile of the graviton wave function) results in the quantization of the graviton mass, which (for an appropriate choice of the quantum number) can therefore be taken to be massless. Usually in the context of AdS_{d+1} gravity duals of CFT_d on ∂AdS_{d+1} at zero temperature, massless graviton implies a vanishing angle between the ETW/KR-brane and ∂AdS_{d+1}, which further implies the islands cease to contribute [17,30]. However, as shown/implied in Sec. III, the ETW-brane in our setup, $x^1 = $ constant, is orthogonal (in the $x^1 - r$-plane) to the thermal bath/QCD-like theory [after having integrated out the angular directions of $\mathcal{M}_6(\theta_{1,2}, \phi_{1,2}, \psi, x^{10})$]. Despite the same, we will show that one obtains a massless graviton in our setup.[9] What is more interesting is that there is a comparable exponential-in-N suppression in the HM-like entanglement entropy which is why the two can be compared at the Page time and one obtains a Page curve.

As in [74], let us write the $D = 11$ metric as:

$$ds^2 = e^{2A(y)}\bar{g}_{\mu\nu}(x)dx^\mu dx^\nu + \hat{g}_{mn}dy^m dy^n. \quad (134)$$

As the resolution parameter a, up to LO in $\frac{g_s M^2}{N}$, is proportional to r_h [47,68,75], strictly speaking (134) is applicable if one disregards $\mathcal{O}(\frac{a^4}{r^4})$ terms (working in the IR-UV interpolating region would ensure the same). The perturbed metric that will be considered is: $\widetilde{ds^2} = e^{2A(y)}(\bar{g}_{\mu\nu} + h_{\mu\nu})dx^\mu dx^\nu + \hat{g}_{mn}dy^m dy^n$, $h_{\mu\nu}(x,y) = h_{\mu\nu}^{[tt]}(x)\psi(y)$ (as ansatz under linear perturbations): $\bar{D}^\mu h_{\mu\nu}^{[tt]} = \bar{g}^{\mu\nu}h_{\mu\nu}^{[tt]} = 0$, and [74]

$$-\frac{e^{-2A(y)}}{\sqrt{|\hat{g}(y)|}}\partial_m(\sqrt{|\hat{g}(y)|}\hat{g}^{mn}e^{4A(y)}\partial_n\psi(y)) = m^2\psi(y). \quad (135)$$

Under the simplifying assumption of localization around, say, $(\theta_1, \theta_2) \sim (\frac{\alpha_{\theta_1}}{N^{\frac{1}{5}}}, \frac{\alpha_{\theta_2}}{N^{\frac{3}{10}}})$ near which one can show that $\psi(r, \theta_{1,2}, \phi_{1,2}, \psi, x^{10}) \to \psi(r, \theta_1)$, the eigenvalue

Eq. (135) up to LO in N in the IR-UV interpolating region reduces to:

$$-\frac{\partial^2\psi(r,\theta_1)}{\partial r^2} + \frac{16(r^4 + r_h^4)}{(r^4 - r_h^4)}\frac{\partial\psi(r,\theta_1)}{\partial r}$$
$$+ \kappa_{r\theta_1}\frac{N^{4/5}r^6}{g_s^3 M^2 N_f^2 (r^2 - 3a^2)^2 (r^4 - r_h^4)(\log N - 9\log r)^2 (\log r)^2}$$
$$\times\left(\frac{\partial^2\psi(r,\theta_1)}{\partial\theta_1^2} - 2\frac{\partial\psi(r,\theta_1)}{\partial\theta_1}\right) - m^2\psi(r,\theta_1) = 0, \quad (136)$$

or, equivalently, using separation of variables $\psi(r,\theta_1) = \mathbb{R}(r)\Theta(\theta_1)$:

$$\left(-\frac{1}{\mathcal{R}(r)}\mathbb{R}''(r) + \frac{1}{\mathbb{R}(r)}\frac{16(r^4 + r_h^4)}{(r^4 - r_h^4)}\mathbb{R}'(r) - m^2\right)$$
$$\left(\kappa_{r\theta_1}\frac{N^{4/5}r^6}{g_s^3 M^2 N_f^2(r^2 - 3a^2)^2(r^4 - r_h^4)(\log N - 9\log r)^2(\log r)^2}\right)^{-1}$$
$$= \frac{1}{\Theta(\theta_1)}(\Theta''(\theta_1) - 2\Theta'(\theta_1)) \equiv \lambda \quad (137)$$

The solution to $\Theta(\theta_1)$ equation in (137):

$$e^{\theta_1(1\pm\sqrt{1+\lambda})}, \quad (138)$$

which can be meaningful if $\lambda = 0$; we hence obtain: $\Theta(\theta_1) = $ Constant.

The EOM for the radial profile $\mathbb{R}$ from (137), is given as under:

$$-\mathbb{R}''(r) + \left(\frac{8}{r - r_h} - \frac{4}{r_h} + \mathcal{O}(r - r_h)\right)\mathbb{R}'(r) - m^2\mathbb{R}(r) = 0. \quad (139)$$

As EOM (135) is homogeneous, $\psi \to m^2\psi(r)$ is also a valid solution which yields:

$$m^2 c_1 U\left(-\frac{8 - 5\sqrt{4 - m^2 r_h^2}}{\sqrt{4 - m^2 r_h^2}}, 10, \frac{2r\sqrt{4 - m^2 r_h^2}}{r_h} - 2\sqrt{4 - m^2 r_h^2}\right)\exp\left(\frac{r(-\sqrt{4 - m^2 r_h^2} - 2) + 9r_h\log(r_h - r)}{r_h}\right)$$
$$+ m^2 c_2 L^9_{\frac{8 - 5\sqrt{4 - m^2 r_h^2}}{\sqrt{4 - m^2 r_h^2}}}\left(\frac{2r\sqrt{4 - m^2 r_h^2}}{r_h} - 2\sqrt{4 - m^2 r_h^2}\right)\exp\left(\frac{r(-\sqrt{4 - m^2 r_h^2} - 2) + 9r_h\log(r_h - r)}{r_h}\right). \quad (140)$$

---

[9]See [73] in the context of islands in black holes in AdS_4 coupled to an external bath embedded in type IIB string theory supporting light gravitons.

If $c_2 = 0$ then

$$m^2 U\left(-\frac{8-5\sqrt{4-m^2 r_h^2}}{\sqrt{4-m^2 r_h^2}}, 10, \frac{2r\sqrt{4-m^2 r_h^2}}{r_h} - 2\sqrt{4-m^2 r_h^2}\right) \exp\left(\frac{r(-\sqrt{4-m^2 r_h^2}-2)+9r_h \log(r_h-r)}{r_h}\right)$$

$$= \frac{e^{-2-\sqrt{4-m^2 r_h^2}}}{\sum_{l=0}^3 c_l(mr_h)^{2l}\Gamma\left(-4-\frac{8}{\sqrt{4-m^2 r_h^2}}\right)}[1+\mathcal{O}((r-r_h)^2)]. \tag{141}$$

If one imposes Dirichlet b.c.[10] at $r = r_h$: $\psi(r = r_h) = 0$ then one sees that one would require $-4 - \frac{8}{\sqrt{4-m^2 r_h^2}} = -n, n \in \mathbb{Z}^+$, i.e.,

$$m = \frac{2\sqrt{n(n-8)}}{4r_h(1-n)} \xrightarrow{n=8} 0. \tag{142}$$

One notes that,

$$U\left(-\frac{8-5\sqrt{4-m^2 r_h^2}}{\sqrt{4-m^2 r_h^2}}, 10, \frac{2r\sqrt{4-m^2 r_h^2}}{r_h} - 2\sqrt{4-m^2 r_h^2}\right)$$

$$\times \exp\left(\frac{r(-\sqrt{4-m^2 r_h^2}-2)+9r_h \log(r_h-r)}{r_h}\right) \xrightarrow{m=0} -\frac{c_1 r_h^9 \Gamma(9, \frac{4r}{r_h}-4)}{262144 e^4}$$

$$= -\frac{315(c_1 r_h^9)}{2048 e^4} + \frac{c_1(r-r_h)^9}{9e^4} + \mathcal{O}((r-r_h)^{10}). \tag{143}$$

If $c_1 = 0$ then $c_2 L^9_{\frac{8-5\sqrt{4-m^2 r_h^2}}{\sqrt{4-m^2 r_h^2}}}\left(\frac{2r\sqrt{4-m^2 r_h^2}}{r_h} - 2\sqrt{4-m^2 r_h^2}\right)$

$\times \exp\left(\frac{r(-\sqrt{4-m^2 r_h^2}-2)+9r_h \log(r_h-r)}{r_h}\right)$ satisfies Dirichlet/ Neumann b.c. $\forall m$. In particular for $m = 0$, the above yields $c_2 e^{-\frac{4r}{r_h}}(r_h - r)^9 L^9_{-1}(\frac{4r}{r_h} - 4)$. Interestingly, $\frac{d^n}{dr^n} L^9_{-1}\left(\frac{4r}{r_h} - 4\right) = (-4)^n \frac{1}{r_h^n} L^{n+9}_{-n-1}\left(\frac{4r}{r_h} - 4\right)$, implying $\lim_{r \to r_h} L^{n+9}_{-n-1}\left(\frac{4r}{r_h} - 4\right) = \binom{8}{n+9} = 0$.

In the UV, the EOM up to LO in $N, N_f^{\text{UV}}, M^{\text{UV}}$, is

$$-\frac{\partial^2 \psi_{\text{UV}}(r,\theta_1)}{\partial r^2} + \frac{16}{r}\frac{\partial \psi_{\text{UV}}(r,\theta_1)}{\partial \theta_1}$$

$$- 2\kappa_{r\theta_1} \frac{N^{4/5}}{g_s^3 M_{\text{UV}}^2 N_{frmUV}^2 (\log N - 9\log r)^2 (\log r)^2 r^2}$$

$$\times \frac{\partial \psi_{\text{UV}}}{\partial \theta_1} - m^2 \psi_{\text{UV}}, \tag{144}$$

whose solution is given as:

$$\psi_{\text{UV}} \sim \frac{1}{m^{17/2}}\left[c_1 \sum_{l_1=0}^3 a_{l_1}(mr)^{2l_1+1}\cos(mr)\right.$$

$$\left. + \left(c_1 \sum_{l_2=0}^4 a_{l_2}(mr)^{2l_2} + c_2 \sum_{l_1=0}^3 (mr)^{2l_1+1}\right)\sin(mr)\right]. \tag{145}$$

As the above, for $m \neq 0$, is ill-behaved in the UV, one is required to set $m = 0$ for which

$$\mathbb{R}_{\text{UV}}(r) = c_1^{\text{UV}} r^{17} + c_2^{\text{UV}}. \tag{146}$$

For $\psi(r)$ to be normalizable, one has to set $c_1^{\text{UV}} = 0$ implying, as expected a constant graviton wave function in the UV.

One thus sees the physical/intuitive reason for the exponentially suppressed entanglement entropy for island surface (124) is that the Laplace-Beltrami equation for the internal coordinates (135) permits a vanishing graviton mass—this is also related to the fact that our computations are in the "near-horizon" limit ($r < (4\pi g_s N)^{1/4}$) wherein even the UV cutoff $r_{\text{UV}} \tilde{<} (4\pi g_s N)^{1/4}$ and hence the internal manifold is not noncompact [74]. This is what is responsible for the very small (involving exponential-in-N suppression) entanglement entropy of the Island surface. What

---

[10]Neumann b.c., $\psi'(r = r_h) = 0$, is identically satisfied $\forall m$.

is nontrivial and therefore extremely interesting is a comparable entanglement entropy of the Hartman-Maldacena-like surface in (90) near the Page time. The vanishing graviton mass further manifests itself at $\mathcal{O}(\beta)$ in the entanglement entropies of the IS-vs-HM-like surfaces in (133)—the former is suppressed relative to the latter.

Now using $r = r_h e^Z$,[11] we can convert Eq. (137) into the following Schrödinger-like equation

$$-R''(Z) + V(Z)R(Z) = 0, \qquad (147)$$

where

$$R(Z) = \mathbb{R}(Z)e^{r_h(-8e^Z + \frac{Z}{2r_h} + 8\tan^{-1}(e^Z) + 8\tanh^{-1}(e^Z))} \approx \mathbb{R}(Z)e^{\frac{Z}{2}}, \qquad (148)$$

and,

$$V(Z) = -\frac{e^{2Z}r_h^2((m^2-64)e^{8Z} - 2(m^2+64)e^{4Z} + m^2 - 64)}{(e^{4Z}-1)^2}$$
$$+ \frac{64e^{5Z}r_h}{(e^{4Z}-1)^2} + \frac{1}{4} \qquad (149)$$

The above potential for massless graviton ($m = 0$) is plotted in Fig. 9; this potential is "volcano"-like with the massless graviton localized near the horizon on the ETW brane. This is similar to [15] wherein one can localize gravity on ETW brane for nonzero brane tension due to appearance of "crater" in "volcano" potential appearing in Schrödinger-like equation of motion of graviton wave function.

In our setup, the ETW-brane has nonzero "tension" (24) and therefore it is possible to localize gravity on ETW-brane. Using (143), one sees that in the massless-limit of the graviton, the graviton wave function is indeed localized near the horizon as shown in Fig. 10. Alternatively, expanding $V(Z)$ of (149) around the horizon $Z = 0$ and obtaining: $V(Z \sim 0) \sim \frac{4r_h(1+4r_h)}{Z^2} + \frac{4r_h(1+8r_h)}{Z} - \frac{1}{12}(-3 + 40r_h - 896r_h^2) + \mathcal{O}(Z)$, one obtains:

$$R(Z) = c_1 M_{-\frac{4\sqrt{3}r_h(8r_h+1)}{\sqrt{896r_h^2-40r_h+3}}, 4r_h+\frac{1}{2}}\left(\frac{\sqrt{896r_h^2 - 40r_h + 3Z}}{\sqrt{3}}\right)$$
$$+ c_2 W_{-\frac{4\sqrt{3}r_h(8r_h+1)}{\sqrt{896r_h^2-40r_h+3}}, 4r_h+\frac{1}{2}}\left(\frac{\sqrt{896r_h^2 - 40r_h + 3Z}}{\sqrt{3}}\right). \qquad (150)$$
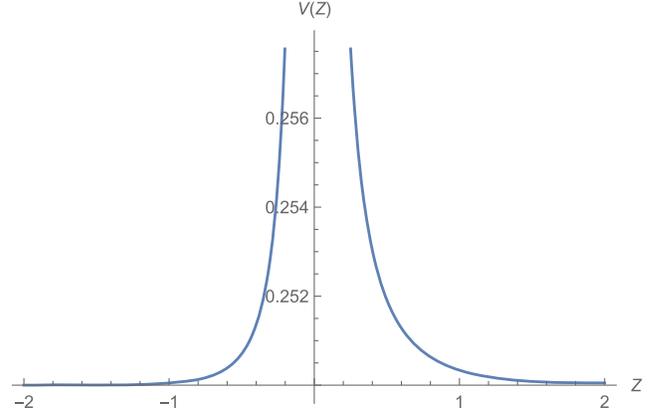
FIG. 9. Volcano potential for massless graviton from (149).
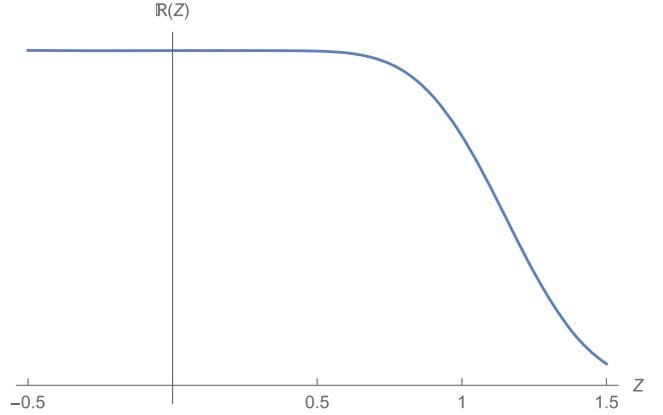
FIG. 10. Localization of the graviton wave function near the horizon from the $m = 0$-limit of the solution (143) of (139).
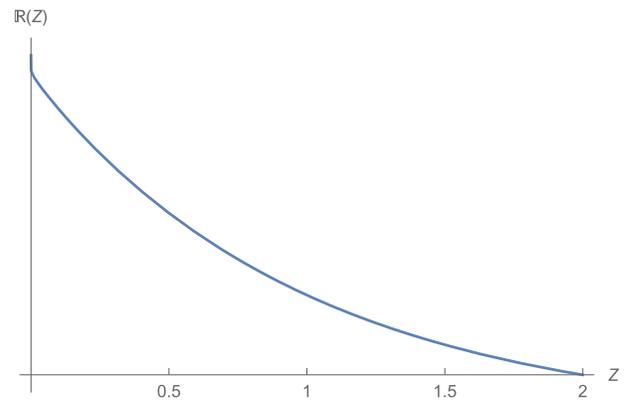

FIG. 11. Localization of the graviton wave function near the horizon from the solution of the Schrödinger-like radial wave Eq. (147).

Now, both Whittaker functions are complex for $Z < 0$, i.e., $r < r_h$. Setting $c_1 = 0$, one obtains

$$\mathbb{R}(Z) = e^{-\frac{Z}{2}} W_{-\frac{4\sqrt{3}r_h(8r_h+1)}{\sqrt{896r_h^2-40r_h+3}}, 4r_h+\frac{1}{2}}\left(\frac{\sqrt{896r_h^2-40r_h+3Z}}{\sqrt{3}}\right), \text{ and hence}$$

the following plot which indicates a decay of the graviton wave function away from the horizon.

VII. SUMMARY

Following is the summary of the key steps and results that were obtained in this paper.

(1) We discussed the doubly holographic setup in the context of M theory background in II B summarized in Fig. 1. The main idea is that we consider an ETW-brane at $x = 0$ in Fig. 2, which contains the black hole and then we couple the ETW-brane to a nonconformal bath (QCD in 3 dimensions after integrating out the angular coordinates and wick rotation along x^3). We then discussed how we can calculate the entanglement entropy of Hawking radiation using the prescription of [10] for higher derivative gravity theories. We derived the ETW-brane embedding in M-theory background in Sec. III. First we considered the Einstein Hilbert term and the GHY term along with the tension of the ETW-brane and obtained the embedding (21). By using the induced metric (20) on the ETW, we computed various terms appearing in Eq. (21) and found that at $\mathcal{O}(\beta^0)$ the embedding of the ETW-brane will be given by constant x [Eq. (25)]. Given that in the MQGP limit of (4), the J_0 dominates over the E_8 and $t_8^2 G^2 R^3$ terms in the $\mathcal{O}(R^4)$ terms in (14), we work with only the J_0 term. We found that the ETW-brane embedding obtained with just EH-GHY terms, continues to hold even with the inclusion of the J_0 term as restricted to the same (embedding) the boundary term involving covariant derivative of the metric variation (that one would have had to cancel by construction of an appropriate boundary term relevant to the J_0 term), vanishes.

(2) Given the robustness of the islands picture, the M-theory dual of large-N thermal QCD at high temperature constructed in [4,36] (based on [34]) too is thus expected to generate a Page curve. The aforementioned top-down M-theory dual however offers the following additional conceptual insights:

(a) There are very few papers (e.g., [22]) wherein the authors discuss doubly holographic setup in higher derivative theory of gravity because of absence of the knowledge of explicit forms of boundary terms on the ETW-brane with the inclusion of higher derivative terms. As we explicitly show in Sec. III B, no boundary terms are generated from the inclusion of the $\mathcal{O}(R^4)$ terms.

(b) To the best of our knowledge, our model/ (aforementioned) M-theory dual is either the only one (from M theory) or one of the very few top-down models that obtain(s) the Page curve for massless graviton[12] in VI.

(c) In our top-down M-theory dual, we find that ETW-brane to be a fluxed hypersurface $\mathcal{W}$ that is a warped product of an asymptotic AdS$_4$ and a six-fold M_6 where M_6 is a warped product of the M-theory circle and a non-Einstenian generalization of $T^{1,1}$; the hypersurface $\mathcal{W}$, can also be thought of as an effective ETW-brane corresponding to fluxed intersecting $M5$-brane wrapping a homologous sum of $S^3 \times [0,1]$ and $S^2 \times S^2$ in a warped product of $\mathbb{R}^2$ and an $SU(4)/\text{Spin}(7)$-structure eight-fold. The ETW-brane, $\mathcal{W}$, then has nonzero "tension" and a massless graviton localized near the horizon by a volcanolike potential.

(d) Further, unlike almost all the papers in the literature wherein the Page curve computation is done for a CFT bath, in our model, the external bath is a non-CFT bath (thermal QCD).

(e) Entanglement entropy contribution from Hartman-Maldacena (HM)-like surface which is responsible for increase of Einstein-Rosen bridge in time, also exhibits a Swiss-cheese structure in the large-N scenario (V B).

(f) With the inclusion of $\mathcal{O}(R^4)$ terms in the action, our aforementioned M-theory dual yields a hierarchy in the entanglement entropies of the HM-like and island surface (IS) with respect to a large-N exponential suppression factor, physically arising from the existence of massless graviton mode on the ETW-brane. This suppression further implies that the Page curve is unaffected by the inclusion of higher derivative—$\mathcal{O}(R^4)$ in particular—terms.

(g) To tame the IR- and large-N enhancement in the IS entanglement entropy per unit BH entropy to ensure the same is around 2 in Sec. IV A, along with dimensional considerations of Sec. IV A, a connection between the Planckian length and the nonextremality parameter (the horizon radius) is shown to arise in Sec. IV A.

(3) In Secs. IV A and IV B, using the Ryu-Takayanagi formula (since we are not considering higher derivative terms in the gravitational action in this part), we calculated the entanglement entropies of HM-like and islands surfaces (IS) by computing the areas of the codimension two surfaces for the HM-like and island surfaces. The entanglement entropy for HM-like surface was calculated in (52) using (47), which shows linear time dependence. If one

---

[12]See [59] in which author has discussed that one can get Page curve for massless graviton in critical Randall-Sundrum II model from a bottom-up approach.

does not consider the island surface then (52) implies that at late times [i.e., beyond the Page time) we have infinite amount of Hawking radiation. The entanglement entropy of the island surface (65) was calculated using (63)]. If we are below the Page time then entanglement entropy of HM-like surface dominates which shows linear time dependence and after the Page time the

entanglement entropy of island surface, which is constant, dominates. Therefore combination of the two produces the Page curve of an eternal black hole in Fig. 3.

In $\mathcal{R}_{D5/\overline{D5}} = 1$-units, using (52), (65), (A7) and $r_h \sim e^{-\kappa_{r_h} N^{\frac{1}{3}}}$ [68], the aforementioned is succinctly captured by:

$$S^{\mathrm{HM}} = \frac{A_{\mathrm{HM}}}{4 G_N^{(11)}} \sim \frac{\mathcal{O}(1) \times 10^{-4} M^2 N_f^6 g_s^{15/4} N^{34/15} \mathbf{e}^{-6\kappa_{r_h} N^{1/3}}}{G_N^{(11)}} t_b, \qquad t_b \leq t_{\mathrm{Page}};$$

$$\mathcal{S}^{IS} = \mathcal{S}^{IS}\left(\tilde{r}_T \equiv \frac{r_T}{r_h} = (1 + \delta_2); r_h\right), \qquad t_b \geq t_{\mathrm{Page}}, \tag{151}$$

where δ_2 in the turning point r_T is as given in (A7).

(4) In Sec. V, we obtained the Page curve of an eternal black hole in the presence of $\mathcal{O}(R^4)$ terms in eleven dimensional supergravity action. For this purpose use the prescription of [10] as given in (66) to calculate the entanglement entropies of HM-like and island surfaces with the inclusion of $\mathcal{O}(R^4)$ terms. Since in the working action (26) only J_0 term is considered (as it is the most dominant in the MQGP limit) therefore we need to calculate two type of terms appearing in (66). These two type of terms are given in (69) and (70) where we have used $z = xe^{it}$. In Sec. VA, the entanglement entropy for HM-like surface is calculated and it turns out that for Einstein-Hilbert term Dong's prescription [10] produces (72). For the J_0 term there are two types of terms mentioned earlier and these terms are given in (74) and (75). Now if we combine the Einstein-Hilbert and J_0 terms's contribution then we obtain the total entanglement entropy (76) in terms of the embedding function of HM-like surface $t(r)$ and its derivatives. We obtained the on-shell entanglement entropy (91) for HM-like surface at $\mathcal{O}(\beta^0)$ by computing the solution to the EOM for the HM-like surface embedding $t(r)$ (80) and substituting back into (76). Interestingly (91) also has linear time dependence similar to (52).

In VB, with c_1 and c_2 being two parameters in the family of HM-like surface embeddings, curiously, $\frac{\delta S_{\mathrm{EE}}^{\mathrm{HM},\beta^0}}{\delta|c_2|} > 0, \frac{\delta S_{\mathrm{EE}}^{\mathrm{HM},\beta^0}}{\delta|c_1|} < 0$, which along with $|c_2| \sim e^{\kappa_{c_2}|c_1|^{\frac{1}{3}}}, |c_1| \sim N$, provides a perfect "Swiss-cheese" (of the "single-big-divisor-single-small-divisor" variety) structure to $S_{\mathrm{EE}}^{\mathrm{HM},\beta^0}(|c_1|, |c_2|)$ (which essentially is a codimension-two volume) wherein $\log|c_2|$ plays the role of the "big divisor" volume and

$\log|c_1|$ plays the role of a solitary "small divisor" volume, realizing what could be dubbed as a "Large N scenario"(LNS). Alternatively, the entanglement entropy for the Hartman-Maldacena-like surface can be viewed as a Swiss-cheese-like open surface in the two-dimensional (in the IR) space of family of HM-like embeddings $\mathbb{R}_+^2(|c_1|, |c_2|)$ augmented by the entanglement entropy that coordinatizes $\mathbb{R}_{\geq 0}(S_{\mathrm{EE}}^{\mathrm{HM},\beta^0})$.

In Sec. VC, we found that entanglement entropy contributions from Einstein-Hilbert and J_0 terms as given in (99), (102), and (103). Combining all these contributions we obtained the total entanglement entropy in (105) in terms of embedding function of island surface and its derivatives. We solved the embedding EOM for the island surface similar to HM-like surface and the solution is given in (115). Now, using the solution we obtained the entanglement entropy for island surface at the level of EH-GHY terms by substituting back in (105). This yields that the entanglement entropy will be of the form given in (118). Given that the turning point lies deep in the IR, the entanglement entropy for HM-like and island surfaces at $\mathcal{O}(\beta^0)$ came out to be proportional to β, an obvious but apparent contradiction. This was resolved by proposing a $\beta/l_p - r_h$ relation as discussed above (120) and its explicit form as given in (123). The on-shell entanglement entropy for island surface turns out to be (124). Upon plotting the entanglement entropy contributions from HM-like (91) and island surfaces (124) we obtained the Page curve shown in Fig. 7.

The aforementioned is neatly summarized below. Using the HM-like embedding (80), and (89) and (90), the on-shell entanglement entropy (EE) for HM-like surface is given by:

$$S_{\text{EE}}^{\beta^0,\text{HM}} \sim e^{-\frac{3\kappa_{l_p} N^{\frac{1}{3}}}{2}} M N^{13/10} N_f^{5/3} \left(1 - \frac{4t_{b_0}}{3c_2}\right) \left(\frac{2}{3}\log\left(\frac{c_2}{c_1}\right) - n_{t_b}\log(N)\right)^{\frac{17}{6}}, \qquad \kappa_{l_p} \equiv \frac{1}{\mathcal{O}(1)},$$

$$c_{1,2} < 0, |c_2| \gg |c_1|; |c_2| \sim e^{\kappa_{c_2}|c_1|^{1/3}}, \qquad \kappa_{c_1} \equiv \mathcal{O}(1)$$

$$t \le t_{\text{Page}}, \tag{152}$$

and using the embedding (115), and (124), (126), (128), and (132), the on-shell EE for island surface is given by:

$$S_{\text{EE}}^{\beta^0,\text{IS}} \sim \frac{M^2 e^{-\frac{3\kappa_{l_p} N^{\frac{1}{3}}}{2}} N_f^{4/3} g_s^{35/6} \log^2(N) |\log(r_h)|^{4/3}}{r_h^{11/2}},$$

$$t \ge t_{\text{Page}}. \tag{153}$$

The above can be shown to be consistent with the RT computation summarized earlier.[13]

(5) Positivity of the Page time—worked out in (126)—is shown to provide an upper bound on the non-extremality parameter—the black-hole horizon radius r_h.

(6) We computed the $\mathcal{O}(\beta)$ contributions to the HM-like and island surfaces as given in (128) and (131) and we show in (133) that there is hierarchy between the $\mathcal{O}(\beta^0)$ and $\mathcal{O}(\beta)$ contributions. To be a bit more specific, as the turning point for the Hartman-Maldacena-like surface $r_*: r_* - r_h \sim \beta^{\frac{2}{3}}$, and that for Island surface $r_T: r_T - r_h \sim \beta^2$, one obtains the following exponential hierarchy: $S_{\text{EE}}^{\text{HM},\beta^0}: S_{\text{EE}}^{\text{IS},\beta^0}: S_{\text{EE}}^{\text{HM},\beta}: S_{\text{EE}}^{\text{IS},\beta} \sim \gamma^{\frac{3}{2}}: \gamma^{\frac{3}{2}}: \gamma^2: \gamma^3$, where $\gamma \equiv e^{-\kappa_{l_p} N^{\frac{1}{3}}}$. Therefore we can neglect the $\mathcal{O}(\beta)$ contributions to the entanglement entropy for both extremal surfaces. The exponentially suppressed $S_{\text{EE}}^{\text{IS},\beta^0}$ and the suppression of $S_{\text{EE}}^{\text{IS},\beta}$ relative to $S_{\text{EE}}^{\text{HM},\beta}$ is argued in Sec. VI to be due to the existence of a massless graviton. It is also rather nontrivial to have a similar exponential suppression in $S_{\text{EE}}^{\text{HM}}$ so that the same could be matched with $S_{\text{EE}}^{\text{IS}}$ at the Page time, and a Page curve obtained.

(7) Motivated by the requirement $\frac{S_{\text{EE}}^{\beta^0,\text{IS}}}{S_{\text{BH}}} \sim e^{-\kappa_{l_p} N^{1/3}}$ $\mathcal{F}(M,N,N_f;r_h)\left[1 + \sum_{n=1}^{\infty} \mathcal{A}_n \left(\frac{a_3}{a_2 r_h}\right)^n\right]$ [as obtained in (122)] to be less than or equal to 2 up to leading order in the dimensionless "$G_N^{(11)}/r_h^9$" [71], which

for us is $\frac{a_3}{a_2 r_h}$ [$a_{2,3}$ parametrizing the IS-surface embedding (115)], one needs to cure the large-N and IR(via small r_h) enhancements in $\frac{S_{\text{EE}}^{\beta^0,\text{IS}}}{S_{\text{BH}}}$. Utilizing the estimate in [68] of the $r = r_0 \sim r_h: N_{\text{eff}}(r_0 = 0)$, and in particular the exponential N-suppression therein we therefore propose $\beta \sim \left(g_s^{\frac{4}{3}} \alpha'^2 e^{-\kappa_{l_p} N^{1/3}} \frac{r_h}{\mathcal{R}_{D5/\overline{D5}}}\right)^{3/2}$. This further requires (see Fig. 6) a lower bound on the non-extremality parameter—the black-hole horizon. With the inclusion of the $\mathcal{O}(R^4)$ terms in M theory, the fact the turning point associated with the xHartman-Maldacena-like surface is in the deep IR, also require the aforementioned β- or $l_p - r_h$ relation.

Some open questions related to our work are

(i) How the holographic complexity will be modified in the presence of $\mathcal{O}(R^4)$ terms in the gravitational action [76]?

(ii) What will be the effect of higher derivative [$\mathcal{O}(R^4)$] terms on the reflected entropy [77]?

We will return to these issues in our future work.

ACKNOWLEDGMENTS

APPENDIX A: HM-LIKE/IS ANALYTICS/ NUMERICS

In this appendix, we discuss (i) the angular integrations which have been used in the paper and have written the expression for the area of Hartman-Maldacena-like surface, and (ii) how to obtain an estimate on the turning point in the context of island surface entanglement entropy.

---

[13]Compatibility of (151) and (152) (using footnote 8) requires $\kappa_{r_h}, \kappa_{l_p}, \kappa_{c_2}: M^2 N_f^6 g_s^{15/4} N^{34/15} e^{-6\kappa_{r_h} N^{1/3}} \sim M N^{13/10} N_f^{5/3}$ $\left(\frac{2}{3}[\kappa_{c_2} N^{1/3} - \log|c_1|] - n_{t_b}\log(N)\right)^{\frac{17}{6}} e^{-\frac{3\kappa_{l_p} N^{1/3}}{2}}$ (for compatibility of $S_{\text{EE}}^{\beta^0,\text{HM}}$ obtained from computation of the area of the HM-like surface and from Wald entanglement entropy) and $11\kappa_{r_h} < 3\kappa_{l_p}$ (for $S_{\text{EE}}^{\beta^0,\text{IS}}$ to be well defined in the large-N limit).

1. HM-like surface area

The angular integrations, in promoting the delocalized results around $(\theta_1, \theta_2) = \left(\frac{\alpha_{\theta_1}}{N^{\frac{1}{5}}}, \frac{\alpha_{\theta_2}}{N^{\frac{3}{10}}}\right)$, to global results, disregarding all contributions of $\mathcal{O}\left(\frac{\mathcal{O}(1)}{N^\alpha}\right)$, $\alpha > 1$, have been performed as under. Promoting $(x, y, z) \to (\phi_1, \phi_2, \psi)$ via [36]:

$$dx = \sqrt{h_2}(g_s N)^{\frac{1}{4}}\left[1 + \mathcal{O}\left(\frac{g_s M^2}{N}\right) + \mathcal{O}\left(\frac{(g_s M^2)(g_s N_f)}{N}\right)\right]\sin\theta_1 d\phi_1,$$

$$dy = \sqrt{h_4}(g_s N)^{\frac{1}{4}}\left[1 + \mathcal{O}\left(\frac{g_s M^2}{N}\right) + \mathcal{O}\left(\frac{(g_s M^2)(g_s N_f)}{N}\right)\right]\sin\theta_2 d\phi_2,$$

$$dz = \sqrt{h_1}(g_s N)^{\frac{1}{4}}\left[1 + \mathcal{O}\left(\frac{g_s M^2}{N}\right) + \mathcal{O}\left(\frac{(g_s M^2)(g_s N_f)}{N}\right)\right]d\psi, \tag{A1}$$

where $h_1 = \frac{1}{9} + \mathcal{O}\left(\frac{g_s M^2}{N}\right), h_2 = \frac{1}{6} + \mathcal{O}\left(\frac{g_s M^2}{N}\right), h_4 = h_2 + \frac{4a^2}{r^2}$ [34,36],

$$\frac{1}{\alpha_{\theta_1}^3 \alpha_{\theta_2}^2} \to \lim_{\epsilon_{1,2}\to 0}\int_{\epsilon_2}^{\pi-\epsilon_2}\sqrt{g_s N}d\theta_2 \sin\theta_2 \int_{\epsilon_1}^{\pi-\epsilon_1}d\theta_1 \sin\theta_1 \frac{1}{(N^{\frac{1}{5}}\sin\theta_1)^3(N^{\frac{3}{10}}\sin\theta_2)^2} \sim \lim_{\epsilon_{1,2}\to 0}\frac{|\log\epsilon_2|}{N^{\frac{7}{10}}\epsilon_1}. \tag{A2}$$

The principal($\mathcal{P}$) value of (A2) is obtained by approximating $|\log\epsilon_2|$ by $\log\mathbb{P} + |\log\epsilon_2|, \mathbb{P} \in \mathbb{Z}^+$ and requiring $\log\mathbb{P} + \log\epsilon_2 = -\epsilon_1$, or $\epsilon_2 = \frac{e^{-\epsilon_1}}{\sqrt{\mathbb{P}}}, \mathbb{P} > 1$. Similarly,

$$\frac{1}{\alpha_{\theta_1}\alpha_{\theta_2}^6} \to \lim_{\epsilon_{1,2}\to 0}\int_{\epsilon_2}^{\pi-\epsilon_2}\sqrt{g_s N}d\theta_2 \sin\theta_2 \int_{\epsilon_1}^{\pi-\epsilon_1}d\theta_1 \sin\theta_1 \frac{1}{(N^{\frac{1}{5}}\sin\theta_1)(N^{\frac{3}{10}}\sin\theta_2)^6} \xrightarrow{\mathcal{P}} \frac{\pi(540\log(2) - 107)\sqrt{g_s}}{720 N^{3/2}}. \tag{A3}$$

Assuming $r_* \in$ IR, approximating $\log r \approx \log r_h$ for $r = v r_h \ \forall \ r \in$ IR, $v = \mathcal{O}(1)$, one obtains the following expression after radial integration of Eq. (48):

$$A_{\text{HM}} \sim \left[EM^2 \sqrt[10]{N} N N_f^6 g_s^{17/4} \log^2(r_h)(\log(N) - 3\log(r_h))^4 \right.$$

$$\times \left(3r_*^5(\log(N) - 9\log(r_h))^2 - 10r_*^3 r_h^2 \log(N)(\log(N) - 9\log(r_h))\right.$$

$$\left.+ 15 r_* r_h^4 \log^2(N) - r_h^5(36\log(N)\log(r_h) + 243\log^2(r_h) + 8\log^2(N))\right)\right]. \tag{A4}$$

2. IS turning point

In the context of IS entanglement entropy (65), to get an estimate of the turning point $\tilde{r}_T$, one notes that: $\frac{H(r_T)}{\sigma(r_T)} = \mathcal{C}^2$, up to LO in N, that obtains:

$$1458 g_s^{5/4} M^2 N^{2/5} N_f^6 r_T^4 (r_T^4 - r_h^4) \log^7(r_T)$$

$$\times (7\log N r_T^2 - 3a^2 \log N)$$

$$- 6561 g_s^{5/4} M^2 N^{2/5} N_f^6 r_T^6 (r_T^4 - r_h^4) \log^8(r_T)$$

$$+ \mathcal{O}\left(\frac{1}{(\log r_h)^6}\right) = \tilde{\mathcal{C}}^2. \tag{A5}$$

Writing $\tilde{r}_T = 1 + \delta_2$, upon substitution into (A5), and assuming $0 < \delta_2 \ll 1$ and thereby approximating $\log r \approx \log r_h$, yields the following:

$$1458\delta_2 r_h^{10} \log^7(r_h)(4(47\delta_2 + 6)\log N$$

$$- 9(15\delta_2 + 2)\log(r_h))$$

$$- 5832\sqrt{3}\delta_2(11\delta_2 + 2)\epsilon \log N r_h^{10} \log^7(r_h)$$

$$= \frac{M^2 N^{2/5} N_f^6 \tilde{\mathcal{C}}^2}{g_s^{5/4}}. \tag{A6}$$

Assuming again $|\log r_h| \gg \log N$, the relevant solution to (A6) is:

$$\delta_2 \approx \frac{M^2 N^{2/5} N_f^6 \tilde{\mathcal{C}}^2}{26244 g_s^{5/4} r_h^{10} \log^8(r_h)} - \frac{2}{15}. \tag{A7}$$

Guided by the estimate of $r = r_0 \sim r_h$: $N_{\text{eff}}(r_0) = 0$ obtained in [68], writing $r_h \sim e^{-\kappa_{r_h} N^{\frac{1}{3}}}$, and assuming $\tilde{\mathcal{C}}^2 = e^{-\kappa_C N^{\frac{1}{3}}}$. Numerically, for $M = N_f = 3, g_s = 0.1, N = 10^{3.3}$ and assuming $\kappa_C = 1.37, \kappa_{r_h} = 0.1, \tilde{\mathcal{C}} = 3 \times 10^{-8}$ one obtains $\delta_2 = 5.6 \times 10^{-4}$.

APPENDIX B: HARTMAN-MALDACENA-LIKE SURFACE MISCELLANIA

In this appendix we have listed various r dependent functions appearing in the entanglement entropy expression for the Hartman-Maldacena-like surface at $\mathcal{O}(\beta^0)$ and $\mathcal{O}(\beta)$. Additionally we have also worked out the equation of motion for the embedding function of the Hartman-Maldacena-like surface.

(i) The r dependent functions appearing in Eq. (72) are,

$$
\begin{aligned}
\alpha(r) &= \kappa_\alpha \frac{r^2 (N_f g_s (2\log(N) - 6\log(r)))^{2/3}}{\sqrt{N} g_s^{3/2}}, \\
\sigma(r) &= \kappa_\sigma \frac{N g_s - 3M^2 N_f g_s^3 \log(r)(\log(N) - 6\log(r))}{(r^4 - r_h{}^4)}, \\
\lambda(r) &= \kappa_\lambda \left(-\frac{MN^{17/10} N_f^{4/3} g_s^{5/2} (r^2 - r_h{}^2)\log(r)(\log(N) - 9\log(r))\sqrt[3]{\log(N) - 3\log(r)}}{r^4 \alpha_{\theta_1}^3 \alpha_{\theta_2}^2} \right) \\
&\sim -\frac{MN^{21/20} N_f^{4/3} g_s^{13/4} (r^2 - r_h^2)\kappa_\lambda \log(r)(\log(N) - 9\log(r))\sqrt[3]{\log(N) - 3\log(r)}}{3r^4},
\end{aligned}
\tag{B1}
$$

where κ_α, κ_σ and κ_λ are numerical pre-factors.

(ii) In Wald entanglement entropy term (74) for HM-like surface, we have the following r dependent functions:

$$
\begin{aligned}
\lambda_1(r) &= \kappa_{\lambda_1} \left(\frac{M^7 N^{7/10} N_f^{7/3} g_s^7 \log^4(r)(\log(N) - 12\log(r))^3(\log(N) - 9\log(r))}{r^2 \alpha_{\theta_1}^3 \alpha_{\theta_2}^2 (\log(N) - 3\log(r))^{5/3}} \right) \\
&\sim \frac{M^7 \sqrt[20]{N} N_f^{7/3} g_s^{31/4} \kappa_{\lambda_1} \log^4(r)(\log(N) - 12\log(r))^3(\log(N) - 9\log(r))}{3r^2 (\log(N) - 3\log(r))^{5/3}}, \\
\lambda_2(r) &= \kappa_{\lambda_2} \left(\frac{M^3 N^{7/10} \sqrt[3]{N_f} g_s^3 \log^2(r)(\log(N) - 12\log(r))(\log(N) - 9\log(r))}{r^2 \alpha_{\theta_1}^3 \alpha_{\theta_2}^2 (\log(N) - 3\log(r))^{5/3}} \right) \\
&\sim \frac{M^3 \sqrt[20]{N} \sqrt[3]{N_f} g_s^{15/4} \kappa_{\lambda_2} \log^2(r)(\log(N) - 12\log(r))(\log(N) - 9\log(r))}{3r^2 (\log(N) - 3\log(r))^{5/3}}.
\end{aligned}
\tag{B2}
$$

κ_{λ_1} and κ_{λ_2} in the above equation are numerical pre-factors.

(iii) In the anomaly term (75) following are the r dependent functions: 6

$$
\begin{aligned}
\mathcal{L}_1 = \mathcal{L}_2 &= \frac{\sqrt{\alpha(r)\left(\sigma(r) - \left(1 - \frac{r_h^4}{r^4}\right)t'(r)^2\right)}}{t'(r)^2 \left(\sigma(r) - \left(1 - \frac{r_h^4}{r^4}\right)t'(r)^2\right)^4} \left(\alpha'(r)\left(\sigma(r) - \left(1 - \frac{r_h^4}{r^4}\right)t'(r)^2\right) \right. \\
&\quad \left. + \alpha(r)\left(\sigma'(r) - t'(r)\left(\frac{4r_h^4}{r^5} t'(r) + 2\left(1 - \frac{r_h^4}{r^4}\right)t''(r) \right) \right) \right)^2 ; \\
\mathcal{L}_3 = \mathcal{L}_4 &= \frac{\sqrt{\alpha(r)\left(\sigma(r) - \left(1 - \frac{r_h^4}{r^4}\right)t'(r)^2\right)}}{t'(r)^2}.
\end{aligned}
\tag{B3}
$$

(iv) Use has been made of the following for the computation of first and second term in entanglement entropy computation in the presence of higher derivative terms:

$$\frac{\delta J_0}{\delta R_{M_1 N_1 P_1 Q_1}} = G^{M_1 M_1} G^{N_1 N_1} G^{P_1 P_1} G^{Q_1 Q_1} \left(R_{PN_1 P_1 Q} R^{Q}{}_{RSQ_1} + \frac{1}{2} R_{PQP_1 Q_1} R^{Q}{}_{RSN_1} \right) R_{M_1}{}^{RSP}$$

$$+ \left(\delta^{Q_1}_Q R^{HN_1 P_1 K} + \frac{1}{2} \delta^{N_1}_Q R^{HKP_1 Q_1} \right) R_H{}^{RSM_1} R^{Q}{}_{RSK}$$

$$+ G^{N_1 N_1} G^{P_1 P_1} G^{Q_1 Q_1} \left(R_{Q_1 MNQ} R^{M_1 MNK} + \frac{1}{2} R_{Q_1 QMN} R^{M_1 KMN} \right) R^{Q}{}_{N_1 P_1 K}$$

$$+ G^{M_1 M_1} \left(R_{PMNM_1} R^{HMNQ_1} + \frac{1}{2} R_{PM_1 MN} R^{HQ_1 MN} \right) R_H{}^{N_1 P_1 P}, \tag{B4}$$

and

$$\frac{\delta^2 J_0}{\delta R_{M_2 N_2 P_2 Q_2} \delta R_{M_1 N_1 P_1 Q_1}} = A_1 + A_2 + A_3 + A_4, \tag{B5}$$

where

$$A_1 = G^{M_1 M_1} G^{N_1 N_1} G^{P_1 P_1} G^{Q_1 Q_1} \left[\delta^{M_2}_{M_1} G^{N_2 N_2} G^{P_2 P_2} G^{Q_2 Q_2} \left(R_{Q_2 N_1 P_1 Q} R^{Q}{}_{N_2 P_2 Q_1} + \frac{1}{2} R_{Q_2 QP_1 Q_1} R^{Q}{}_{N_2 P_2 N_1} \right) \right.$$

$$+ \left(\delta^{M_2}_P \delta^{N_2}_{N_1} \delta^{P_2}_{P_1} \delta^{Q_2}_Q R^{Q}{}_{RSQ_1} R_{M_1}{}^{RSP} + \frac{1}{2} \delta^{M_2}_P \delta^{N_2}_Q \delta^{P_2}_{P_1} \delta^{Q_2}_{Q_1} R^{Q}{}_{RSN_1} R_{M_1}{}^{RSP} \right)$$

$$+ \left. \left(G^{M_2 M_2} \delta^{N_2}_R \delta^{P_2}_S \delta^{Q_2}_{Q_1} R_{M_1}{}^{RSP} R_{PN_1 P_1 M_2} + \frac{1}{2} G^{M_2 M_2} \delta^{N_2}_R \delta^{P_2}_S \delta^{Q_2}_{N_1} R_{M_1}{}^{RSP} R_{PM_2 P_1 Q_1} \right) \right]$$

$$\equiv G^{M_1 M_1} G^{N_1 N_1} G^{P_1 P_1} G^{Q_1 Q_1} \left[\delta^{M_2}_{M_1} G^{N_2 N_2} G^{P_2 P_2} G^{Q_2 Q_2} \left(R_{Q_2 N_1 P_1 Q} R^{Q}{}_{N_2 P_2 Q_1} + \frac{1}{2} R_{Q_2 QP_1 Q_1} R^{Q}{}_{N_2 P_2 N_1} \right) \right.$$

$$+ \left(\delta^{N_2}_{N_1} \delta^{P_2}_{P_1} R^{Q_2}{}_{RSQ_1} R_{M_1}{}^{RSM_2} + \frac{1}{2} \delta^{P_2}_{P_1} \delta^{Q_2}_{Q_1} R^{N_2}{}_{RSN_1} R_{M_1}{}^{RSM_2} \right)$$

$$+ \left. \left(G^{M_2 M_2} \delta^{Q_2}_{Q_1} R_{M_1}{}^{N_2 P_2 P} R_{PN_1 P_1 M_2} + \frac{1}{2} G^{M_2 M_2} \delta^{Q_2}_{N_1} R_{M_1}{}^{N_2 P_2 P} R_{PM_2 P_1 Q_1} \right) \right],$$

$$A_2 = \left[\left(G^{M_2 M_2} G^{Q_2 Q_2} G^{N_2 N_1} G^{P_2 P_1} R^{Q_1}{}_{RSQ_2} + \frac{1}{2} G^{M_2 M_2} G^{N_2 N_2} G^{P_2 P_1} G^{Q_2 Q_1} R^{N_1}{}_{RSN_2} \right) R_{M_2}{}^{RSM_1} \right.$$

$$+ \left(G^{Q_2 M_1} G^{N_2 N_2} G^{P_2 P_2} R^{M_2 N_1 P_1 K} + \frac{1}{2} G^{Q_2 M_1} G^{N_2 N_2} G^{P_2 P_2} R^{M_2 KP_1 Q_1} \right) R^{N_1}{}_{N_2 P_2 Ka}$$

$$+ \left. \left(G^{M_2 Q_1} R^{HN_1 P_1 Q_2} + \frac{1}{2} G^{M_2 N_1} R^{HQ_2 P_1 Q_1} \right) R_H{}^{N_2 P_2 M_1} \right],$$

$$A_3 = \left[G^{N_1 N_1} G^{P_1 P_1} G^{Q_1 Q_1} \left[\left(\delta^{M_2}_{Q_1} \delta^{Q_2}_Q R^{M_1 N_2 P_2 K} + G^{M_2 M_1} G^{N_2 N_2} G^{P_2 P_2} G^{Q_2 K} R_{Q_1 N_2 P_2 Q} \right. \right. \right.$$

$$+ \frac{1}{2} \delta^{M_2}_{Q_1} \delta^{N_2}_Q R^{M_1 KP_2 Q_2} + \frac{1}{2} G^{M_2 M_1} G^{N_2 K} G^{P_2 P_2} G^{Q_2 Q_2} R_{Q_1 QP_2 Q_2} \right) R^{Q}{}_{N_1 P_1 K}$$

$$+ \left. \left. G^{M_2 M_2} \delta^{N_2}_{N_1} \delta^{P_2}_{P_1} \left(R_{Q_1 MNM_2} R^{M_1 MNQ_2} + \frac{1}{2} R_{Q_1 M_2 MN} R^{M_1 Q_2 MN} \right) \right] \right],$$

$$A_4 = G^{M_1 M_1} \left[\left(\delta^{M_2}_P \delta^{Q_2}_{M_1} R^{HN_2 P_2 Q_1} + G^{M_2 H} G^{N_2 N_2} G^{P_2 P_2} G^{Q_2 Q_1} R_{PN_2 P_2 M_1} \right. \right.$$

$$+ \frac{1}{2} \delta^{M_2}_P \delta^{N_2}_{M_1} R^{HQ_1 P_2 Q_2} + \frac{1}{2} G^{M_2 H} G^{N_2 Q_1} G^{P_2 P_2} G^{Q_2 Q_2} R_{PM_1 P_2 Q_2} \right) R_H{}^{N_1 P_1 P}$$

$$+ \left. G^{N_2 N_1} G^{P_2 P_1} G^{Q_2 Q_2} \left(R_{Q_2 MNM_1} R^{M_2 MNQ_1} + \frac{1}{2} R_{Q_2 M_1 MN} R^{M_2 Q_1 MN} \right) \right]. \tag{B6}$$

(v) The *r*-dependent functions appearing in Eq. (75) are given below:

$$Z(r) = -\kappa_Z \frac{MN^{37/10}g_s^{35/6}\log(r)(\log(N) - 9\log(r))}{r^{14}\alpha_{\theta_1}^3\alpha_{\theta_2}^2 N_f^{4/3}(\log(N) - 3\log(r))^{7/3}}$$

$$\sim -\frac{\pi^{23/6}MN^{61/20}g_s^{79/12}\kappa_Z\log(r)(\log(N) - 9\log(r))}{r^{14}N_f^{4/3}(\log(N) - 3\log(r))^{7/3}},$$

$$W(r) = -\kappa_W \frac{MN^{37/10}g_s^{35/6}\log(r)(\log(N) - 9\log(r))}{r^{14}\alpha_{\theta_1}^3\alpha_{\theta_2}^2 N_f^{4/3}(\log(N) - 3\log(r))^{7/3}}$$

$$\sim -\frac{MN^{61/20}g_s^{79/12}\kappa_W\log(r)(\log(N) - 9\log(r))}{r^{14}N_f^{4/3}(\log(N) - 3\log(r))^{7/3}},$$

$$U(r) = -\kappa_U \frac{M^2 N N_f g_s^3 \log(r)(\log(N) - 45\log(r))}{r^4\alpha_{\theta_1}\alpha_{\theta_2}^6(\log(N) - 3\log(r))^3}$$

$$\sim -\frac{M^2 N_f g_s^{15/4}\kappa_U\log(r)(\log(N) - 45\log(r))}{\sqrt[4]{N}r^4(\log(N) - 3\log(r))^3},$$

$$V(r) = \kappa_V \frac{M^2 N N_f g_s^3}{r^4\alpha_{\theta_1}\alpha_{\theta_2}^6\log^2(r)} \sim \frac{M^2 N_f g_s^{15/4}\kappa_V}{\sqrt[4]{N}r^4\log^2(r)}, \tag{B7}$$

where κ_Z, κ_W, κ_U and κ_V are the numerical factors including $\left(\frac{8}{q_\alpha + 1}\right)$.

(vi) To obtain the EOM for $t(r)$ we need to calculate the following derivatives from Eqs. (72), (74)–(76):

$$\frac{\delta\mathcal{L}_{\text{Total}}^{\text{HM}}}{\delta t'(r)} = \beta\left(\frac{(r - r_h)^{3/2}p_4^\beta(r_h)(\mathcal{A}_1 t'(r) + \mathcal{A}_2 t''(r))}{N^{7/10}t'(r)^2} + \frac{p_5^\beta(r_h)(\mathcal{A}_3 t'(r) + \mathcal{A}_4 t''(r))}{N^{7/10}t'(r)^2} + \frac{(r - r_h)^{13/2}p_7^\beta(r_h)}{N^{57/10}t'(r)^4}\right.$$

$$+ \frac{p_6^\beta(r_h)}{(r - r_h)N^{7/10}t'(r)} + \frac{(r - r_h)^{3/2}p_1^\beta(r_h)}{N^{5/4}t'(r)} + \frac{N^{3/10}p_8^\beta(r_h)}{\sqrt{r - r_h}t'(r)^3} + \frac{N^{3/10}p_9^\beta(r_h)}{\sqrt{r - r_h}t'(r)^3} + \frac{p_2^\beta(r_h)}{\sqrt{r - r_h}t'(r)^3}$$

$$\left. + \frac{p_3^\beta(r_h)}{\sqrt{r - r_h}t'(r)^3} + N^{3/10}(r - r_h)^{3/2}Y_5(r_h)t'(r)\right) + N^{3/10}(r - r_h)^{5/2}p_1(r_h)t'(r), \tag{B8}$$

and

$$\frac{\delta\mathcal{L}_{\text{Total}}^{\text{HM}}}{\delta t''(r)} = \frac{\beta\mathcal{F}^\beta(r_h)(r - r_h)^{5/2}}{N^{7/10}t'(r)}, \tag{B9}$$

where

$$p_1(r_h) = \kappa_{p_1}\left(\frac{MN_f^{5/3}g_s^{7/3}\sqrt{\kappa_\alpha}\kappa_\lambda\log(r_h)(\log(N) - 9\log(r_h))(\log(N) - 3\log(r_h))^{5/6}}{r_h^{3/2}\sqrt{\kappa_\sigma}}\right),$$

$$p_1^\beta(r_h) = -\kappa_{p_1^\beta}\left(\frac{M^2\sqrt[4]{N}x_R^2 N_f^{4/3}g_s^{17/6}\sqrt{\kappa_\alpha}\kappa_U\log(r_h)(\log(N) - 45\log(r_h))}{r_h^{5/2}\sqrt{\kappa_\sigma}(\log(N) - 3\log(r_h))^{5/2}}\right),$$

$$p_2^\beta(r_h) = \kappa_{p_2^\beta}\left(\frac{M^2 x_R^2 N_f^{4/3}g_s^{23/6}\kappa_U\log(r_h)\sqrt{\kappa_\alpha\kappa_\sigma}(\log(N) - 45\log(r_h))}{r_h^{9/2}(\log(N) - 3\log(r_h))^{5/2}}\right),$$

$$p_3^\beta(r_h) = -\kappa_{p_3^\beta}\left(\frac{M^2 x_R^2(540\log(2) - 107)N_f^{4/3}g_s^{23/6}\sqrt{\kappa_\alpha\kappa_\sigma}}{r_h^{9/2}\log^2(r_h)(\log(N) - 3\log(r_h))^{5/2}}\right.$$

$$\left. \times (28\kappa_V(\log(N) - 3\log(r_h))^3 - 27\kappa_U\log^3(r_h)(\log(N) - 45\log(r_h)))\right),$$

$$p_4^\beta(r_h) = \kappa_{p_4^\beta} F(g_s, r_h, N_f, M),$$

$$p_5^\beta(r_h) = \kappa_{p_5^\beta} F(g_s, r_h, N_f, M),$$

$$p_6^\beta(r_h) = -\kappa_{p_6^\beta} \left(\frac{M x_R^4 \sqrt[3]{N_f} g_s^2 \kappa_W \log(r_h)(\kappa_\alpha \kappa_\sigma)^{5/2}(\log(N) - 9\log(r_h))\sqrt[6]{\log(N) - 3\log(r_h)}}{r_h^{5/2}\kappa_\sigma^5} \right),$$

$$p_7^\beta(r_h) = -\kappa_{p_7^\beta} \left(\frac{M \sqrt[3]{N_f} r_h^{25/2} \kappa_Z \log(r_h)(\kappa_\alpha \kappa_\sigma)^{5/2}(\log(N) - 9\log(r_h))\sqrt[6]{\log(N) - 3\log(r_h)}}{g_s^3 \kappa_\sigma^{10}} \right),$$

$$p_8^\beta(r_h) = \kappa_{p_8^\beta} \left(\frac{M x_R^4 \sqrt[3]{N_f} g_s^3 \kappa_W \log(r_h)(\kappa_\alpha \kappa_\sigma)^{5/2}(\log(N) - 9\log(r_h))\sqrt[6]{\log(N) - 3\log(r_h)}}{r_h^{9/2}\kappa_\sigma^4} \right),$$

$$p_9^\beta(r_h) = \kappa_{p_9^\beta} \left(\frac{M \sqrt[3]{N_f} g_s^3 \kappa_Z \log(r_h)(\kappa_\alpha \kappa_\sigma)^{5/2}(\log(N) - 9\log(r_h))\sqrt[6]{\log(N) - 3\log(r_h)}}{r_h^{9/2}\kappa_\sigma^4} \right),$$

$$\mathcal{F}^\beta = -\kappa_{\mathcal{F}^\beta} \left(\frac{M \sqrt[3]{N_f} g_s^2 \kappa_\alpha^{5/2} \log(r_h)(\log(N) - 9\log(r_h))\sqrt[6]{\log(N) - 3\log(r_h)}(x_R^4 \kappa_W + 2\kappa_Z)}{r_h^{5/2}\kappa_\sigma^{5/2}} \right), \tag{B10}$$

where $\kappa_{p_1}, \kappa_{p_{i=1,\ldots,9}^\beta}$ and $\kappa_{\mathcal{F}^\beta}$ are the numerical factors. From Eq. (76) and using Eqs. (B8) and (B9), the EOM corresponding to the embedding $t(r)$, given by $\frac{d(\frac{\delta\mathcal{L}}{\delta t'(r)})}{dr} = \frac{d^2(\frac{\delta\mathcal{L}}{\delta t''(r)})}{dr^2}$ turns out to be

$$\beta \left(-\frac{N^{3/10} p_8^\beta(r_h)}{2(r - r_h)^{3/2} t'(r)^3} - \frac{N^{3/10} p_9^\beta(r_h)}{2(r - r_h)^{3/2} t'(r)^3} - \frac{3N^{3/10} t''(r) p_8^\beta(r_h)}{\sqrt{r - r_h} t'(r)^4} - \frac{3N^{3/10} t''(r) p_9^\beta(r_h)}{\sqrt{r - r_h} t'(r)^4} \right)$$

$$+ N^{3/10}(r - r_h)^{5/2} p_1(r_h) t''(r) + \frac{5}{2} N^{3/10}(r - r_h)^{3/2} p_1(r_h) t'(r)$$

$$= -\frac{\beta M \sqrt[3]{N_f} g_s^2 \sqrt{r - r_h}\kappa_\alpha^{5/2} \log(r_h)(\log(N) - 9\log(r_h))\sqrt[6]{\log(N) - 3\log(r_h)}(x_R^4 \kappa_W + 2\kappa_Z)}{4N^{7/10} r_h^{5/2}\kappa_\sigma^{5/2} t'(r)^3}$$

$$\times (8(r - r_h)^2 t''(r)^2 - 4(r - r_h)t'(r)((r - r_h)t^{(3)}(r) + 5t''(r)) + 15t'(r)^2). \tag{B11}$$

APPENDIX C: ISLAND SURFACE MISCELLANIA

In this appendix we are listing the various functions appearing in the entanglement entropy of the island surface at $\mathcal{O}(\beta)$. We have also computed the derivatives of the Lagrangian of the island surface here which have been used in obtaining the equation of motion of the embedding function of the island surface.

(i) $\lambda_{3,4}(r)$ appearing in the Wald entanglement entropy term (102) of the island surface are given below:

$$\lambda_3(r) = \kappa_{\lambda_3} \frac{M^7 N^{7/10} N_f^{7/3} g_s^7 r_h^{14} \log(N)\log^7(r)(5\log(N) - 12\log(r))^3}{r^{16}\alpha_{\theta_1}^3 \alpha_{\theta_2}^2 (\log(N) - 3\log(r))^{14/3}}$$

$$\sim \frac{M^7 \sqrt[20]{N} \log(2)(\log(64) - 1)N_f^{7/3} g_s^{31/4} r_h^{14} \kappa_{\lambda_3} \log(N)\log^7(r)(5\log(N) - 12\log(r))^3}{r^{16}(\log(N) - 3\log(r))^{14/3}},$$

$$\lambda_4(r) = \kappa_{\lambda_4} \frac{M^3 N^{7/10} \sqrt[3]{N_f} g_s^3 r_h^{14} \log(N)\log^3(r)(5\log(N) - 12\log(r))}{r^{16}\alpha_{\theta_1}^3 \alpha_{\theta_2}^2 (\log(N) - 3\log(r))^{8/3}}$$

$$\sim \frac{M^3 \sqrt[20]{N} \log(2)(\log(64) - 1)\sqrt[3]{N_f} g_s^{15/4} r_h^{14} \kappa_{\lambda_4} \log(N)\log^3(r)(5\log(N) - 12\log(r))}{r^{16}(\log(N) - 3\log(r))^{8/3}}, \tag{C1}$$

where κ_{λ_3} and κ_{λ_4} are the numerical factors.

(ii) In the anomaly term (103) following are the r dependent functions:

$$
Z_1(r) = \kappa_{Z_1} \frac{MN^{37/10} g_s^{35/6} r_h^2 \log(N) \log(r)}{r^{16} \alpha_{\theta_1}^3 \alpha_{\theta_2}^2 N_f^{4/3} (\log(N) - 3\log(r))^{7/3}}
$$
$$
\sim \frac{MN^{61/20} \log(2)(\log(64) - 1) g_s^{79/12} r_h^2 \log(N) \log(r) \kappa_{Z_1}}{r^{16} N_f^{4/3} (\log(N) - 3\log(r))^{7/3}},
$$

$$
W_1(r) = \kappa_{W_1} \frac{MN^{37/10} g_s^{35/6} \log(N) \log(r)}{r^8 \alpha_{\theta_1}^3 \alpha_{\theta_2}^2 N_f^{4/3} r_h^6 (\log(N) - 3\log(r))^{7/3}}
$$
$$
\sim \frac{MN^{61/20} \log(2)(\log(64) - 1) g_s^{79/12} \kappa_{W_1} \log(N) \log(r)}{r^8 N_f^{4/3} r_h^6 (\log(N) - 3\log(r))^{7/3}},
$$

$$
U_1(r) = \kappa_{U_1} \frac{M^2 N N_f g_s^3 r_h^{12} \log^2(N) \log^3(r)(\log(N) - 17\log(r))(\log(N) - 9\log(r))}{r^{15} \alpha_{\theta_1} \alpha_{\theta_2}^6 (\log(N) - 3\log(r))^4},
$$
$$
\sim \frac{M^2 N_f g_s^{15/4} r_h^{12} \kappa_{U_1} \log^2(N) \log^3(r)(\log(N) - 17\log(r))(\log(N) - 9\log(r))}{\sqrt[4]{N} r^{15} (\log(N) - 3\log(r))^4},
$$

$$
V_1(r) = -\kappa_{V_1} \frac{M^2 N N_f g_s^3 r_h^8 \log^5(N) \log^3(r)(\log(N) - 6\log(r))}{r^{11} \alpha_{\theta_1} \alpha_{\theta_2}^6 (\log(N) - 9\log(r))^3 (\log(N) - 3\log(r))^3}
$$
$$
\sim -\frac{M^2 N_f g_s^{15/4} r_h^8 \kappa_{V_1} \log^5(N) \log^3(r)(\log(N) - 6\log(r))}{\sqrt[4]{N} r^{11} (\log(N) - 9\log(r))^3 (\log(N) - 3\log(r))^3}, \tag{C2}
$$

where $\kappa_{Z_1}, \kappa_{W_1}, \kappa_{U_1}$ and κ_{V_1} are the numerical prefactors which also includes $\left(\frac{8}{q_\alpha + 1}\right)$.

(iii) Using Eqs. (99), (102)–(105) we obtain:

$$
\frac{\delta \mathcal{L}_{\text{Total}}^{\text{IS}}}{\delta x(r)} = \beta \left(\frac{N^{3/10} f_1^\beta(r_h) x(r)}{\sqrt{r - r_h}} + \left(\frac{f_2^\beta(r_h)}{\sqrt{r - r_h}} + \frac{f_3^\beta(r_h)}{N^{1/4} \sqrt{r - r_h}} \right) \frac{x(r)}{x'(r)^2} + \frac{N^{3/10} f_4^\beta(r_h) x(r)^3}{\sqrt{r - r_h} x'(r)^2} + \frac{N^{13/10} x(r) Y_1(r_h)}{\sqrt{r - r_h}} \right)
$$
$$
+ \frac{N^{13/10} f_1(r_h) x(r)}{\sqrt{r - r_h}}, \tag{C3}
$$

$$
\frac{\delta \mathcal{L}_{\text{Total}}^{\text{IS}}}{\delta x'(r)} = \beta \left[\frac{F_1^\beta(r_h) \sqrt{r - r_h} x(r)^2 x'(r)}{N^{7/10}} + \frac{F_{10}^\beta(r_h) \sqrt{r - r_h} x(r)^4}{N^{7/10} x'(r)} + \frac{F_{11}^\beta(r_h) \sqrt{r - r_h}}{N^{7/10} x'(r)} + \frac{N^{3/10} F_{12}^\beta(r_h) x(r)^4}{\sqrt{r - r_h} x'(r)^3} \right.
$$
$$
+ \frac{N^{3/10} F_{13}^\beta(r_h)}{\sqrt{r - r_h} x'(r)^3} + \frac{F_2^\beta(r_h) \sqrt{r - r_h} x(r)^2}{N x'(r)} + \frac{F_3^\beta(r_h) \sqrt{r - r_h} x(r)^2}{N^{5/4} x'(r)} + \frac{F_4^\beta(r_h) x(r)^2}{\sqrt{r - r_h} x'(r)^3} + \frac{F_5^\beta(r_h) x(r)^2}{N^{1/4} \sqrt{r - r_h} x'(r)^3}
$$
$$
+ \frac{F_6^\beta(r_h)(r - r_h)^{3/2} x(r)^4 (2x'(r) + r x''(r))}{N^{7/10} x'(r)^2} + \frac{F_7^\beta(r_h)(r - r_h)^{3/2}(2x'(r) + r x''(r))}{N^{7/10} x'(r)^2}
$$
$$
\left. + \frac{F_8^\beta(r_h) \sqrt{r - r_h} x(r)^4}{N^{7/10} x'(r)} + \frac{F_9^\beta(r_h) \sqrt{r - r_h}}{N^{7/10} x'(r)} + N^{3/10} x(r)^2 Y_3(r_h) x'(r) \right] + N^{3/10} F_1(r_h) \sqrt{r - r_h} x(r)^2 x'(r), \tag{C4}
$$

and,

$$
\frac{\delta \mathcal{L}_{\text{Total}}^{\text{IS}}}{\delta x''(r)} = \beta \left(\frac{\mathcal{F}_1^\beta(r_h)(r - r_h)^{3/2}}{N^{7/10}} + \frac{\mathcal{F}_2^\beta(r_h)(r - r_h)^{3/2}}{N^{7/10}} \right), \tag{C5}
$$

where we have defined $F_1(r_h), F_{i=1,\ldots,13}^\beta(r_h), f_1(r_h), f_{i=1,\ldots,4}^\beta(r_h)$, and $Y_{i=1,3}(r_h)$ for the island surface as:

$$F_1(r_h) = \frac{\kappa_{F_1} M \log(2)(\log(64)-1) N_f^{5/3} g_s^{7/3} \sqrt{r_h} \kappa_\alpha \kappa_{\lambda_5} \log(N) \log(r_h)(\log(N)-3\log(r_h))^{2/3}}{\sqrt{\kappa_\alpha \kappa_\sigma}},$$

$$F_1^\beta(r_h) = \frac{\kappa_{F_1^\beta} M^3 \log(2)(\log(64)-1) N_f^{2/3} g_s^{17/6} \sqrt{r_h} \kappa_\alpha \log(N) \log^3(r_h)(5\log(N)-12\log(r_h))}{\sqrt{\kappa_\alpha \kappa_\sigma}(\log(N)-3\log(r_h))^{13/3}}$$
$$\times (81(16+\sqrt{2})M^4 N_f^2 g_s^4 \kappa_{\lambda_3} \log^4(r_h)(5\log(N)-12\log(r_h))^2 + 4096(4+\sqrt{2})\pi^4 \kappa_{\lambda_4}(\log(N)-3\log(r_h))^2),$$

$$F_2^\beta(r_h) = -\frac{\kappa_{F_2^\beta} M^2 g_s^{3/2} \kappa_\alpha \kappa_{U_1} \log^2(N) \log^3(r)(\log(N)-17\log(r_h))(\log(N)-9\log(r_h))(N_f g_s(\log(N)-3\log(r_h)))^{4/3}}{\sqrt{r_h}\sqrt{\kappa_\alpha \kappa_\sigma}(\log(N)-3\log(r_h))^5},$$

$$F_3^\beta(r_h) = \frac{\kappa_{F_3^\beta} M^4 N_f^{7/3} g_s^{79/12} \kappa_\alpha \log^4(N) \log^6(r_h)}{r_h^{7/2} \sqrt{\kappa_\alpha \kappa_\sigma}(\log(N)-9\log(r_h))^6(\log(N)-3\log(r_h))^{23/3}}$$
$$\times ((\kappa_{V_1} \log^3(N)(-9\log(N)\log(r_h)+18\log^2(r_h)+\log^2(N))$$
$$-6\kappa_{U_1}(\log(N)-17\log(r_h))(\log(N)-9\log(r_h))^4)^2),$$

$$F_4^\beta(r_h) = \frac{\kappa_{F_4^\beta} M^2 N_f^{4/3} g_s^{23/6} \kappa_{U_1} \log^2(N) \log^3(r_h)\sqrt{\kappa_\alpha \kappa_\sigma}(\log(N)-17\log(r_h))(\log(N)-9\log(r_h))}{r_h^{7/2}(\log(N)-3\log(r_h))^{11/3}},$$

$$F_5^\beta(r_h) = -\frac{\kappa_{F_5^\beta} M^4 g_s^{21/4} \log^4(N) \sqrt{\kappa_\alpha \kappa_\sigma}(N_f g_s(\log(N)-3\log(r_h)))^{7/3}}{r_h^{13/2}(\log(N)-9\log(r_h))^6(\log(N)-3\log(r_h))^{10}}$$
$$\times (\kappa_{V_1} \log^3(N)\log^3(r_h)(-9\log(N)\log(r_h)+18\log^2(r_h)+\log^2(N))$$
$$-6\kappa_{U_1} \log^3(r)(\log(N)-17\log(r_h))(\log(N)-9\log(r_h))^4)^2;$$

$$F_6^\beta(r_h) = -\frac{\kappa_{F_6^\beta} M \sqrt[3]{N_f} g_s^2 \kappa_{W_1} \log(N) \log(r_h)(\kappa_\alpha \kappa_\sigma)^{5/2}}{r_h^{5/2} \kappa_\sigma^5 (\log(N)-3\log(r_h))^{2/3}},$$

$$F_7^\beta(r_h) = -\frac{\kappa_{F_7^\beta} M \log(2)(\log(64)-1)\sqrt[3]{N_f} g_s^2 \kappa_{Z_1} \log(N) \log(r_h)(\kappa_\alpha \kappa_\sigma)^{5/2}}{r_h^{5/2} \kappa_\sigma^5 (\log(N)-3\log(r_h))^{2/3}},$$

$$F_8^\beta(r_h) = \frac{\kappa_{F_8^\beta} M \log(2)(\log(64)-1)\sqrt[3]{N_f} g_s^2 \kappa_{W_1} \log(N) \log(r_h)(\kappa_\alpha \kappa_\sigma)^{5/2}}{r_h^{3/2} \kappa_\sigma^5 (\log(N)-3\log(r_h))^{2/3}},$$

$$F_9^\beta(r_h) = \frac{\kappa_{F_9^\beta} M \log(2)(\log(64)-1)\sqrt[3]{N_f} g_s^2 \kappa_{Z_1} \log(N) \log(r_h)(\kappa_\alpha \kappa_\sigma)^{5/2}}{r_h^{3/2} \kappa_\sigma^5 (\log(N)-3\log(r_h))^{2/3}},$$

$$F_{10}^\beta(r_h) = -\frac{\kappa_{F_{10}^\beta} M \log(2)(\log(64)-1)\sqrt[3]{N_f} g_s^2 \kappa_{W_1} \log(N) \log(r_h)(\kappa_\alpha \kappa_\sigma)^{5/2}}{r_h^{3/2} \kappa_\sigma^5 (\log(N)-3\log(r_h))^{2/3}};$$

$$F_{11}^\beta(r_h) = -\frac{\kappa_{F_{11}^\beta} M \log(2)(\log(64)-1)\sqrt[3]{N_f} g_s^2 \kappa_{Z_1} \log(N) \log(r_h)(\kappa_\alpha \kappa_\sigma)^{5/2}}{r_h^{3/2} \kappa_\sigma^5 (\log(N)-3\log(r_h))^{2/3}},$$

$$F_{12}^\beta(r_h) = -\frac{\kappa_{F_{12}^\beta} M \log(2)(\log(64)-1)\sqrt[3]{N_f} g_s^3 \kappa_{W_1} \log(N) \log(r_h)(\kappa_\alpha \kappa_\sigma)^{5/2}}{r_h^{9/2} \kappa_\sigma^4 (\log(N)-3\log(r_h))^{2/3}},$$

$$F_{13}^\beta(r_h) = -\frac{\kappa_{F_{13}^\beta} M \log(2)(\log(64)-1)\sqrt[3]{N_f} g_s^3 \kappa_{Z_1} \log(N) \log(r_h)(\kappa_\alpha \kappa_\sigma)^{5/2}}{r_h^{9/2} \kappa_\sigma^4 (\log(N)-3\log(r_h))^{2/3}};$$

$$f_1(r_h) = \frac{\kappa_{f_1} M \log(2)(\log(64)-1) N_f^{5/3} g_s^{10/3} \kappa_{\lambda_5} \log(N) \log(r_h) \sqrt{\kappa_\alpha \kappa_\sigma}(\log(N) - 3\log(r_h))^{2/3}}{r_h^{5/2}},$$

$$f_1^\beta(r_h) = \frac{\kappa_{f_1^\beta} M^3 N_f^{2/3} g_s^{23/6} \log(N) \log^3(r_h) \sqrt{\kappa_\alpha \kappa_\sigma}(5\log(N) - 12\log(r_h))}{r_h^{5/2}(\log(N) - 3\log(r_h))^{13/3}}$$
$$\times \left(\frac{M^3 \log(2)(\log(64)-1) N_f^{2/3} g_s^{23/6} \log(N) \log^3(r_h) \sqrt{\kappa_\alpha \kappa_\sigma}(5\log(N) - 12\log(r_h))}{1572864 \sqrt[3]{2} 3^{5/6} \pi^{77/12} r_h^{5/2}(\log(N) - 3\log(r_h))^{13/3}} \right),$$

$$f_2^\beta(r_h) = -\frac{\kappa_{f_2^\beta} M^2 N_f^{4/3} g_s^{23/6} \kappa_{U_1} \log^2(N) \log^3(r_h) \sqrt{\kappa_\alpha \kappa_\sigma}(\log(N) - 17\log(r_h))(\log(N) - 9\log(r_h))}{r_h^{7/2}(\log(N) - 3\log(r_h))^{11/3}},$$

$$f_3^\beta(r_h) = \frac{\kappa_{f_3^\beta} M^4 g_s^{21/4} \log^4(N) \sqrt{\kappa_\alpha \kappa_\sigma}(N_f g_s(\log(N) - 3\log(r_h)))^{7/3}}{r_h^{13/2}(\log(N) - 9\log(r_h))^6(\log(N) - 3\log(r_h))^{10}}$$
$$\times (\kappa_{V_1} \log^3(N) \log^3(r_h)(-9\log(N) \log(r_h) + 18\log^2(r_h) + \log^2(N))$$
$$- 6\kappa_{U_1} \log^3(r)(\log(N) - 17\log(r_h))(\log(N) - 9\log(r_h))^4)^2,$$

$$f_4^\beta(r_h) = \frac{\kappa_{f_4^\beta} M \log(2)(\log(64)-1) \sqrt[3]{N_f} g_s^3 \kappa_{W_1} \log(N) \log(r_h)(\kappa_\alpha \kappa_\sigma)^{5/2}}{r_h^{9/2} \kappa_\sigma^4 (\log(N) - 3\log(r_h))^{2/3}}; \tag{C6}$$

$$\mathcal{F}_1^\beta(r_h) = -\frac{\kappa_{\mathcal{F}_1^\beta} M \log(2)(\log(64)-1) \sqrt[3]{N_f} g_s^2 \kappa_\alpha^{5/2} \kappa_{W_1} \log(N) \log(r_h)}{r_h^{3/2} \kappa_\sigma^{5/2}(\log(N) - 3\log(r_h))^{2/3}},$$

$$\mathcal{F}_2^\beta(r_h) = -\frac{\kappa_{\mathcal{F}_1^\beta} M \log(2)(\log(64)-1) \sqrt[3]{N_f} g_s^2 \kappa_\alpha^{5/2} \kappa_{Z_1} \log(N) \log(r_h)}{r_h^{3/2} \kappa_\sigma^{5/2}(\log(N) - 3\log(r_h))^{2/3}}, \tag{C7}$$

and,

$$Y_1(r_h) = \frac{\kappa_{Y_1} \mathcal{C}_{\theta_1 x} M N_f^{5/3} g_s^{10/3} \log^2(r_h) \sqrt{\kappa_\alpha \kappa_\sigma}(\log(N) - 3\log(r_h))^{2/3}}{r_h^{3/2}},$$

$$Y_3(r_h) = \frac{\kappa_{Y_3} \mathcal{C}_{\theta_1 x} M N_f^{5/3} g_s^{7/3} r_h^{3/2} \kappa_\alpha \log^2(r_h)(\log(N) - 3\log(r_h))^{2/3}}{\sqrt{\kappa_\alpha \kappa_\sigma}}, \tag{C8}$$

where $\kappa_{F_1}, \kappa_{F_{i=1,...,13}^\beta}, \kappa_{f_1}, \kappa_{f_{i=1,...,4}^\beta}, \kappa_{\mathcal{F}_{1,2}^\beta}, \kappa_{Y_{1,3}}$ are numerical factors and $\mathcal{C}_{\theta_1 x}$ is the constant of integration appearing in the solution to $\mathcal{O}(l_p^6)$ correction to the metric component along the toroidal analog $T^2(\theta_1, x)$ of the vanishing two-cycle $S^2(\theta_1, \phi_1)$.

APPENDIX D: POSSIBLE TERMS APPEARING IN HOLOGRAPHIC ENTANGLEMENT ENTROPIES

In this appendix we have listed all the possible terms that we obtain from differentiating Lagrangian of the M-theory dual inclusive of $\mathcal{O}(R^4)$ corrections. In appendix D 1, we have listed all the terms for Hartman-Maldacena-like surface and in appendix D 2 we have listed all the possible terms for the island surface.

1. Hartman-Maldacena-like surface

Square root of the determinant of the induced metric (35) for the Hartman-Maldacena-like surface scale as $N^{7/10}$ and is given below:

$$\sqrt{-g} \sim \left(\frac{MN^{7/10}\sqrt{g_s}(N_f(\log(N) - 3\log(r)))^{5/3}\sqrt{\alpha(r)(\sigma(r) - \left(1 - \frac{r_h^4}{r^4}\right)t'(r)^2)}}{\alpha_{\theta_1}^3 \alpha_{\theta_2}^2} (N_f g_s(r^2(\log(N)(2\log(r) + 1)) \right.$$

$$\left. + 3(1 - 6\log(r))\log(r)) - r_h^2(\log(N)(2\log(r) + 1) - 18(6r + 1)\log^2(r))) + 8\pi(r_h^2 - r^2)\log(r)) \right). \tag{D1}$$

There are four terms that we obtain from $\frac{\partial J_0}{\partial R_{txtx}}$:

(i) $\int d\mathcal{V}_9 \sqrt{-g}\left((G^{xx})^2(G^{tt})^2\left(R_{PxtQ} + \frac{1}{2}R_{PQtx}\right)R_t^{RSP}R^Q_{RSx}\right)$

$\sim \int d\mathcal{V}_9 \sqrt{-g}\left(-\frac{r_h^8(-9\log^2(N)(\log(N) - 6\log(r))^2 - 13(\log(N) - 3\log(r))^4 - 21(\log(N) - 3\log(r))^2)}{\sqrt{N}r^{12}N_f^{10/3}\sqrt{g_s}(\log(N) - 3\log(r))^{22/3}}\right);$

(ii) $\int d\mathcal{V}_9 \sqrt{-g}\left(R^{HxtK}R_H{}^{RSt}R^x{}_{RSK} + \frac{1}{2}R^{HKtx}R_H{}^{RSt}R^Q{}_{RSK}\right) \sim \int d\mathcal{V}_9 \sqrt{-g}\left(\frac{1}{\sqrt{N}r^{12}N_f^{22/3}\sqrt{g_s}r_h^8(\log(N) - 3\log(r))^{22/3}}\right);$

(iii) $\int d\mathcal{V}_9 \sqrt{-g}\left((G^{xx})^2 G^{tt}\left(R_{PxtQ} + \frac{1}{2}R_{PQtx}\right)R_t^{RSP}R^Q{}_{RSx}\right) \sim \int d\mathcal{V}_9\left(\lambda_1(r)\sqrt{\alpha(r)\left(\sigma(r) - \left(1 - \frac{r_h^4}{r^4}\right)t'(r)^2\right)}\right);$

(iv) $\int d\mathcal{V}_9 \sqrt{-g}\left(G^{tt}\left(R^{HMNx}R_{PMNt} + \frac{1}{2}R^{HxMN}R_{PtMN}\right)R_H{}^{xtP}\right) \sim \int d\mathcal{V}_9\left(\lambda_2(r)\sqrt{\alpha(r)\left(\sigma(r) - \left(1 - \frac{r_h^4}{r^4}\right)t'(r)^2\right)}\right). \tag{D2}$

From Eq. (B2) it is clear that (iii) and (iv) terms scale as $N^{7/10}$ whereas from Eqs. (D1) and (D2) we can see that (i) and (ii) terms scale as $N^{1/5}$. Therefore (iii) and (iv) terms are the most dominant terms in the large-N limit.

We obtain thirteen terms from $\frac{\partial^2 J_0}{\partial R_{xixj}\partial R_{xmxl}}K_{tij}K_{tml}$ which are listed below:

(i) $\int d\mathcal{V}_9 \sqrt{-g}(G^{xx})^2(G^{mm})(G^{ll})\delta_m^i R_r{}^{TSx}R^j{}_{TSl}K_{tij}K_{tml} \sim \int d\mathcal{V}_9 \sqrt{-g}$

$\left(-\frac{M^2NN_f g_s^3 \log^3(r)(23\log(N) - 72\log(r))^2(29\log(N) - 72\log(r))(2\log(N) - 3\log(r))\sqrt{\alpha(r)(\sigma(r) - t'(r)^2)}}{r^4\alpha_{\theta_1}\alpha_{\theta_2}^6(\log(N) - 9\log(r))^3(\log(N) - 3\log(r))^6 t'(r)^2}\right),$

(ii) $\int d\mathcal{V}_9 \sqrt{-g}(G^{xx})^3(G^{ii})(G^{jj})(G^{mm})(G^{ll})R_{jmxQ}R^Q{}_{ixl}K_{tij}K_{tml} \sim 0,$

(iii) $\int d\mathcal{V}_9 \sqrt{-g}\frac{1}{2}(G^{xx})^2(G^{mm})(G^{jl})R_r{}^{TSx}R^i{}_{TSx}K_{tij}K_{tml} \sim 0,$

(iv) $\int d\mathcal{V}_9 \sqrt{-g}\frac{1}{2}(G^{xx})^2(G^{ii})(G^{jl})R_r{}^{TSx}R^m{}_{TSi}K_{tij}K_{tml}$

$\sim \int d\mathcal{V}_9 \sqrt{-g}\left(\frac{M^3N^{13/10}\alpha_{\theta_1}N_f^2 g_s^{9/2}\log^3(N)(\log(N) - 23\log(r))^3(\log(N) + 18\log^2(r))\sqrt{\alpha(r)(\sigma(r) - t'(r)^2)}}{r^4\alpha_{\theta_2}^{10}\log^2(r)(\log(N) - 9\log(r))^3(\log(N) - 3\log(r))^5 t'(r)^2}\right),$

(v) $\int d\mathcal{V}_9 \sqrt{-g} \frac{1}{2}(G^{xx})^3(G^{ii})(G^{ll})(G^{mm})(G^{jj})R_{jQxl}R^Q{}_{ixm}K_{tij}K_{tml} \sim \int d\mathcal{V}_9\left(\frac{Z(r)}{2}\mathcal{L}_1\right),$

(vi) $\int d\mathcal{V}_9 \sqrt{-g} \frac{1}{2}(G^{xx})^3(G^{jm})(G^{ll})R_{Pxxl}R_x{}^{ixP}K_{tij}K_{tml}$

$\sim \int d\mathcal{V}_9 \sqrt{-g}\left(-\frac{M^2 N N_f g_s^3 \log^6(N)(\log(N)-51\log(r))(\log(N)-23\log(r))\sqrt{\alpha(r)(1-\sigma(r)r'(t)^2)}}{r^4 \alpha_{\theta_1}\alpha_{\theta_2}^6 \log^3(r)(\log(N)-9\log(r))^3(\log(N)-3\log(r))^5 t'(r)^2}\right),$

(vii) $\int d\mathcal{V}_9 \sqrt{-g}(G^{xx})^2(G^{im})(G^{ll})R^{xMNj}R_{lMNx}K_{tij}K_{tml} \sim 0,$

(viii) $\int d\mathcal{V}_9 \sqrt{-g}(G^{xx})^2(G^{jj})(G^{im})R^{xMNl}R_{jMNx}K_{tij}K_{tml} \sim 0,$

(ix) $\int d\mathcal{V}_9 \sqrt{-g}(G^{xx})^3(G^{ii})(G^{jj})(G^{ll})(G^{mm})R^Q{}_{mxj}R_{lixQ}K_{tij}K_{tml} \sim 0,$

(x) $\int d\mathcal{V}_9 \sqrt{-g}\frac{1}{2}(G^{xx})^2(G^{im})(G^{ll})R^{xjMN}R_{lxMN}K_{tij}K_{tml}$

$\sim \int d\mathcal{V}_9 \sqrt{-g}\Bigg[-\frac{MN^{7/10}r^2 N_f^{8/3} g_s^{3/2}\log(r)(\log(N)-9\log(r))(\log(N)-3\log(r))^{5/3}\sqrt{\alpha(r)(\sigma(r)-t'(r)^2)}}{\alpha_{\theta_1}^3 \alpha_{\theta_2}^2 t'(r)^2}$

$\times \left(76800 G_1(r) - \frac{29\sqrt[3]{6}M^4 g_s^4 \log^2(N)\log^2(r)(\log(N)-12\log(r))^2(\log(N)-6\log(r))^2}{\pi^{4/3}r^4\alpha(r)^2 N_f^{2/3}(\log(N)-3\log(r))^{20/3}(\sigma(r)-t'(r)^2)^2}\right.$

$\times (\sigma(r)\alpha'(r)-\alpha'(r)t'(r)^2+\alpha(r)(\sigma'(r)-2t'(r)t''(r)))^2\Bigg],$

(xi) $\int d\mathcal{V}_9 \sqrt{-g}\frac{1}{2}(G^{xx})^2(G^{im})(G^{jj})R^{xlMN}R_{jxMN}K_{tij}K_{tml}$

$\sim \int d\mathcal{V}_9 \sqrt{-g}\Bigg[-\frac{MN^{7/10}r^2 N_f^{8/3} g_s^{3/2}\log(r)(\log(N)-9\log(r))(2\log(N)-\log(r))^{5/3}\sqrt{\alpha(r)(\sigma(r)-t'(r)^2)}}{129600\sqrt{2}3^{5/6}\pi^{19/6}\alpha_{\theta_1}^3\alpha_{\theta_2}^2 t'(r)^2}$

$\times \left(450 G_2(r) - \frac{87\sqrt[3]{3}M^4 g_s^4\log^2(N)\log^2(r)(\log(N)-12\log(r))^2(\log(N)-6\log(r))^2(\log(N)-3\log(r))^2}{}\right.$

$\times (\sigma(r)\alpha'(r)-\alpha'(r)t'(r)^2+\alpha(r)(\sigma'(r)-2t'(r)t''(r)))^2\pi^{4/3}r^4\alpha(r)^2 N_f^{2/3}(2\log(N)-\log(r))^{26/3}(\sigma(r)-t'(r)^2)^2\Bigg],$

(xii) $\int d\mathcal{V}_9 \sqrt{-g}\frac{1}{2}(G^{xx})^3(G^{ii})(G^{jj})(G^{ll})(G^{mm})R^Q{}_{mxi}R_{lQxj}K_{tij}K_{tml} \sim \int d\mathcal{V}_9\left(\frac{Z(r)}{2}\mathcal{L}_1\right),$

(xiii) $\int d\mathcal{V}_9 \sqrt{-g}\frac{1}{2}(G^{xx})^3(G^{jj})(G^{il})R_x{}^{mxP}R_{Pxxj}K_{tij}K_{tml}$

$\sim \int d\mathcal{V}_9 \sqrt{-g}\left(-\frac{M^2 N N_f g_s^3\log^5(N)(5\log(N)-211\log(r))(\log(N)-23\log(r))\sqrt{\alpha(r)(\sigma(r)-t'(r)^2)}}{r^4\alpha_{\theta_1}\alpha_{\theta_2}^6\log(r)(\log(N)-9\log(r))^3(\log(N)-3\log(r))^5 t'(r)^2}\right),$ (D3)

where $G_1(r)$ and $G_2(r)$ are N independent functions. Out of all the terms listed above (v) and (xii) terms are the most dominant in the large N limit.

Similarly find that there are thirteen terms arising from $\frac{\partial^2 J_0}{\partial R_{titj}\partial R_{tmtl}}K_{tij}K_{tml}$ which are listed below:

(i) $\int d\mathcal{V}_9\sqrt{-g}(G^{tt})^2(G^{mm})(G^{ll})\delta^i_m R_t{}^{TSt}R^j{}_{TSl}K_{tij}K_{tml}$

$\sim \int d\mathcal{V}_9\sqrt{-g}\left(-\dfrac{M^2NN_f g_s^3\log^5(N)(23\log(N)-72\log(r))^2(\log(N)-27\log(r))\sqrt{\alpha(r)(\sigma(r)-t'(r)^2)}}{r^4\alpha_{\theta_1}\alpha_{\theta_2}^6(\log(N)-9\log(r))^4(\log(N)-3\log(r))^6 t'(r)^2}\right),$

(ii) $\int d\mathcal{V}_9\sqrt{-g}(G^{tt})^3(G^{ii})(G^{jj})(G^{mm})(G^{ll})R_{jmtQ}R^Q{}_{itl}K_{tij}K_{tml}\sim 0,$

(iii) $\int d\mathcal{V}_9\sqrt{-g}\dfrac{1}{2}(G^{tt})^2(G^{mm})(G^{jl})R_t{}^{TSt}R^i{}_{TSt}K_{tij}K_{tml}\sim 0,$

(iv) $\int d\mathcal{V}_9\sqrt{-g}\dfrac{1}{2}(G^{tt})^2(G^{ii})(G^{jl})R_t{}^{TSt}R^m{}_{TSi}K_{tij}K_{tml}$

$\sim \int d\mathcal{V}_9\sqrt{-g}\left(\dfrac{M^3N^{13/10}\alpha_{\theta_1}N_f^2 g_s^{9/2}\log^3(N)(\log(N)-23\log(r))^3(\log(N)+18\log^2(r))\sqrt{\alpha(r)(\sigma(r)-t'(r)^2)}}{1728\sqrt{6}\pi^{7/2}r^4\alpha_{\theta_2}^{10}\log^2(r)(\log(N)-9\log(r))^3(\log(N)-3\log(r))^5 t'(r)^2}\right),$

(v) $\int d\mathcal{V}_9\sqrt{-g}\dfrac{1}{2}(G^{tt})^3(G^{ii})(G^{ll})(G^{mm})(G^{jj})R_{jQtl}R^Q{}_{itm}K_{tij}K_{tml}\sim \int d\mathcal{V}_9\left(\dfrac{W(r)}{2}\mathcal{L}_2\right),$ (D4)

(vi) $\int d\mathcal{V}_9\sqrt{-g}\dfrac{1}{2}(G^{tt})^3(G^{jm})(G^{ll})R_{Pttl}R_t{}^{itP}K_{tij}K_{tml}$

$\sim \int d\mathcal{V}_9\sqrt{-g}\left(\dfrac{M^2NN_f g_s^3\log^5(N)(5\log(N)-211\log(r))(\log(N)-23\log(r))\sqrt{\alpha(r)(\sigma(r)-t'(r)^2)}}{r^4\alpha_{\theta_1}\alpha_{\theta_2}^6\log(r)(\log(N)-9\log(r))^3(\log(N)-3\log(r))^5 t'(r)^2}\right),$

(vii) $\int d\mathcal{V}_9\sqrt{-g}(G^{tt})^2(G^{im})(G^{ll})R^{tMNj}R_{lMNt}K_{tij}K_{tml}\sim 0,$

(viii) $\int d\mathcal{V}_9\sqrt{-g}(G^{tt})^2(G^{jj})(G^{im})R^{tMNl}R_{jMNt}K_{tij}K_{tml}\sim 0,$

(ix) $\int d\mathcal{V}_9\sqrt{-g}(G^{tt})^3(G^{ii})(G^{jj})(G^{ll})(G^{mm})R^Q{}_{mtj}R_{litQ}K_{tij}K_{tml}\sim 0,$

(x) $\int d\mathcal{V}_9\sqrt{-g}\dfrac{1}{2}(G^{tt})^2(G^{im})(G^{ll})R^{tjMN}R_{ltMN}K_{tij}K_{tml}$

$\sim \int d\mathcal{V}_9\sqrt{-g}\left[\dfrac{M^5N^{7/10}N_f^2 g_s^{11/2}G_3(r)\log^3(N)\log^3(r)(\log(N)-24\log(r))(\log(N)-9\log(r))(\log(N)-6\log(r))^2}{r^2\alpha_{\theta_1}^3\alpha_{\theta_2}^2\alpha(r)^2(\log(N)-3\log(r))^5}\right.$

$\times \dfrac{\sqrt{\alpha(r)(\sigma(r)-t'(r)^2)}(\sigma(r)\alpha'(r)-\alpha'(r)t'(r)^2+\alpha(r)(\sigma'(r)-2t'(r)t''(r)))^2}{t'(r)^4(\sigma(r)-t'(r)^2)^2}\Bigg],$

(xi) $\int d\mathcal{V}_9\sqrt{-g}\dfrac{1}{2}(G^{tt})^2(G^{im})(G^{jj})R^{tlMN}R_{jtMN}K_{tij}K_{tml}$

$\sim \int d\mathcal{V}_9\sqrt{-g}\left[-\dfrac{MN^{7/10}r^2N_f^{8/3}g_s^{3/2}\log(r)(\log(N)-9\log(r))(2\log(N)-\log(r))^{5/3}\sqrt{\alpha(r)(\sigma(r)-t'(r)^2)}}{\alpha_{\theta_1}^3\alpha_{\theta_2}^2 t'(r)^2}\right.$

$\times\left(G_4(r)-\dfrac{52\sqrt[3]{6}M^4 g_s^4\log^2(r)(\log(N)-12\log(r))^2(\sigma(r)\alpha'(r)-\alpha'(r)t'(r)^2+\alpha(r)(\sigma'(r)-2t'(r)t''(r)))^2}{\pi^{4/3}r^4\alpha(r)^2N_f^{2/3}(\log(N)-3\log(r))^{8/3}(\sigma(r)-t'(r)^2)^2}\right)\Bigg],$

(xii) $\int dV_9 \sqrt{-g} \frac{1}{2} (G^{tt})^3 (G^{ii})(G^{jj})(G^{ll})(G^{mm}) R^Q{}_{mti} R_{lQtj} K_{tij} K_{tml} \sim \int dV_9 \left(\frac{W(r)}{2} \mathcal{L}_2 \right),$

(xiii) $\int dV_9 \sqrt{-g} \frac{1}{2} (G^{tt})^3 (G^{jj})(G^{il}) R_t{}^{mtP} R_{Pttj} K_{tij} K_{tml}$

$$\sim \int dV_9 \sqrt{-g} \left(-\frac{M^2 N N_f g_s^3 \log^6(N)(\log(N) - 51\log(r))(\log(N) - 23\log(r))\sqrt{\alpha(r)(\sigma(r) - t'(r)^2)}}{r^4 \alpha_{\theta_1} \alpha_{\theta_2}^6 \log^3(r)(\log(N) - 9\log(r))^3 (\log(N) - 3\log(r))^5 t'(r)^2} \right), \quad \text{(D5)}$$

where $G_3(r)$ and $G_4(r)$ are N independent functions. Out of all the thirteen terms listed above (v) and (xii) terms are the most dominant terms in the large-N limit.

We find that at $\mathcal{O}(R^4)$, there are six terms coming from $\frac{\partial^2 J_0}{\partial R_{titj} \partial R_{xmxl}} K_{tij} K_{tml}$ and listed below:

(i) $\int dV_9 \sqrt{-g} (G^{xx})^2 (G^{mm})(G^{ll}) \delta_m^i \delta_P^t \delta_R^t \delta_Q^j R_x{}^{TSP} R^Q{}_{TSl} K_{tij} K_{tml} \sim \int dV_9 (U(r)\mathcal{L}_3),$

(ii) $\int dV_9 \sqrt{-g} (G^{xx})^2 (G^{ii})(G^{jj})(G^{mm})(G^{ll})(G^{tt}) \delta_x^t R_{jmxQ} R^Q{}_{itl} K_{tij} K_{tml} \sim 0,$

(iii) $\int dV_9 \sqrt{-g} (G^{xx})^2 (G^{mm})(G^{ll})(G^{tt}) \delta_T^i \delta_S^t \delta_l^j R_{Pmxt} R_x{}^{TSP} K_{tij} K_{tml} \sim 0,$

(iv) $\int dV_9 \sqrt{-g} \frac{1}{2} (G^{xx})^2 (G^{mm})(G^{ll})(G^{tt}) \delta_T^i \delta_S^t \delta_m^j R_{Ptxl} R_x{}^{TSP} K_{tij} K_{tml} \sim 0,$

(v) $\int dV_9 \sqrt{-g} (G^{xx})(G^{tt})^2 (G^{ii})(G^{jl}) R_t{}^{mxP} R_{Pitx} K_{tij} K_{tml} \sim 0,$

(vi) $\int dV_9 \sqrt{-g} \frac{1}{2} (G^{tt})^2 (G^{xx})(G^{jj})(G^{iK}) \delta_K^l R_t{}^{mxP} R_{Pxtj} K_{tij} K_{tml} \sim 0. \quad \text{(D6)}$

From the above terms we can see that it is the only first term which is nonzero. Therefore only this term will contribute to the Lagrangian.

Similarly we found that at $\mathcal{O}(R^4)$, there are four terms coming from $\frac{\partial^2 J_0}{\partial R_{tixj} \partial R_{xmtl}} K_{tij} K_{tml}$ which are listed below:

(i) $\int dV_9 \sqrt{-g} (G^{xx})^2 (G^{mm})(G^{ll}) \delta_m^i R_x{}^{TSx} R^j{}_{TSl} K_{tij} K_{tml} \sim \int dV_9 (U(r)\mathcal{L}_4),$

(ii) $\int dV_9 \sqrt{-g} (G^{xx})^3 (G^{ii})(G^{jj})(G^{ll})(G^{mm}) R_{jmxQ} R^Q{}_{ixl} K_{tij} K_{tml} \sim 0,$

(iii) $\int dV_9 \sqrt{-g} \frac{1}{2} (G^{xx})(G^{tt})^2 (G^{jm})(G^{ll}) R_x{}^{ixP} R_{Pttl} K_{tij} K_{tml} \sim \int dV_9 (V(r)\mathcal{L}_4),$

(iv) $\int dV_9 \sqrt{-g} \frac{1}{2} (G^{xx})^2 (G^{tt})(G^{jj})(G^{il}) R_t{}^{mtP} R_{Pxxj} K_{tij} K_{tml} \sim \int dV_9 (V(r)\mathcal{L}_4). \quad \text{(D7)}$

From Eq. (B7) it is clear that all the three nonzero terms scale as N. Therefore we will keep all nonzero terms in the Lagrangian.

2. Island surface

Square root of minus of determinant of the induced metric (53) for the island surface scale as $N^{7/10}$ is given below:

$$\sqrt{-g} = \frac{M N^{7/10} \sqrt{g_s} (N_f (\log(N) - 3\log(r)))^{5/3} \sqrt{\alpha(r)(\sigma(r) + x'(r)^2)}}{144 \, 6^{5/6} \pi^{19/6} \alpha_{\theta_1}^3 \alpha_{\theta_2}^2} (18 N_f g_s \log^2(r)(r^2 - 3b^2(6r+1)r_h^2)$$

$$+ \log(r)(8\pi(r^2 - 3b^2 r_h^2) - 3r^2 N_f g_s) - N_f g_s \log(N)(2\log(r) + 1)(r^2 - 3b^2 r_h^2)). \quad \text{(D8)}$$

Similar to Hartman-Maldacena-like surface, there are four terms that we obtain from $\frac{\partial J_0}{\partial R_{txtx}}$:

(i) $\int d\mathcal{V}_9\sqrt{-g}\left((G^{xx})^2(G^{tt})^2\left(R_{PxtQ}+\frac{1}{2}R_{PQtx}\right)R_t{}^{RSP}R^Q{}_{RSx}\right)$

$\sim\int d\mathcal{V}_9\sqrt{-g}\left(\frac{r_h^8(13(\log(N)-3\log(r))^4+21(\log(N)-3\log(r))^2+9\log(r)(6\log(N)-9\log(r))^2)}{\sqrt{N}r^{12}N_f^{10/3}\sqrt{g_s}(\log(N)-3\log(r))^{22/3}}\right);$

(ii) $\int d\mathcal{V}_9\sqrt{-g}\left(R^{HxtK}R_H{}^{RSt}R^x{}_{RSK}+\frac{1}{2}R^{HKtx}R_H{}^{RSt}R^Q{}_{RSK}\right)$

$\sim\int d\mathcal{V}_9\sqrt{-g}\left(\frac{r_h^8(-2g_s\log^2(N)(\log(N)-12\log(r))^2-5(\log(N)-9\log(r))^2(\log(N)-3\log(r))^2)}{\sqrt{N}r^{12}N_f^{10/3}\sqrt{g_s}(\log(N)-9\log(r))^2(\log(N)-3\log(r))^{16/3}}\right);$

(iii) $\int d\mathcal{V}_9\sqrt{-g}\left((G^{xx})^2G^{tt}\left(R_{PxtQ}+\frac{1}{2}R_{PQtx}\right)R_t{}^{RSP}R^Q{}_{RSx}\right)$

$\sim\int d\mathcal{V}_9(\lambda_3(r)\sqrt{\alpha(r)(\sigma(r)+x'(r)^2)});$

(iv) $\int d\mathcal{V}_9\sqrt{-g}\left(G^{tt}\left(R^{HMNx}R_{PMNt}+\frac{1}{2}R^{HxMN}R_{PtMN}\right)R_H{}^{xtP}\right)$

$\sim\int d\mathcal{V}_9(\lambda_4(r)\sqrt{\alpha(r)(\sigma(r)+x'(r)^2)}).$ (D9)

We find that (iii) and (iv) terms are the most dominant terms in the large N limit. There are thirteen terms that obtain from $\frac{\partial^2 J_0}{\partial R_{xixj}\partial R_{xmxl}}K_{xij}K_{xml}$ which are listed below:

(i) $\int d\mathcal{V}_9\sqrt{-g}(G^{xx})^2(G^{mm})(G^{ll})\delta^i_m R_r{}^{TSx}R^j{}_{TSl}K_{xij}K_{xml}$

$\sim\int d\mathcal{V}_9\sqrt{-g}\left(-\frac{M^2NN_fg_s^3\log^2(r)(23\log(N)-72\log(r))^3}{r^4\alpha_{\theta_1}\alpha_{\theta_2}^6(\log(N)-9\log(r))^2(\log(N)-3\log(r))^6x'(r)^2}\right),$

(ii) $\int d\mathcal{V}_9\sqrt{-g}(G^{xx})^3(G^{ii})(G^{jj})(G^{mm})(G^{ll})R_{jmxQ}R^Q{}_{ixl}K_{xij}K_{xml}\sim 0,$

(iii) $\int d\mathcal{V}_9\sqrt{-g}\frac{1}{2}(G^{xx})^2(G^{mm})(G^{jl})R_r{}^{TSx}R^i{}_{TSx}K_{xij}K_{xml}\sim 0,$

(iv) $\int d\mathcal{V}_9\sqrt{-g})\frac{1}{2}(G^{xx})^2(G^{ii})(G^{jl})R_r{}^{TSx}R^m{}_{TSi}K_{xij}K_{xml}$

$\sim\int d\mathcal{V}_9\sqrt{-g}\left(\frac{M^3N^{13/10}\alpha_{\theta_1}N_f^5g_s^{15/2}\log(r)(23\log(N)-72\log(r))^3(\log(N)+18\log^2(r))\sqrt{\alpha(r)(\sigma(r)+x'(r)^2)}}{r^4\alpha_{\theta_2}^{10}(\log(N)-3\log(r))^5x'(r)^2(4\pi-N_fg_s(\log(N)-9\log(r)))^3}\right),$

(v) $\int d\mathcal{V}_9\sqrt{-g}\frac{1}{2}(G^{xx})^3(G^{ii})(G^{ll})(G^{mm})(G^{jj})R_{jQxl}R^Q{}_{ixm}K_{xij}K_{xml}\sim\int d\mathcal{V}_9\left(\frac{Z_1(r)}{2}\mathcal{L}_1\right),$

(vi) $\int d\mathcal{V}_9\sqrt{-g}\frac{1}{2}(G^{xx})^3(G^{jm})(G^{ll})R_{Pxxl}R_x{}^{ixP}K_{xij}K_{xml}$

$\sim\int d\mathcal{V}_9\sqrt{-g}\left(\frac{M^2NN_fg_s^3\log^3(N)(5\log(N)-196\log(r))(23\log(N)-72\log(r))\sqrt{\alpha(r)(\sigma(r)+x'(r)^2)}}{r^4\alpha_{\theta_1}\alpha_{\theta_2}^6(\log(N)-9\log(r))^3(\log(N)-3\log(r))^4x'(r)^2}\right),$

(vii) $\int d\mathcal{V}_9 \sqrt{-g}(G^{xx})^2(G^{im})(G^{ll})R^{xMNj}R_{lMNx}K_{xij}K_{xml} \sim 0,$

(viii) $\int d\mathcal{V}_9 \sqrt{-g}(G^{xx})^2(G^{jj})(G^{im})R^{xMNl}R_{jMNx}K_{xij}K_{xml} \sim 0,$

(ix) $\int d\mathcal{V}_9 \sqrt{-g}(G^{xx})^3(G^{ii})(G^{jj})(G^{ll})(G^{mm})R^{Q}_{\ mxj}R_{lixQ}K_{xij}K_{xml} \sim 0,$

(x) $\int d\mathcal{V}_9 \sqrt{-g}\frac{1}{2}(G^{xx})^2(G^{im})(G^{ll})R^{xjMN}R_{lxMN}K_{xij}K_{xml}$

$\sim \int d\mathcal{V}_9 \sqrt{-g}\Bigg[\frac{MN^{7/10}r^2N_f^{8/3}g_s^{3/2}\log(r)(\log(N)-9\log(r))(\log(N)-3\log(r))^{5/3}\sqrt{\alpha(r)(\sigma(r)+x'(r)^2)}}{\alpha_{\theta_1}^3\alpha_{\theta_2}^2 x'(r)^2}$

$\times \Bigg(\frac{M^4 g_s^4 \log^2(r)(\log(N)-12\log(r))^2(\sigma(r)\alpha'(r)+\alpha'(r)x'(r)^2+\alpha(r)(\sigma'(r)+2x'(r)x''(r)))^2}{64\,6^{2/3}\pi^{4/3}r^4\alpha(r)^2N_f^{2/3}(\log(N)-3\log(r))^{8/3}(\sigma(r)+x'(r)^2)^2} - 200G_5(r)\Bigg)\Bigg],$

(xi) $\int d\mathcal{V}_9 \sqrt{-g}\frac{1}{2}(G^{xx})^2(G^{im})(G^{jj})R^{xlMN}R_{jxMN}K_{xij}K_{xml}$

$\sim \int d\mathcal{V}_9 \sqrt{-g}\Bigg[\frac{MN^{7/10}r^2N_f^{8/3}g_s^{3/2}\log(r)(\log(N)-9\log(r))(\log(N)-3\log(r))^{5/3}\sqrt{\alpha(r)(\sigma(r)+x'(r)^2)}}{14400\,6^{5/6}\pi^{19/6}\alpha_{\theta_1}^3\alpha_{\theta_2}^2 x'(r)^2}$

$\times \Bigg(\frac{29M^4 g_s^4 \log^2(r)(\log(N)-12\log(r))^2(\sigma(r)\alpha'(r)+\alpha'(r)x'(r)^2+\alpha(r)(\sigma'(r)+2x'(r)x''(r)))^2}{64\,6^{2/3}\pi^{4/3}r^4\alpha(r)^2N_f^{2/3}(\log(N)-3\log(r))^{8/3}(\sigma(r)+x'(r)^2)^2} - 200G_6(r)\Bigg)\Bigg],$

(xii) $\int d\mathcal{V}_9 \sqrt{-g}\frac{1}{2}(G^{xx})^3(G^{ii})(G^{jj})(G^{ll})(G^{mm})R^{Q}_{\ mxi}R_{lQxj}K_{xij}K_{xml} \sim \int d\mathcal{V}_9 \left(\frac{Z_1(r)}{2}\mathcal{L}_1\right),$

(xiii) $\int d\mathcal{V}_9 \sqrt{-g}\frac{1}{2}(G^{xx})^3(G^{jj})(G^{il})R_x^{\ mxP}R_{Pxxj}K_{xij}K_{xml}$

$\sim \int d\mathcal{V}_9 \sqrt{-g}\left(-\frac{M^2NN_f g_s^3\log^3(N)(5\log(N)-196\log(r))(23\log(N)-72\log(r))\sqrt{\alpha(r)(\sigma(r)+x'(r)^2)}}{r^4\alpha_{\theta_1}\alpha_{\theta_2}^6(\log(N)-9\log(r))^3(\log(N)-3\log(r))^4 x'(r)^2}\right),$ (D10)

where $G_5(r)$ and $G_6(r)$ are N independent functions. We find that (v) and (xii) terms are the most dominant terms in the large N limit. There are thirteen terms that are obtained from $\frac{\partial^2 J_0}{\partial R_{titj}\partial R_{tmtl}}K_{xij}K_{xml}$:

(i) $\int d\mathcal{V}_9 \sqrt{-g}(G^{tt})^2(G^{mm})(G^{ll})\delta^i_m R_t^{\ TSt}R^j_{\ TSl}K_{xij}K_{xml}$

$\sim \int d\mathcal{V}_9 \sqrt{-g}\left(-\frac{M^2NN_f g_s^3 \log^4(N)\log^2(r)(23\log(N)-72\log(r))^2(\log(N)-27\log(r))\sqrt{\alpha(r)(\sigma(r)+x'(r)^2)}}{r^4\alpha_{\theta_1}\alpha_{\theta_2}^6(\log(N)-9\log(r))^4(\log(N)-3\log(r))^6 x'(r)^2}\right),$

(ii) $\int d\mathcal{V}_9 \sqrt{-g}(G^{tt})^3(G^{ii})(G^{jj})(G^{mm})(G^{ll})R_{jmtQ}R^Q_{\ itl}K_{xij}K_{xml} \sim 0,$

(iii) $\int d\mathcal{V}_9 \sqrt{-g}\frac{1}{2}(G^{tt})^2(G^{mm})(G^{jl})R_t^{\ TSt}R^i_{\ TSt}K_{xij}K_{xml} \sim 0,$

(iv) $\int d\mathcal{V}_9 \sqrt{-g}\frac{1}{2}(G^{tt})^2(G^{ii})(G^{jl})R_t^{\ TSt}R^m_{\ TSi}K_{xij}K_{xml}$

$\sim \int d\mathcal{V}_9 \sqrt{-g}\left(-\frac{M^3N^{13/10}\alpha_{\theta_1}N_f^2 g_s^{9/2}\log(r)(23\log(N)-72\log(r))^3(\log(N)+18\log^2(r))\sqrt{\alpha(r)(\sigma(r)+x'(r)^2)}}{r^4\alpha_{\theta_2}^{10}(\log(N)-9\log(r))^3(\log(N)-3\log(r))^5 x'(r)^2}\right),$

(v) $\int d\mathcal{V}_9 \sqrt{-g} \frac{1}{2}(G^{tt})^3(G^{ii})(G^{ll})(G^{mm})(G^{jj})R_{jQtl}R^Q{}_{itm}K_{xij}K_{xml} \sim \int d\mathcal{V}_9\left(\frac{W_1(r)}{2}\mathcal{L}_2\right),$

(vi) $\int d\mathcal{V}_9 \sqrt{-g} \frac{1}{2}(G^{tt})^3(G^{jm})(G^{ll})R_{Pttl}R_t{}^{itP}K_{xij}K_{xml} \sim \int d\mathcal{V}_9 \sqrt{-g}$

$$\left(\frac{M^2 N N_f g_s^3 \log^3(N)(5\log(N)-196\log(r))(23\log(N)-72\log(r))(\log(N)-3\log(r)-1)^2\sqrt{\alpha(r)(\sigma(r)+x'(r)^2)}}{r^4 \alpha_{\theta_1}\alpha_{\theta_2}^6 (\log(N)-9\log(r))^3(\log(N)-3\log(r))^6 x'(r)^2}\right),$$

(vii) $\int d\mathcal{V}_9 \sqrt{-g}(G^{tt})^2(G^{im})(G^{ll})R^{tMNj}R_{lMNt}K_{xij}K_{xml} \sim 0,$

(viii) $\int d\mathcal{V}_9 \sqrt{-g}(G^{tt})^2(G^{jj})(G^{im})R^{tMNl}R_{jMNt}K_{xij}K_{xml} \sim 0,$

(ix) $\int d\mathcal{V}_9 \sqrt{-g}(G^{tt})^3(G^{ii})(G^{jj})(G^{ll})(G^{mm})R^Q{}_{mtj}R_{litQ}K_{xij}K_{xml} \sim 0,$

(x) $\int d\mathcal{V}_9 \sqrt{-g}\frac{1}{2}(G^{tt})^2(G^{im})(G^{ll})R^{tjMN}R_{ltMN}K_{xij}K_{xml}$

$$\sim \int d\mathcal{V}_9 \sqrt{-g}\left[\frac{MN^{7/10}r^2 N_f^{8/3} g_s^{3/2}\log(r)(\log(N)-9\log(r))(\log(N)-3\log(r))^{5/3}\sqrt{\alpha(r)(\sigma(r)+x'(r)^2)}}{\alpha_{\theta_1}^3 \alpha_{\theta_2}^2 x'(r)^2}\right.$$

$$\left.\times\left(\frac{13M^4 g_s^4 \log^2(r)(\log(N)-12\log(r))^2(\sigma(r)\alpha'(r)+\alpha'(r)x'(r)^2+\alpha(r)(\sigma'(r)+2x'(r)x''(r)))^2}{64 6^{2/3}\pi^{4/3}r^4\alpha(r)^2(\log(N)-3\log(r))^2(N_f(\log(N)-3\log(r)))^{2/3}(\sigma(r)+x'(r)^2)^2}-25G_7(r)\right)\right],$$

(xi) $\int d\mathcal{V}_9 \sqrt{-g}\frac{1}{2}(G^{tt})^2(G^{im})(G^{jj})R^{tlMN}R_{jtMN}K_{xij}K_{xml}$

$$\sim \int d\mathcal{V}_9 \sqrt{-g}\left[\frac{MN^{7/10}r^2 N_f^{8/3} g_s^{3/2}\log(r)(\log(N)-9\log(r))(\log(N)-3\log(r))^{5/3}\sqrt{\alpha(r)(\sigma(r)+x'(r)^2)}}{\alpha_{\theta_1}^3 \alpha_{\theta_2}^2 x'(r)^2}\right.$$

$$\left.\times\left(\frac{13M^4 g_s^4 \log^2(r)(\log(N)-12\log(r))^2(\sigma(r)\alpha'(r)+\alpha'(r)x'(r)^2+\alpha(r)(\sigma'(r)+2x'(r)x''(r)))^2}{64 6^{2/3}\pi^{4/3}r^4\alpha(r)^2(\log(N)-3\log(r))^2(N_f(\log(N)-3\log(r)))^{2/3}(\sigma(r)+x'(r)^2)^2}-25G_8(r)\right)\right],$$

(xii) $\int d\mathcal{V}_9 \sqrt{-g}\frac{1}{2}(G^{tt})^3(G^{ii})(G^{jj})(G^{ll})(G^{mm})R^Q{}_{mti}R_{lQtj}K_{xij}K_{xml} \sim \int d\mathcal{V}_9\left(\frac{W_1(r)}{2}\mathcal{L}_2\right),$

(xiii) $\int d\mathcal{V}_9 \sqrt{-g}\frac{1}{2}(G^{tt})^3(G^{jj})(G^{il})R_t{}^{mtP}R_{Pttj}K_{xij}K_{xml}$

$$\sim \int d\mathcal{V}_9 \sqrt{-g}\left(\frac{M^2 N N_f g_s^3 \log^3(N)(5\log(N)-196\log(r))(23\log(N)-72\log(r))\sqrt{\alpha(r)(\sigma(r)+x'(r)^2)}}{r^4 \alpha_{\theta_1}\alpha_{\theta_2}^6 (\log(N)-9\log(r))^3(\log(N)-3\log(r))^4 x'(r)^2}\right), \tag{D11}$$

where $G_7(r)$ and $G_8(r)$ are N independent functions and (v) and (xii) terms are the most dominant terms in the large-N limit. Similar to Hartman-Maldacena-like surface, there are six terms that we obtain from $\frac{\partial^2 J_0}{\partial R_{titj}\partial R_{xmxl}}K_{xij}K_{xml}$ and only first term is nonzero.

(i) $\int d\mathcal{V}_9 \sqrt{-g}(G^{xx})^2(G^{mm})(G^{ll})\delta_m^i \delta_P^t \delta_R^t \delta_Q^j R_x{}^{TSP}R^Q{}_{TSl}K_{xij}K_{xml} \sim \int d\mathcal{V}_9(U_1(r)\mathcal{L}_3),$

(ii) $\int d\mathcal{V}_9 \sqrt{-g}(G^{xx})^2(G^{ii})(G^{jj})(G^{mm})(G^{ll})(G^{tt})\delta_x^t R_{jmxQ}R^Q{}_{itl}K_{xij}K_{xml} \sim 0,$

(iii) $\int d\mathcal{V}_9 \sqrt{-g}(G^{xx})^2(G^{mm})(G^{ll})(G^{tt})\delta_T^i \delta_S^t \delta_l^j R_{Pmxt}R_x{}^{TSP}K_{xij}K_{xml} \sim 0,$

(iv) $\int d\mathcal{V}_9 \sqrt{-g} \frac{1}{2} (G^{xx})^2 (G^{mm})(G^{ll})(G^{tt}) \delta^i_T \delta^t_S \delta^j_m R_{Ptxl} R_x{}^{TSP} K_{xij} K_{xml} \sim 0,$

(v) $\int d\mathcal{V}_9 \sqrt{-g} (G^{xx})(G^{tt})^2 (G^{ii})(G^{jl}) R_t^{mxP} R_{Pitx} K_{xij} K_{xml} \sim 0,$

(vi) $\int d\mathcal{V}_9 \sqrt{-g} \frac{1}{2} (G^{tt})^2 (G^{xx})(G^{jj})(G^{iK}) \delta^l_K R_t^{mxP} R_{Pxtj} K_{xij} K_{xml} \sim 0.$ (D12)

Similar to Hartman-Maldacena-like surface, there are four terms that we obtain from $\frac{\partial^2 J_0}{\partial R_{tixj} \partial R_{xmtl}} K_{xij} K_{xml}$ and three terms are nonzero and they scale as same power of N.

(i) $\int d\mathcal{V}_9 \sqrt{-g} (G^{xx})^2 (G^{mm})(G^{ll}) \delta^i_m R_x{}^{TSx} R^j{}_{TSl} K_{xij} K_{xml} \sim \int d\mathcal{V}_9 (U_1(r)\mathcal{L}_4),$

(ii) $\int d\mathcal{V}_9 \sqrt{-g} (G^{xx})^3 (G^{ii})(G^{jj})(G^{ll})(G^{mm}) R_{jmxQ} R^Q{}_{ixl} K_{xij} K_{xml} \sim 0,$

(iii) $\int d\mathcal{V}_9 \sqrt{-g} \frac{1}{2} (G^{xx})(G^{tt})^2 (G^{jm})(G^{ll}) R_x{}^{ixP} R_{Pttl} K_{xij} K_{xml} \sim \int d\mathcal{V}_9 (V_1(r)\mathcal{L}_4),$

(iv) $\int d\mathcal{V}_9 \sqrt{-g} \frac{1}{2} (G^{xx})^2 (G^{tt})(G^{jj})(G^{il}) R_t{}^{mtP} R_{Pxxj} K_{xij} K_{xml} \sim \int d\mathcal{V}_9 (V_1(r)\mathcal{L}_4).$ (D13)

We have multiplied each term by $\frac{8}{(q_\alpha+1)}$.

---

[1] S. W. Hawking, Particle creation by black holes, Commun. Math. Phys. **43**, 199 (1975); **46**, 206(E) (1976).

[2] D. N. Page, Information in Black Hole Radiation, Phys. Rev. Lett. **71**, 3743 (1993).

[3] J. M. Maldacena, The large N limit of superconformal field theories and supergravity, Int. J. Theor. Phys. **38**, 1113 (1999).

[4] A. Misra and V. Yadav, On M-theory dual of large-N thermal QCD-like theories up to $\mathcal{O}(R^4)$ and G-structure classification of underlying nonsupersymmetric geometries, arXiv:2004.07259 [Adv. Theor. Math. Phys. issue 26.10 (to be published)].

[5] S. Raju, Lessons from the information paradox, Phys. Rep. **943**, 1 (2022).

[6] D. Harlow, Jerusalem lectures on black holes and quantum information, Rev. Mod. Phys. **88**, 015002 (2016).

[7] S. Ryu and T. Takayanagi, Holographic Derivation of Entanglement Entropy from AdS/CFT, Phys. Rev. Lett. **96**, 181602 (2006).

[8] I. R. Klebanov, D. Kutasov, and A. Murugan, Entanglement as a probe of confinement, Nucl. Phys. **B796**, 274 (2008).

[9] G. Yadav, V. Yadav, and A. Misra, $\mathcal{M}$cTEQ ($\mathcal{M}$chiral perturbation theory-compatible deconfinement temperature and entanglement entropy up to terms quartic in curvature) and FM(Flavor Memory), J. High Energy Phys. 10 (2021) 220.

[10] Xi Dong, Holographic entanglement entropy for general higher derivative gravity, J. High Energy Phys. 01 (2014) 044.

[11] N. Engelhardt and A. C. Wall, Quantum extremal surfaces: Holographic entanglement entropy beyond the classical regime, J. High Energy Phys. 01 (2015) 073.

[12] A. Almheiri, R. Mahajan, J. Maldacena, and Y. Zhao, The Page curve of Hawking radiation from semiclassical geometry, J. High Energy Phys. 03 (2020) 143.

[13] A. Almheiri, R. Mahajan, and J. E. Santos, Entanglement islands in higher dimensions, SciPost Phys. **9**, 001 (2020).

[14] T. Hartman and J. Maldacena, Time evolution of entanglement entropy from black hole interiors, J. High Energy Phys. 05 (2013) 014.

[15] A. Karch and L. Randall, Locally localized gravity, J. High Energy Phys. 05 (2001) 008.

[16] A. Karch and L. Randall, Open and closed string interpretation of SUSY CFT's on branes with boundaries, J. High Energy Phys. 06 (2001) 063.

[17] H. Geng, A. Karch, C. P. Pardavila, S. Raju, L. Randall, M. Riojas, and S. Shashi, Information transfer with a gravitating bath, SciPost Phys. **10**, 103 (2021).

[18] E. Caceres, A. Kundu, Ayan K. Patra, and S. Shashi, Page curves and bath deformations, SciPost Phys. Core **5**, 033 (2022).

[19] E. Caceres, A. Kundu, Ayan K. Patra, and S. Shashi, Warped information and entanglement islands in AdS/WCFT, J. High Energy Phys. 07 (2021) 004.

[20] A. Bhattacharya, A. Bhattacharyya, P. Nandy, and A. K. Patra, Islands and complexity of eternal black hole and radiation subsystems for a doubly holographic model, J. High Energy Phys. 05 (2021) 135.

[21] A. Bhattacharya, A. Bhattacharyya, P. Nandy, and A. K. Patra, Bath deformations, islands and holographic complexity, Phys. Rev. D **105**, 066019 (2022).

[22] Q. L. Hu, D. Li, R. X. Miao, and Y. Q. Zeng, AdS/BCFT and island for curvature-squared gravity, J. High Energy Phys. 09 (2022) 037.

[23] P. Calabrese and J. Cardy, Entanglement entropy and quantum field theory: A non-technical introduction, Int. J. Quantum. Inform. **04**, 429 (2006).

[24] M. Alishahiha, A. F. Astaneh, and A. Naseh, Island in the presence of higher derivative terms, J. High Energy Phys. 02 (2021) 035.

[25] X. Wang, R. Li, and J. Wang, Islands and Page curves of Reissner-Nordstrom black holes, J. High Energy Phys. 04 (2021) 103.

[26] M. H. Yu and X. H. Ge, Page curves and islands in charged dilaton black holes, Eur. Phys. J. C **82**, 167 (2022).

[27] K. Hoshimoto, N. Iizuka, and N. Matsuo, Islands in Schwarzschild black holes, J. High Energy Phys. 06 (2020) 085.

[28] F. Omidi, Entropy of Hawking radiation for two-sided hyperscaling violating black branes, J. High Energy Phys. 04 (2022) 022.

[29] C. F. Uhlemann, Islands and Page curves in 4d from type IIB, J. High Energy Phys. 08 (2021) 104.

[30] S. Demulder, A. Gnecchi, I. Lavdas, and D. Lust, Island and light gravitons in type IIB string theory, J. High Energy Phys. 02 (2023) 016.

[31] A. Karch, H. Sun, and C. F. Uhlemann, Double holography in string theory, J. High Energy Phys. 10 (2022) 012.

[32] C. Krishnan, V. Patil, and J. Pereira, Page curve and the information paradox in flat space, arXiv:2005.02993.

[33] G. Yadav, Page curves of Reissner-Nordström black hole in HD gravity, Eur. Phys. J. C **82**, 904 (2022).

[34] M. Mia, K. Dasgupta, C. Gale, and S. Jeon, Five easy pieces: The dynamics of quarks in strongly coupled plasmas, Nucl. Phys. **B839**, 187 (2010).

[35] K. Sil and A. Misra, On aspects of holographic thermal QCD at finite coupling, Nucl. Phys. **B910**, 754 (2016).

[36] M. Dhuria and A. Misra, Towards MQGP, J. High Energy Phys. 11 (2013) 001.

[37] K. Sil and A. Misra, New insights into properties of large-N holographic thermal QCD at finite gauge coupling at (the non-conformal/next-to) leading order in N, Eur. Phys. J. C **76**, 618 (2016).

[38] K. Sil, V. Yadav, and A. Misra, Top-down holographic G-structure glueball spectroscopy at (N)LO in N and finite coupling, Eur. Phys. J. C **77**, 381 (2017).

[39] V. Yadav, A. Misra, and K. Sil, Delocalized SYZ mirrors and confronting top-down $SU(3)$-structure holographic meson masses at finite g and N_c with p(article) d(ata) g (roup) values, Eur. Phys. J. C **77**, 656 (2017).

[40] V. Yadav and A. Misra, M-theory exotic scalar glueball decays to mesons at finite coupling, J. High Energy Phys. 09 (2018) 133.

[41] V. Yadav, G. Yadav, and A. Misra, (Phenomenology/lattice-compatible) $SU(3)$ MχPT HD up to $\mathcal{O}(p^4)$ and the $\mathcal{O}(R^4)$-large-N connection, J. High Energy Phys. 08 (2021) 151.

[42] G. Yadav, Deconfinement temperature of rotating QGP at intermediate coupling from M-theory, Phys. Lett. B **841**, 137925 (2023).

[43] P. Ouyang, Holomorphic D7-branes and flavored $N = 1$ gauge theories, Nucl. Phys. **B699**, 207 (2004).

[44] A. Misra and C. Gale, The QCD trace anomaly at strong coupling from M-theory, Eur. Phys. J. C **80**, 620 (2020).

[45] U. Gursoy, E. Kiritsis, L. Mazzanti, and F. Nitti, Deconfinement and Gluon Plasma Dynamics in Improved Holographic QCD, Phys. Rev. Lett. **101**, 181601 (2008).

[46] M. Ionel and M. Min-Oo, Cohomogeneity one special Lagrangian 3-folds in the deformed and the resolved conifolds, Ill. J. Math. **52**, 3 (2008).

[47] K. Sil and A. Misra, New insights into properties of large-N holographic thermal QCD at finite gauge coupling at (the non-conformal/next-to) leading order in N, Eur. Phys. J. C **76**, 618 (2016).

[48] M. Becker, K. Dasgupta, A. Knauf, and R. Tatar, Geometric transitions, flops and nonKahler manifolds. I., Nucl. Phys. **B702**, 207 (2004).

[49] A. Knauf, Geometric transitions on non-Kaehler manifolds, Fortschr. Phys. **55**, 5 (2007).

[50] K. Dasgupta, M. Grisaru, R. Gwyn, S. H. Katz, A. Knauf, and R. Tatar, Gauge-gravity dualities, dipoles and new non-Kahler manifolds, Nucl. Phys. **B755**, 21 (2006).

[51] D. M. McAvity and H. Osborn, Conformal field theories near a boundary in general dimensions, Nucl. Phys. **B455**, 522 (1995).

[52] J. L. Cardy, Boundary conformal field theory, arXiv:hep-th/0411189.

[53] L. Randall and R. Sundrum, An Alternative to Compactification, Phys. Rev. Lett. **83**, 4690 (1999).

[54] S. Detournay, T. Hartman, and D. M. Hofman, Warped conformal field theory, Phys. Rev. D **86**, 124018 (2012).

[55] Y. Ling, Y. Liu, and Z. Y. Xian, Island in charged black holes, J. High Energy Phys. 03 (2021) 251.

[56] H. Omiya and Z. Wei, Causal structures and nonlocality in double holography, J. High Energy Phys. 07 (2022) 128.

[57] Y. Ling, P. Liu, Y. Liu, C. Niu, Z. Y. Xian, and C. Y. Zhang, Reflected entropy in double holography, J. High Energy Phys. 02 (2022) 037.

[58] H. Geng, A. Karch, C. P. Pardavila, S. Raju, and L. Randall, Entanglement phase structure of a holographic BCFT in a black hole background, J. High Energy Phys. 05 (2022) 153.

[59] C. Krishnan, Critical islands, J. High Energy Phys. 01 (2021) 179.

[60] M. Afrasiar, J. K. Basak, A. Chandra, and G. Sengupta, Islands for entanglement negativity in communicating black holes, arXiv:2205.07903.

[61] D. Basu, H. Parihar, V. Raj, and G. Sengupta, Defect extremal surfaces for entanglement negativity, arXiv:2205.07905.

[62] Y. Liu, Z. Y. Xian, C. Peng, and Y. Ling, Black holes entangled by radiation, J. High Energy Phys. 11 (2022) 043.

[63] Z. Li and R. Q. Yang, Upper bounds of holographic entanglement entropy growth rate for thermofield double states, J. High Energy Phys. 10 (2022) 072.

[64] H. Geng, A. Karch, C. P. Pardavila, S. Raju, L. Randall, M. Riojas, and S. Shashi, Jackiw-Teitelboim Gravity from the

Karch-Randall Braneworld, Phys. Rev. Lett. **129,** 231601 (2022).

[65] F. Deng, Y. S. An, and Y. Zhou, JT gravity from partial reduction and defect extremal surface, J. High Energy Phys. 02 (2023) 219.

[66] H. Geng, Aspects of AdS_2 quantum gravity and the Karch-Randall braneworld, J. High Energy Phys. 09 (2022) 024.

[67] T. Takayanagi, Holographic Dual of BCFT, Phys. Rev. Lett. **107,** 101602 (2011).

[68] A. Czajka, K. Dasgupta, C. Gale, S. Jeon, A. Misra, M. Richard, and K. Sil, Bulk viscosity at extreme limits: From kinetic theory to strings, J. High Energy Phys. 07 (2019) 145.

[69] V. Balasubramanian, P. Berglund, J. P. Conlon, and F. Quevedo, Systematics of moduli stabilisation in Calabi-Yau flux compactifications, J. High Energy Phys. 03 (2005) 007.

[70] J. P. Conlon, F. Quevedo, and K. Suruliz, Large-volume flux compactifications: Moduli spectrum and D3/D7 soft supersymmetry breaking, J. High Energy Phys. 08 (2005) 007.

[71] A. Almheiri, T. Hartman, J. Maldacena, E. Shaghoulian, and A. Tajdini, The entropy of Hawking radiation, Rev. Mod. Phys. **93,** 035002 (2021); K. Hashimoto, N. Iizuka, and Y. Matsuo, Islands in Schwarzschild black holes, J. High Energy Phys. 06 (2020) 085; X. Wang, R. Li, and J. Wang, Islands and Page curves of Reissner-Nordström black holes, J. High Energy Phys. 04 (2021) 103.

[72] A. Buchel, C. P. Herzog, I. R. Klebanov, L. A. Pando Zayas, and A. A. Tseytlin, Nonextremal gravity duals for fractional D-3 branes on the conifold, J. High Energy Phys. 04 (2001) 033.

[73] S. Demulder, A. Gnecchi, I. Lavdas, and D. Lust, Islands and light gravitons in type IIB string theory, arXiv:2204. 03669.

[74] C. Bachas and J. Estes, Spin-2 spectrum of defect theories, J. High Energy Phys. 06 (2011) 005.

[75] M. Mia, F. Chen, K. Dasgupta, P. Franche, and S. Vaidya, Non-extremality, chemical potential and the infrared limit of large N thermal QCD, Phys. Rev. D **86,** 086002 (2012).

[76] M. Alishahiha, A. F. Astaneh, A. Naseh, and M. H. Vahidinia, On complexity of $F(R)$ and critical gravity, J. High Energy Phys. 05 (2017) 009.

[77] S. Dutta and T. Faulkner, A canonical purification for the entanglement wedge cross-section, J. High Energy Phys. 03 (2021) 178.